

**Post-translational Events Control Pattern Recognition Receptor  
Trafficking to Preserve PAMP Responsiveness in Plant Immunity**

**Sara Ben Khaled**

A thesis submitted to the University of East Anglia for the degree of Doctor of Philosophy

**The Sainsbury Laboratory**

Norwich Research Park

Norwich, UK

2016

This copy of the thesis has been supplied on condition that anyone who consults it is understood to recognise that its copyright rests with the author and that use of any information derived there from must be in accordance with current UK Copyright Law. In addition, any quotation or extract must include full attribution.

## Abstract

Pattern recognition receptors (PRRs) are localized at the cell surface to recognize conserved microbial patterns and activate plant immunity. The activation status regulates the localization of ligand-bound PRRs and routing to late endocytic trafficking for vacuolar degradation. This ligand-induced endocytosis is conserved across PRR families, and best characterized for the receptor kinases flagellin-sensing 2 (FLS2) and EF-Tu receptor (EFR), both mediating anti-bacterial immunity. However, the molecular determinants of FLS2 and EFR endocytic trafficking, as well as the biological relevance of these processes remain poorly understood.

In this study, I have dissected the molecular code underlying ligand-mediated endocytosis. I show that flagellin induced the interaction of FLS2 with vacuolar protein sorting (VPS) 37-1, a subunit of the endosomal complex required for transport-I (ESCRT-I) that recognizes internalized ubiquitinated proteins for vacuolar sorting. This led me to investigate the role of ubiquitination in FLS2 endocytosis. Using mass-spectrometry and mutational approaches, I identified ubiquitinated FLS2 lysine residues potentially involved in FLS2 endocytic trafficking. Additionally, I revealed an involvement of the E3 ligases KEP and the two redundant plant U-box (PUB) 12 and PUB13 in FLS2 trafficking.

I showed that PUB12/PUB13-mediated monoubiquitination of FLS2 is a key regulatory process for internalisation of activated receptors, while EFR endocytic degradation is regulated by receptor phosphorylation on the tyrosine residues 875 and 877. For both FLS2 and EFR, altering ligand-induced endocytosis did not impact the initiation of downstream signalling, demonstrating that these processes are uncoupled. Instead, my results showed that ligand-mediated endocytosis of FLS2 and EFR plays a pivotal role in maintaining chronic immune signalling responses upon long term ligand stimulation.

Overall, my results uncover an important molecular mechanism regulating the subcellular trafficking of the central immune components FLS2 and EFR, and extend our understanding on how plant responsiveness to its surrounding pathogens is maintained.

## Table of Contents

<b>Abstract.....</b>	2
<b>Table of Contents .....</b>	3
<b>List of Tables .....</b>	6
<b>List of Figures.....</b>	7
<b>List of Publications Arising From the Work in This Thesis .....</b>	10
<b>Acknowledgements.....</b>	11
<b>Abbreviations .....</b>	12
<b>Chapter 1: General Introduction.....</b>	16
1.    General Concepts of Plant Innate Immunity .....	16
1.1    Co-evolution of Plants and Pathogens .....	16
1.2    Perception of PAMPs.....	17
1.3    Effectors of Pathogenic Bacteria .....	20
2.    A Moving View: Subcellular Trafficking Processes in PRR– Triggered Plant Immunity; From (Ben Khaled, Postma, and Robatzek 2015).....	21
2.1 An Overview of the Plant Endomembrane Compartments .....	21
2.2    Subcellular Trafficking in Plant Immunity.....	24
2.3    Subcellular Trafficking of PRRs .....	26
3.    Post-translational Modifications (PTMs) as Regulators of Endocytosis .....	40
4.    Prologue .....	43
<b>Chapter 2: Involvement of Ubiquitination in FLS2 Subcellular Trafficking .....</b>	45
1.    ESCRT-I Mediates FLS2 Endosomal Sorting; From (Spallek et al. 2013) .....	45

1.1	Introduction .....	45
1.2	Activated FLS2 associates and co-localizes with VPS37-1 at endosomes .....	46
1.3	Materials and Methods .....	46
1.4	Discussion .....	48
2.	Towards the Characterisation of the FLS2 Ubiquitin-Endocytic Trafficking Map.....	48
2.1	Introduction .....	48
2.2	Results and Discussion.....	50
2.3	Material and Methods.....	59
3.	Ubiquitin-Mediated FLS2 Endocytosis is Required for Maintaining Responsiveness to Flagellin .....	62
3.1	Abstract.....	62
3.2	Introduction .....	62
3.3	FLS2 is Monoubiquitinated After flg22 Stimulation in a PUB12/PUB13-Dependent Manner .....	64
3.4	PUB12/PUB13-Mediated Ubiquitination of FLS2 Controls Early Endocytic Events in FLS2 Trafficking.....	67
3.5	Inhibition of FLS2 Endocytosis in <i>pub12 pub13</i> Does Not Contribute to Sustaining or Restricting PTI Signalling.....	71
3.6	FLS2 Endocytosis is Required for Maintaining flg22 Responsiveness after Repeated PAMP treatments .....	74
3.6	Discussion .....	78
3.7	Materials and Methods .....	84
<b>Chapter 3: Ligand-Dependent EFR Endocytosis is a Determinant of Long-Term Cellular Responsiveness to EF-Tu and is Regulated by Tyrosine Phosphorylation (PAPER2)</b>	.....	88
1.	Abstract.....	88

2. Introduction .....	89
3. Results .....	90
3.1 Y875 and Y877 are Required for Ligand-Induced EFR Endocytosis and Degradation	90
3.2 Y875- or Y877-Mediated Internalization of EFR is Uncoupled from elf-Triggered Immune Signalling .....	92
3.3 Y-Mediated EFR Endocytosis is Required to Maintain elf18 Responsiveness.....	99
4. Discussion.....	101
5. Materials and Methods .....	105
<b>Chapter 4: General Discussion and Outlook .....</b>	<b>111</b>
<b>References .....</b>	<b>115</b>

## List of Tables

<b>2.2 Table 1.</b> Overview of identified FLS2 interacting proteins.....	52
<b>2.2 Table 2.</b> Summary of identified candidate <i>in vivo</i> FLS2 ubiquitination sites by LC-MS/MS Analysis.....	56
<b>Table 1.</b> List of primers used in the thesis.....	110

## List of Figures

<b>1.2 Figure 1.</b> Schematic overview of pattern recognition receptor (PRR) subcellular trafficking, including localizations at various endomembrane compartments and potential regulators.....	23
<b>2.1 Figure 1.</b> FLS2 is present at ESCRT-I-positive compartments and forms an inducible complex with VPS37-1.....	47
<b>2.2 Figure 1.</b> KEG regulates flg22-induced FLS2 trafficking and degradation.....	54
<b>2.2 Figure 2.</b> Schematic representation of the FLS2 showing the location of the candidate ubiquitinated Ks.....	56
<b>2.2 Figure 3.</b> FLS2 <sup>K1120A</sup> -GFP exhibits altered flg22-induced receptor-mediated trafficking.....	58
<b>2.3 Figure 1.</b> Flg22 induces monoubiquitination of FLS2 in vivo in a PUB12/PUB13-dependent manner.....	66
<b>2.3 Figure 1 —figure supplement 1.</b> FLS2 is not targeted by K63 and K48 polyubiquitin chains.....	67
<b>2.3 Figure 2.</b> PUB12 and PUB13 translocate from the cytosol to intracellular vesicles upon flg22 stimuli.....	68
<b>2.3 Figure 3.</b> PUB12 and PUB13 are required for FLS2 endocytosis.....	69

<b>2.3 Figure 4.</b> PUB12 and PUB13 are required for flg22 uptake.....	70
<b>2.3 Figure 4 —figure supplement 1.</b> <i>Pub12</i> and <i>pub13</i> single mutants are delayed in TAMRA-flg22 internalization.....	70
<b>2.3 Figure 5.</b> FLS2 endocytosis is uncoupled from PTI signalling.....	73
<b>2.3 Figure 5—figure supplement 1.</b> Light intensity has an impact on flg22-induced MAPK activation and FLS2 accumulation.....	74
<b>2.3 Figure 5—figure supplement 2.</b> <i>Pub12 pub13</i> adult plants show enhanced resistance to bacteria but similar flg22- and elf18-induced resistance as WT.....	75
<b>2.3 Figure 6.</b> Ligand-dependent endocytosis and degradation of FLS2 is required for maintaining a signalling competent pool of FLS2.....	77
<b>2.3 Figure 6—figure supplement 1.</b> Flg22-induced resistance is lost in <i>pub12 pub13</i> plants repeatedly sprayed with the PAMP.....	78
<b>2.3 Figure 7.</b> Model of regulation of FLS2 endocytosis by dynamic ubiquitination and its requirement for immunity after repeated PAMP stimulation.....	79
<b>3 Figure1.</b> Mutational screen identifies Y residues in EFR cytoplasmic domain required for elf18-induced endocytosis.....	91
<b>3 Figure1—figure supplement 1.</b> Mutation of most Y residues in the EFR cytoplasmic domain did not affect ligand-induced endocytosis.....	92

<b>3 Figure 2.</b> Y875 and Y877 are not required for the formation of signalling-competent receptor complexes.....	94
<b>3 Figure2—figure supplement 1.</b> Detection of in vivo phosphorylation of EFR Y875 and Y877 by LC-MS/MS.....	95
<b>3 Figure2—figure supplement 2.</b> Y875 and Y877 are required for ligand-mediated degradation of EFR.....	96
<b>3 Figure 3.</b> Mutation of EFR Y875 or Y877 does not compromise elf18-triggered PTI responses.....	97
<b>3 Figure 3—figure supplement 1.</b> Elf18-triggered responses are not affected by mutation of Y875 and Y877.....	98
<b>3 Figure 4.</b> Ligand-dependent endocytosis is required for maintaining a signalling competent pool of EFR.....	100
<b>3 Figure4—figure supplement 1.</b> Elf18- but not flg22-induced resistance is lost in EFR <sup>Y875F</sup> -EFR <sup>Y875F</sup> -expressing plants repeatedly sprayed with elf18.....	101
<b>3 Figure 5.</b> Schematic overview of EFR subcellular trafficking regulation.....	105

**Note: In this thesis I used “we” as a writing style. However, unless mentioned otherwise in the text, all of the results were produced from my own work.**

## **List of Publications Arising From the Work in This Thesis**

### **Chapter 1.2**

Ben Khaled S., Postma J. and Robatzek S. A Moving View: Subcellular Trafficking Processes in Pattern Recognition Receptor–Triggered Plant Immunity. *Ann. Rev. Phytopathol.* 2015

### **Chapter 2.1**

Spallek T., Beck M., Ben Khaled S., Salomon S., Bourdais G., Schellmann S. and Robatzek S. ESCRT-I Mediates FLS2 Endosomal Sorting and Plant Immunity. *Plos Genetics* 2013

### **Chapter 2.3**

Ben Khaled S., Rybak K., Hawecker H. and Robatzek S. Ubiquitin-Mediated FLS2 Endocytosis is Required for Maintaining Responsiveness to Bacterial Flagellin. *Elife*, in preparation.

### **Chapter 3**

Ben Khaled S., Macho A., Couto D., Kopischke M., Sklenar J., Derbyshire P., Hawecker H., Siwoszek A., Menke F., Zipfel C. and Robatzek S. Ligand-Dependent EFR Endocytosis is a Determinant of Long-Term Cellular Responsiveness to EF-Tu and is regulated by Tyrosine Phosphorylation. *Cell Host & Microbe*, in preparation.

## Acknowledgements

I would like to express my sincere gratitude to my PhD supervisor Silke Robatzek for giving me the opportunity to work as part of her team and the freedom to develop my ideas. Thank you for all your support, help and faith in me.

I would like to thank the members of my supervisory team Sophien Kamoun and Brande Wolf for their guidance, support and all the inspiring discussions that we had throughout these years.

A big thank you to the people who helped me scientifically and personally during the past four years. In particular, Alberto Macho and Rosa Lozano-Duran, I wouldn't have made it without you!

Thank you to all SR lab members for the good spirit and the great atmosphere in the lab, and for pulling up with my strong opinions.

Thank you to the TSL support teams for making our work go so smoothly.

Thank you to my friends: Cyrine, Zied, Jan, Seb, Andy, Will, Christoph, Michaela, Martin, Kasia, Aga, Jelle, Hannah... for all the moments we enjoyed together.

Thank you Papi for being my sunshine.

Finally, I owe my deepest gratitude to my parents and sister for making me who I am, for giving me strength in moments of doubt, for always believing in me and loving me unconditionally.

## Abbreviations

ABC	ATP binding cassette
ABI5	Abscisic acid insensitive 5
ACD6	Accelerated cell death 6
ANK	Ankyrin
APM1	Associated protease M1
ARF	ADP ribosylation factor
At	<i>Arabidopsis thaliana</i>
AUX1	Auxin resistant 1
BAK1	BRI1-associated kinase 1
BFA	Brefeldin A
BIK1	Botrytis-induced kinase 1
BIR	BAK1-interacting RLK
BOR1	Boron transporter 1
BRI1	Brassinosteroid insensitive 1
CCV	Clathrin-coated vesicle
CDPK	Calcium-dependent protein kinase
CEBIP	Chitin elicitor-binding protein
CERK1	Chitin elicitor receptor kinase 1
CHC	Clathrin heavy chain
CHMP	Charged multivesicular body protein
CLC	Clathrin light chain
CME	Clathrin-mediated endocytosis
Col0	<i>Columbia 0</i>
ConcA	Concanamycin A
DAMP	Damage-associated molecular pattern
DN	Dominant negative
DRP	Dynamin-related protein

DUB	Deubiquitinating enzyme
E	Enzyme
EE	Early endosome
EFR	EF-Tu receptor
EF-Tu	Elongation factor Tu
EGF	Epidermal growth factor
EGFR	EGF receptor
EHM	Extra-haustorial membrane
EIX	Ethylene-inducing xynalase
ER	Endoplasmic reticulum
ERQC	ER quality control
ESCRT	Endosomal complex required for transport
ETI	Effector-triggered immunity
ETS	Effector-triggered susceptibility
EV	Empty vector
FLS2	Flagellin-sensing 2
GEF	Guanine exchange factor
GFP	Green fluorescent protein
GSL	Glucan synthase-like
HR	Hypersensitive response
HRP	Hypersensitive response and pathogenicity
ICD	INF1-triggered cell death
ILV	Intraluminal vesicle
K	Lysine
KAK	KAKTUS
KEG	Keep on going
LC-MS/MS	Liquid chromatography-tandem mass spectrometry
LE	Late endosome
LORE	Lipooligosaccharide -specific reduced elicitation

LPS	Lipopolysaccharide
LRR	Leucine-rich repeat
LysM	Lysine motif
MAPK	Mitogen-associated protein kinase
MVB	Multivesicular body
Nb	<i>Nicotiana benthamiana</i>
NB-LRR	Nucleotide binding-leucine rich repeat
Os	<i>Oryza sativa</i>
P.	<i>Phytophthora</i>
Pto	<i>Pseudomonas syringae</i> pv. tomato
PAMP	Pathogen-associated molecular pattern
PEN	Penetration resistance
PEPR	Pep receptor
PIN1	Pinformed 1
PM	Plasma membrane
PR1	Pathogenesis-related 1
PRA1	Prenylated RAB acceptor 1
PRR	Pattern recognition receptor
PTI	PAMP-triggered immunity
PTM	Post-translational modification
PUB	Plant U-box
Pv.	Pathovar
R	Resistance
RBOH	Respiratory burst oxidase homolog
RFP	Red fluorescent protein
RLK	Receptor-like kinase
RLP	Receptor-like protein
ROI	Region of interest
ROS	Reactive oxygen species

RTLNB	Reticulon-like proteins group B
RV	Recycling vesicle
SA	Salicylic acid
SCD1	Stomatal cytokinesis-defective 1
SE	Standard error
SERK	Somatic embryogenesis related kinase
SGI	Seedling growth inhibition
SID2	SA induction deficient 2
SKD1	Suppressor of K <sup>+</sup> transport growth defect 1
SI	<i>Solanum lycopersicum</i>
SOBIR1	Suppressor of BIR1
SV	Secretory vesicle
TGN	<i>Trans</i> -Golgi network
TLR	Toll-like receptor
TTSS	Type three secretion system
Ub	Ubiquitin
UPL3	Ubiquitin protein ligase 3
VIGS	Virus-induced gene silencing
VPS	Vacuolar protein sorting
Wm	Wortmannin
WT	Wild type
Xoo	<i>Xanthomonas oryzae</i> pv. <i>oryzae</i>
Y	Tyrosine

# Chapter 1: General Introduction

## 1. General Concepts of Plant Innate Immunity

Plant perception of phytopathogens establishes a molecular dialogue between the two protagonists leading to the activation of immune signalling. An effective immune response enables the host to arrest microbial threats, while maintaining a tolerance threshold to avoid autoimmune diseases and allow cell growth and expansion of the host.

### 1.1 Co-evolution of Plants and Pathogens

Interactions between plants and pathogens are often compared to an evolutionary arms race, whereby each organism evolves molecular weapons to defeat its contender (Boller and He, 2009). The over time evolution of the host and invader proteins, as well as the outcome of these evolutionary events on plant resistance and microbial pathogenicity, are represented by Jones and Dangl (2006). Plants sense pathogen-associated molecular patterns (PAMPs), epitopes within molecules fundamental to pathogen fitness and widely distributed across whole classes of microbes (Akira et al., 2006). This recognition is mediated by surface-localized pattern recognition receptors (PRRs), and ultimately leads to the establishment of PAMP-triggered immunity (PTI). Thriving pathogens evolve to overcome this level of resistance by acquiring virulence factors, referred to as effectors, which disrupt PTI to promote successful infection. This results in effector-triggered susceptibility (ETS), and the pathogen involved is considered virulent. In turn, plants evolve so-called resistance (R) proteins, typically these are cytosolic nucleotide binding-leucine rich repeat (NB-LRR) proteins but can also include cell surface-localized PRRs. Both types of receptors recognize directly or indirectly effectors, inducing the second layer plant resistance referred to as effector-triggered immunity (ETI). This resistance is frequently associated with the development of a rapid and localized cell death, the hypersensitive response (HR), and the pathogen in this case is avirulent. These ongoing co-evolutionary events continuously promote the selection of new effectors to avoid and suppress recognition of the

pathogen, and new alleles of R genes to confer the recognition of these new effectors by the plant (Jones and Dangl, 2006).

## 1.2 Perception of PAMPs

Host cells perceive different types of molecules derived from potentially pathogenic microbes, and modified host components arising from pathogen attacks. In animals, Toll-like receptors (TLRs) recognize distinct PAMPs, and play critical roles in innate immune responses. For instance, TLR5 binds flagellin, a major component of the bacterial motility organ (Macnab, 2003, Smith et al., 2003). In *Arabidopsis*, flagellin perception is mediated by the receptor-like kinase (RLK) flagellin-sensing 2 (FLS2), the functional homologue of TLR5 in plants (Gomez-Gomez and Boller, 2000). Other than sharing common features in their extracellular domains, no notable amino acid similarity indicates an evolutionary relationship between FLS2 and TLR5 (Smith et al., 2003). In fact, these two receptors recognize structurally different sites of flagellin (Felix et al., 1999). Thus, plants and animals seem to have independently evolved leucine-rich repeat receptors (LRRs) to sense bacterial flagellin and activate host defence mechanisms.

*Arabidopsis thaliana* recognizes flagellin through a 22 amino acid conserved epitope at its N-terminal region, called flg22 (Felix et al., 1999, Gomez-Gomez and Boller, 2000, Gomez-Gomez et al., 1999). Binding to flg22 induces the interaction between FLS2 and brassinosteroid insensitive 1 (BRI1)-associated kinase 1 (BAK1), a member of the somatic embryogenesis receptor kinase (SERK) family. This interaction facilitates the flg22-induced activation of the receptor complex to trigger PTI (Chinchilla et al., 2006, Chinchilla et al., 2007, Schulze et al., 2010, Schwessinger et al., 2011). PTI is a multi-layered defence and can be divided into early and late events with different branches and hierarchies (Boller and Felix, 2009, Boudsocq et al., 2010, Segonzac et al., 2011) and at different spatial scales. Early events are typically induced within 5 min and decrease within a time frame of 30 min. They include apoplastic alkalinization, a reactive oxygen species (ROS) burst, an intracellular calcium burst, and phosphorylation of mitogen-activated protein kinases (MAPKs) and calcium-dependent protein kinases (CDPKs) (Asai et al., 2002, Boller and Felix, 2009, Romeis et al., 2001). Late events are typically induced within several

hours to days and include the upregulation of defence genes such as pathogenesis-related 1 (PR1), the production of salicylic acid (SA), the accumulation of callose, and ultimately the inhibition of growth (Boller and Felix, 2009, Couto and Zipfel, 2016). Although generally not associated with PTI, in some cases, late flg22-induced events can also result in the development of programmed cell death (Hann and Rathjen, 2007). Intermediate events include the upregulation of a large number of defence genes, the production of ethylene, cellular responses such as the closure of stomata and plasmodesmata, and the remodelling of the actin cytoskeleton (Boller and Felix, 2009, Faulkner et al., 2013, Henty-Ridilla et al., 2013, Melotto et al., 2006). Yet, it is not fully understood how these events are all positively and negatively regulated and to what extent the different defence responses contribute to the establishment of PTI.

The collection of PRRs involved in plant-microbe recognition has grown considerably over the past decade. In addition to FLS2, well studied examples of such PRRs in plants are the *Arabidopsis thaliana* EF-Tu receptor (EFR) and the rice *Xanthomonas oryzae* pv. *oryzae* (*Xoo*) resistance protein OsXa21, both RLKs with significant roles in defence against bacterial infections (Song et al., 1995, Zipfel et al., 2006). EFR recognizes a conserved peptide in bacterial EF-Tu (or its eliciting epitope elf18), whereas OsXa21 detects RaxX, a protein secreted by *Xoo* (Pruitt et al., 2015, Song et al., 1995, Zipfel et al., 2006). The tomato receptor-like proteins (RLPs) ethylene-inducing xylanase 1 and 2 (Eix1 and Eix 2) and members of the Cf family confer immunity against different infectious fungi: Eix1 and Eix2 detect xylanase from *Trichoderma viride*, and the Cf receptors sense specific apoplastic effectors secreted by *Cladosporium fulvum* (de Jonge et al., 2012, Kaku et al., 2006, Miya et al., 2007). For example, *C. fulvum* secretes the Avr4 effector into the apoplast to bind chitin, thus preventing its host-induced enzymatic breakdown and possibly subsequent recognition by PRRs. However, Avr4 itself is detected by Cf-4, a PRR present in resistant tomato, which triggers HR (Thomas et al., 1997).

Additional PRRs include the *Brassicaceae*-specific receptor for enigmatic MAMP of *Xanthomonas* (ReMAX) which, as its name indicates, recognizes a currently unknown ligand from *Xanthomonas* (Jehle et al., 2013), and the lysine motif (LysM) RLK chitin elicitor receptor kinase 1 (CERK1),

involved in detection of fungal chitin (Miya et al., 2007). Chitin-induced immune signalling in *Arabidopsis* require two additional LysM-RLKs, LYK4 and LYK5 (Cao et al., 2014, Wan et al., 2012). The *AtCERK1* homologue in rice, *OsCERK1* has no chitin oligosaccharide binding activity, although it is essential for chitin-induced signalling (Shimizu et al., 2010). *OsCERK1* acts cooperatively with the chitin oligosaccharide elicitor binding protein (*OsCEBiP*) (Shimizu et al., 2010). The LysM motif is also involved in peptidoglycan (PGN) binding. This is mediated by the LysM-domain proteins (LYM) 1 and LYM3 in *Arabidopsis* (Willmann et al., 2011), and LYP4 and LYP5 in rice, all of which found in complex with CERK1 (Gust, 2015).

Recently, the PRR lipooligosaccharide-specific reduced elicitation (LORE) has been associated with plant recognition of lipopolysaccharides (LPS) from *Pseudomonas* and *Xanthomonas* bacteria, and the subsequent induction of immune signalling (Ranf et al., 2015). LORE-mediated perception of LPS is restricted to the *Brassicaceae* family of plants, although direct binding activity has not been demonstrated so far (Ranf et al., 2015).

Detection of modified host components, also referred to as damage-associated molecular patterns (DAMPs), may equally induce defence pathways or serve as amplification loops of immune responses (Boller and Felix, 2009, Boller and He, 2009). DAMPs are frequently found in the apoplast and can be cell wall fragments or monomers of cutin. In addition, secreted peptides resulting from wounding or PAMP perception act as DAMPs. For instance, the *Arabidopsis* 23-amino acid peptide Pep1, secreted upon activation of FLS2 and EFR pathways, is perceived by the PEPR1/PEPR2 RLK pair to triggers PTI (Yamaguchi et al., 2006).

Though PTI is a very robust and effective immune response against most invaders, some adapted pathogens can overcome this form of resistance by evolving effector proteins.

### 1.3 Effectors of Pathogenic Bacteria

Adapted pathogens evolved effector proteins to overcome recognition by their hosts, often through targeting different branches of the PTI signalling pathway. To deliver these effectors, pathogenic bacteria use secretion systems, of which the type three secretion system (TTSS) is the most widely distributed among phytopathogenic bacteria (Buttner and Bonas, 2002, He et al., 2004). The TTSS is a multiprotein complex assembled as a transmembrane syringe-like structure, allowing the secretion of type three effectors directly inside the host cell (Costa et al., 2015). Proteins of this complex are encoded by genes grouped into a cluster in the genome of the bacterium called *hrp* (for hypersensitive response and pathogenicity). Accordingly, mutants lacking this cluster are no longer able to trigger HR in resistant plants or to induce disease in hosts otherwise sensitive to the wild-type strain (Alfano and Collmer, 2003, Collmer, 1998).

The biochemical activity of bacterial effectors has been extensively studied over the past decade and can include: cysteine protease, ubiquitin-like protease, E3 ubiquitin ligase, and protein phosphatase (Abramovitch et al., 2006). For example, the *Pseudomonas syringae* pv. *tomato* DC3000 (*Pto* DC3000) type three effector AvrPtoB, carries an E3 ligase domain in its C-terminus (Janjusevic et al., 2006). AvrPtoB interacts directly with PRRs such as FLS2 in vivo (Shan et al., 2008, Gimenez-Ibanez et al., 2009), leading to the E3 ligase-dependent degradation of FLS2 (Gohre et al., 2008). Other *Pseudomonas syringae* effectors that target PRRs complexes include AvrPto, which binds to FLS2 and EFR to suppress immune responses, and the tyrosine phosphatase HopAO1, which targets the tyrosine phosphorylation of PRRs, such as EFR, inhibiting their ligand-induced activation and downstream immune signalling (Macho et al., 2014). Nonetheless, most effectors have no sequence similarity to any known proteins and their mode of virulence remains elusive.

Other pathogens such as oomycetes and fungi also secrete effectors, although this will not be covered in this introduction.

## **2. A Moving View: Subcellular Trafficking Processes in PRR– Triggered Plant Immunity; From (Ben Khaled et al., 2015)**

In addition to communicating the presence of a non-self-organism and its nature, the plant immune system engages the subcellular trafficking pathways. A role of both secretory and endocytic trafficking in defence against different pathogens is suggested by the transcriptional and posttranslational changes of many trafficking regulators upon elicitation with PAMPs and apoplastic effectors. The following section addresses the links between subcellular trafficking and plant immunity with a focus on PRRs as transported cargos.

### **2.1 An Overview of the Plant Endomembrane Compartments**

The plant endomembrane system is involved in the synthesis, uptake, sorting, and degradation of cargo molecules. It consists of an inter-related membrane system including the nuclear envelope, the endoplasmic reticulum (ER), the Golgi apparatus (consisting of *cis* and *trans* cisternae) and *trans*-Golgi network (TGN), endosomes, the tonoplast around the vacuole, and the plasma membrane (PM) enveloping the cell. Several endocytic pathways have been characterised in eukaryotic cells, of which clathrin-mediated endocytosis (CME) is the most prevalent and the best characterised so far. In CME, three classes of intracellular vesicles can be distinguished: clathrin-coated vesicles (CCVs), *trans*-Golgi network that in plants also functions as early endosome (EE), late endosomes that mature into multivesicular bodies (LEs/MVBs).

#### **Clathrin-Coated Vesicles**

In eukaryotes, PM proteins and their respective ligands can be internalized into endosomes via CCVs (1.2 Figure 1). CCV formation proceeds through five stages: initiation, cargo recruitment, coat assembly, scission and uncoating (McMahon and Boucrot, 2011). Clathrin coats are composed of a three-legged molecule, called the triskelion, in which each leg consists of a clathrin heavy chain (CHC) and a clathrin light chain (CLC) (Fotin et al., 2004). The *Arabidopsis* genome contains two genes encoding CHC and three encoding CLC (Fujimoto et al., 2010). In plant cells,

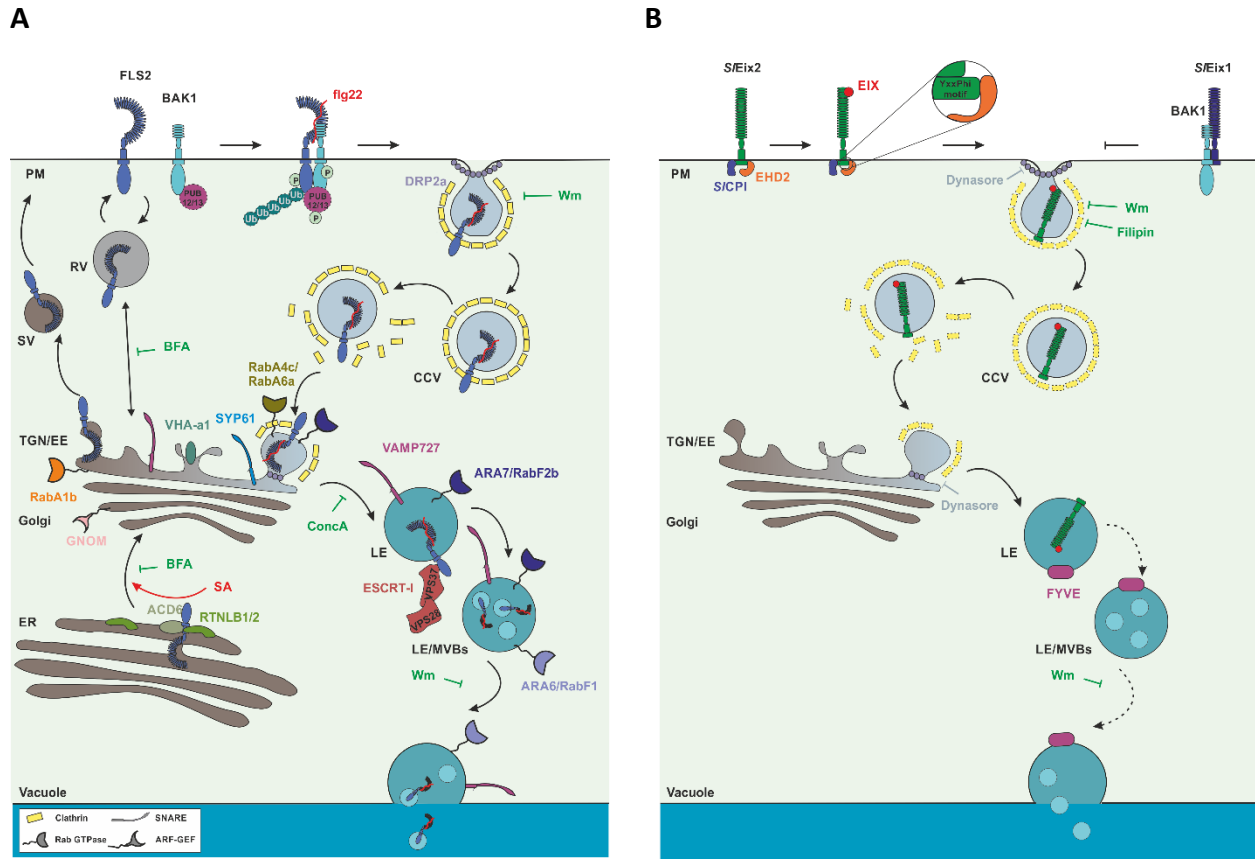
clathrin was predominantly localized to TGN and for a minor part to the PM and LE/MVBs (Ito et al., 2012).

### **Trans-Golgi Network/ Early Endosomes**

The first compartment to which a newly formed endocytic vesicle delivers its cargo is defined as the early endosome (Bolte et al., 2004). To the contrary of animal cells, the plant TGN takes on the function of an EE, rather than existing as a separate organelle (Lama et al., 2007) (1.2 Figure 1). The TGN derives from a maturation process of the *trans*-most Golgi cisterna of the Golgi stack, and cycles between a Golgi-associated and a Golgi-free status (Scheuring and Robinson, 2007). The Golgi-free state is temporary and eventually leads to the release of secretory vesicles and CCVs. The remaining membranes are likely to be involved in the formation of LEs (Kang et al., 2011). The TGN-derived CCVs were suggested to be vehicles for cargo recycling to the PM, although this has not been experimentally proven in plant cells (Robinson and Pimpl, 2014). Intriguingly, a recycling endosome (RE) in plants has not yet been characterized morphologically and could possibly consist of a subdomain of the TGN. Furthermore, an *Arabidopsis* mutant lacking a component required for TGN function was defective in secretory trafficking whereas endocytosis was unaltered, suggesting a separation of these two functions of the TGN (Gendrea et al., 2011). Therefore, the plant TGN constitutes a hub, with distinct subdomains specialized in secretion, recycling and internalization of proteins.

### **Late Endosomes/Multivesicular Bodies**

LE/MVBs are the sorting station in the endocytic route preceding vacuolar fusion (1.2 Figure 1). They are characterized by a multivesicular appearance, in which the external endosomal membrane buds inward the lumen to produce internal vesicles, also called intraluminal vesicles (ILVs), that become isolated from the cytoplasm (Raposo and Stoorvogel, 2013). This structure allows delivery of cargo molecules to the vacuole, through fusion of the MVB outer membrane with the tonoplast (Raposo and Stoorvogel, 2013, Reyes et al., 2011).



## 1.2 Figure 1

### Schematic overview of pattern recognition receptor (PRR) subcellular trafficking, including localizations at various endomembrane compartments and potential regulators.

Trafficking regulators that are associated with specific endomembrane compartments and used as marker proteins are indicated. Chemical interference of subcellular transport is accompanied by a drop symbol and is shown in green when validated in plants and in grey when not validated in plants.

(A) Known subcellular localizations of FLS2 at the endoplasmic reticulum (ER), the Golgi apparatus, the *trans*-Golgi network (TGN), the plasma membrane (PM), the late endosome (LE), and the multivesicular bodies (MVBs). Arrows indicate trafficking through the secretory pathways via secretory vesicles (SV), and endocytic pathways via recycling vesicles (RV), and clathrin-coated vesicles (CCV). Chemical inhibition by Brefeldin A (BFA), Concanamycin A (ConcA), and Wortmannin (Wm) is indicated at the different steps of subcellular transport. Dashed symbols for ubiquitination (Ub) and PUB12/PUB13 indicate potential involvement in endocytosis. (B) Known subcellular localizations of S/Eix2 at the PM and MVBs. Dashed symbols for clathrin relate to indirect evidence in S/Eix2 endocytosis. Abbreviations: ARF: ADP ribosylation factor, GEF: guanine nucleotide exchange factor.

## 2.2 Subcellular Trafficking in Plant Immunity

Intracellular protein trafficking is a fundamental and complex mechanism that is of particular importance during environmental challenges such as pathogen attack. Localization, abundance, and activity of essential components of the plant innate immune system are regulated by subcellular trafficking, both in preparation and during execution of defence.

### Delivery to the Cell Surface

Prominently, default secretory trafficking from the ER via the Golgi apparatus and TGN is important in plant immunity to charge the PM with PRRs and the extracellular space with defence compounds (1.2 Figure 1). These include peptides with antimicrobial activities, e.g., PR1, defensins, and thionins (Caaveiro et al., 1997, Carmona et al., 1993, Gaspar et al., 2014, Wang et al., 2005), as well as several proteases (Bozkurt et al., 2011). Plants also have the ability to direct their trafficking pathways to the location of pathogen attack. RabE1d, a member of the Rab8 GTPase-related RabE family implicated in secretory trafficking, localizes to Golgi and the PM, and locally accumulates in response to bacterial infection (Speth et al., 2009). Similarly, flg22 focuses the secretory trafficking of the penetration resistance 1 (PEN1) syntaxin (also known as SYP121) to mediate its local accumulation at the PM (Underwood and Somerville, 2013). PEN1 is differentially phosphorylated in response to flg22, although the functional significance of this modification is still unknown. In addition, transport processes independent of secretion confer microbe-induced PM focal accumulation of defence proteins, such as PEN3, an ATP binding cassette (ABC) transporter (Underwood and Somerville, 2013, Xin et al., 2013). Intriguingly, FLS2 but not BAK1 is required for flg22-induced PEN3 focal accumulation, thus the mechanisms to concentrate defence proteins at microbial contact sites remain to be understood.

Focal accumulation is one of the most significant transport processes of defence against filamentous pathogens (Underwood and Somerville, 2008). Perception of powdery mildew fungi induces the local delivery of PEN1, PEN3, and callose from MVBs (Meyer et al., 2009). In support

of a role for MVBs in this process, these organelles cluster around fungal penetration sites (An et al., 2006a, An et al., 2006b, Bohlenius et al., 2010). Exocytosis releases PEN1 and callose into the apoplast, where they accumulate at papillae underneath fungal hyphae (Meyer et al., 2009). Significantly, loss of PEN1 permits entry of powdery mildew fungi into non-host cells (Collins et al., 2003). This correlates with delayed callose deposition at fungal contact sites but does not depend on PEN1 itself (Asai et al., 2002). Focal accumulation of PEN1, and also callose, is delayed in plants with impaired function of GNOM (Nielsen et al., 2012), a TGN-associated ADP ribosylation factor (ARF)-guanine nucleotide exchange factor (GEF). This correlates with enhanced fungal entry rates, suggesting that GNOM-regulated post-Golgi trafficking is required for full penetration resistance.

### **Uptake from the Cell Surface**

Internalization and late endosomal sorting also contribute to plant immunity. Endocytosis is accomplished by the invagination of the PM and release of a CCV by scission through dynamins (1.2 Figure 1A). Mutants in genes coding for dynamin-related proteins (DRPs) are impaired in endocytic uptake (Collings et al., 2008). Growth of virulent and effector-disarmed *Pto* DC3000 is enhanced in *drp2b* mutants (Smith et al., 2014), suggesting that basal and PAMP-triggered immunity depend on endocytic trafficking from the PM. *Pto* DC3000 infection is similarly enhanced in mutants of two subunits of the endosomal complex required for transport-I (ESCRT-I), *vps28-2* and *vps37-1* (Spallek et al., 2013). The ESCRT-I to -III complex localizes at TGN/EE and LE/MVB compartments and recognizes internalized ubiquitinated proteins to sort them to the lumen of MVBs for vacuolar degradation (Scheuring et al., 2011). These ESCRT-I mutants show enhanced susceptibility to *Hyaloperonospora arabidopsis* (Lu et al., 2012). Thus, mis-sorting of late endosomal cargo compromises immunity against at least two types of pathogens, evidencing a broader role of late endocytic trafficking in defence.

## Effector Interference with Subcellular Trafficking

Plant subcellular trafficking processes are subject to interference by effectors secreted by pathogens, substantiating the significance of membrane trafficking in plant immunity. The AVRblb2 effector from *Phytophthora infestans* localizes at the extrahaustorial membrane (EHM), a plant-derived membrane that separates the haustorium of infectious filamentous microbes from the host cytoplasm (O'Connell and Panstruga, 2006). AVRblb2 targets the papain-like cysteine protease C14 to prevent its secretion into the apoplast, thereby promoting *P. infestans* virulence (Bozkurt et al., 2011). AVR3a, another *P. infestans*-secreted effector, associates with host DRPs to interfere with BAK1-dependent PAMP-triggered defence responses (Chaparro-Garcia et al., 2014).

Likewise, *Pto* DC3000 bacteria secrete HopM1, which localizes to the host TGN to interfere with post-Golgi trafficking mediated by the ARF-GEF family member BIG5, also known as MIN7 or BEN1 (Nomura et al., 2011, Richter et al., 2014, Tanaka et al., 2009). HopM1 degrades MIN7, which results in reduced callose deposition, and in turn enhanced bacterial virulence (Nomura et al., 2006). Interestingly, microbe-induced callose is mainly produced by glucan synthase-like 5 (GSL5, also known as PMR4), which is found at TGN compartments (Drakakaki et al., 2012). Recent work revealed several molecular regulators of plant subcellular transport as potential effector targets. These include components of CME, Rab GTPases and their regulators, and proteins associated with the cytoskeleton (Mukhtar et al., 2011, Wessling et al., 2014, Nomura et al., 2006, Nomura et al., 2011, Kang et al., 2014, Lee et al., 2012a, Bogdanove and Martin, 2000, Chaparro-Garcia et al., 2014, Schmidt et al., 2014). Pathogens thus translocate several effectors that interfere with secretory and endocytic trafficking to promote successful infection.

### 2.3 Subcellular Trafficking of PRRs

In addition to their presence at the PM to sense apoplastic microbes, PRRs distribution changes inside in a dynamic manner (Robatzek et al., 2006). This potentially influences PAMP recognition,

PRR abundance and defence activation. By using functional fluorescent PRR fusions combined with cell biology, genetic, molecular, biochemical, and chemical approaches, increasing knowledge is gained about the pathways and trafficking processes regulating the spatiotemporal dynamics of several plant PRRs.

## **Secretion**

Newly synthesized PRRs first localize to the ER, where they are processed and folded into their correct structures (1.2 Figure 1A). This requires the ER quality control (ERQC) machinery and N-glycosylation that, when impaired, cause the accumulation of EFR in this organelle (Farid et al., 2013, Haweker et al., 2010, Li et al., 2009, Lu et al., 2009, Nekrasov et al., 2009). Consequently, loss-of-function mutants in these ERQC components are insensitive to elf18 stimulus and show enhanced susceptibility to bacterial infection (Haweker et al., 2010). Notably, these ERQC mutants respond normally to flg22 (Haweker et al., 2010). This indicates that FLS2 and EFR rely on different subsets of the ERQC machinery.

PRRs carry a typical N-terminal signal peptide that directs them for export from the ER to enter the secretory pathway. For this, FLS2 associates with reticulon-like proteins group B (RTNLB) 1 and 2, ER-resident reticulons involved in ER tubule formation and vesicle trafficking (Lee et al., 2012b, Sparkes et al., 2010). When absent, ER-to-Golgi exit of FLS2 is impaired, resulting in the accumulation of the receptor in the ER (Lee et al., 2012b).

The ER is often in contact with endosomes, and this is thought to regulate vesicle trafficking (Raiborg et al., 2015, Rocha et al., 2009), fusion (van der Kant et al., 2013), and fission (Rowland et al., 2014). Recently, our understanding of the complexity of the ER function has expanded to orchestrating endosomal maturation and cargo trafficking, including signalling receptors, in space and time (Jongsma et al., 2016). In mammalian cells, this is mediated by the ER-localised E3 ligase Ring finger protein 26 (RNF26). RNF26 acts by attracting ubiquitin-binding domains (UBDs) of various vesicle membrane adaptors, which results in restraining the movement of the

cognate vesicles (early, recycling, and late endosomes/lysosomes) (Jongsma et al., 2016). Release of these vesicles from the perinuclear cloud towards the cell periphery is mediated by the catalytic opposition of the deubiquitinating enzyme (DUB) USP15 (Jongsma et al., 2016). It would be interesting to determine whether an RNF26 plant counterpart is also involved in similar functions, though our understanding of the regulation of plant PRR sorting to the PM is still at its early times (1.2 Figure 1A). A distinct member of the RabA/Rab11 GTPase family, RabA1b is involved in transport of FLS2 to the PM (Choi et al., 2013). Co-expression of dominant-negative (DN)-RabA1b and FLS2-GFP in *Nicotiana benthamiana* significantly reduces FLS2 PM localization, while FLS2 fluorescent signals appear in small vesicles. As DN-RabA1b expression causes morphological changes to SYP61-positive TGN compartments, this suggests that RabA1b is required for FLS2 transport from the TGN to the PM. This trafficking pathway appears to represent a default secretory route to the PM.

SA-induced secretory trafficking also seems to be engaged in PRR delivery to the PM. SA upregulates FLS2 expression and enhances the PM pool of both FLS2 and BAK1 (Tateda et al., 2014). This is dependent on accelerated cell death 6 (ACD6), a membrane-associated protein involved in positive feedback regulation with SA. ACD6 forms complexes with FLS2 and ER chaperones, possibly to facilitate the folding and delivery of FLS2 under SA-inducing conditions (Zhang et al., 2014).

### **PM Localization of PRRs**

Recent studies have indicated that PRRs are not only generally present at the PM (Beck et al., 2012a) but can be found at specific PM locations. For example, PRRs, including FLS2, are enriched at plasmodesmata, specific channels that traverse the cell wall and connect neighbouring cells (Faulkner et al., 2013). Plasmodesmata regulate the molecular flux in symplastic cell-to-cell communication to ensure cell-specific responses (Epel, 1994). The extent of cell-to-cell communication upon pathogen stimuli can be regulated through the activation of PRRs (Faulkner et al., 2013). Consistent with the presence of FLS2 at plasmodesmata, flg22 reduces the

molecular flux mediated by these cellular structures. Evidence suggests that the PM lining the plasmodesmata has characteristics typical of specialized PM microdomains (Tilsner et al., 2011). FLS2 has also been identified in detergent-resistant PM microdomains, and this localization was further enhanced upon flg22 stimulus (Keinath et al., 2010). Thus, a feature of PRR localization at the PM is the ability to associate with PM microdomains, which could reduce the lateral mobility of these receptors (Ali et al., 2007). This is supported by flg22-induced differential phosphorylation of remorins, which preferentially associate with PM microdomains (Jarsch et al., 2014). PM microdomains may enrich PRRs at specific locations to define sites of signal transduction, such as plasmodesmata, and to ensure specific entry to the endocytic trafficking route.

Colocalization studies and chemical interference revealed that FLS2 receptors constitutively recycle between the PM and endosomal compartments via an endocytic route sensitive to Brefeldin A (BFA) (Beck et al., 2012c). Delivery of FLS2 to BFA bodies is independent of flg22 stimulus and BAK1, and is not affected by binding of the antagonistic ligand flg22 delta2. This separates receptor complex activation from a constitutive endocytic recycling pathway of non-activated FLS2 (1.2 Figure 1A). The BFA sensitivity of this pathway suggests roles for the ARF-GEFs GNOM and BIG5/AtMIN7/BEN1 (Tanaka et al., 2009). The latter is degraded by the bacterial effector HopM1, which underlines that pathogens target BFA-sensitive trafficking (Nomura et al., 2006).

### **Ligand-Induced Endocytosis**

Upon flg22 stimulation, FLS2 translocates from the PM and transiently accumulates at internal mobile vesicles (Robatzek et al., 2006). Colocalization with FM4-64, a lipophilic probe tracing time-dependent endocytic uptake (Bolte et al., 2004), showed that activated FLS2 receptors localize to bona fide endosomes (Beck et al., 2012c). Activated FLS2 traffics along the late endosomal pathway in a BFA-insensitive manner. In contrast to the constitutive endocytic

recycling of FLS2, its flg22-induced endocytosis requires BAK1. Thus, FLS2 enters two distinct endocytic trafficking routes depending on its activation status (Beck et al., 2012c) (1.2 Figure 1A).

flg22-induced FLS2 endocytosis is transient, with a maximum number of FLS2-GFP endosomes approximately 1 h after elicitation of *Arabidopsis* leaves (Beck et al., 2012c, Robatzek et al., 2006) and approximately 2 h in *N. benthamiana* (Choi et al., 2013). Colocalization studies using defined endosomal compartment markers combined with chemical interference identified the endocytic route through which flg22-activated FLS2 receptors traffic: FLS2-GFP is mainly present at compartments labelled by ARA7/RabF2b and ARA6/RabF1, which are members of the Rab5 GTPase family predominantly present at TGN/EEs or LEs and LE/MVBs, respectively (Beck et al., 2012c). In agreement, most activated FLS2 receptors colocalize with ARA7/RabF2b and VAMP727 in *N. benthamiana* (Choi et al., 2013). Activated FLS2 thus appears to sequentially traffic through ARA7/RabF2b and ARA6/RabF1 compartments along the late endocytic route with a large proportion of the receptors in constant association with LE/MVB compartments (1.2 Figure 1A). Presence of activated FLS2 at TGN/EE compartments occurs to a much lesser extent. In *N. benthamiana*, only a third of FLS2-positive endosomes initially colocalizes with SYP61, a TGN-resident syntaxin, which then decreases over the time of flg22 elicitation (Choi et al., 2013). In addition, activated FLS2 does not colocalize but rather closely associate with VHAa1, one of three isoforms of a vacuolar-type H<sup>+</sup>-ATPase subunit specifically present at the TGN (Choi et al., 2013). Consistently, impairment of TGN to LE trafficking by Concanamycin A (ConcA), which inhibits VHA function (Huss et al., 2002), increases the number of flg22-activated FLS2 endosomes in *Arabidopsis* (Beck et al., 2012c). Thus, the half-life of activated FLS2 at the TGN is limited, suggesting active sorting to prevent the recycling of flg22-bound receptors to the PM.

### **Regulation of Ligand-Induced Endocytic Trafficking**

Identification of the trafficking machinery responsible for endosomal transport of PRRs is an area of active research. At the PM, flg22 induces the enrichment of FLS2 into detergent-resistant microdomains and the translocation into endosomes (Beck et al., 2012c, Choi et al., 2013, Keinath

et al., 2010). This raises the question of what mediates the internalization of activated receptors from the PM. Evidence exists that a significant proportion of FLS2 endosomes is generated via CME. Tyrphostin A23, a tyrosine kinase inhibitor known to affect clathrin adaptors (Dhonukshe et al., 2007), decreases flg22-induced FLS2 endosomal numbers in *Arabidopsis* (Beck et al., 2012c), and transient knockdown of clathrin heavy chain genes in *N. benthamiana* strongly reduced the number of FLS2 endosomes (Mbengue et al., 2016). Clathrin is potentially targeted by effectors (Mukhtar et al., 2011, Wessling et al., 2014), which could be to abolish the endocytosis of FLS2 and other immune-related cargos. Consistent with a role for clathrin-mediated endocytosis in trafficking of PRRs, recent work has implicated dynamin GTPases in this process (1.2 Figure 1a) (Chaparro-Garcia et al., 2014, Smith et al., 2014). In *Arabidopsis*, the closely related DRP2A and DRP2B represent typical dynamin GTPases that scissor and release clathrin coated vesicles (Fujimoto et al., 2010). Single *drp2b*, but not the related *drp2a* mutants, shows a 20% reduction in flg22-induced FLS2 endosomes (Smith et al., 2014). This is correlated with a smaller decrease of PM-localized FLS2 in *drp2b* mutants after flg22 elicitation (Smith et al., 2014), in agreement with a role of DRP2B at the PM (Fujimoto et al., 2008). However, as FLS2-GFP endosomes are still formed in *drp2b* mutants, it thus appears that this dynamin GTPase is only partially required for FLS2 internalization from the PM and at least another of the 16 DRP family members in *Arabidopsis* is likely to be involved (Huang et al., 2015). Although endocytosis of activated FLS2 is accomplished by clathrin and dynamin GTPases, the mechanisms underlying the recruitment of this machinery to the receptor are unclear. To this end, DRP2A and DRP2B are phosphorylated upon flg22 stimulus (Benschop et al., 2007), which could recruit and activate these dynamins to internalize FLS2. Interestingly, DRP2 is targeted by the *P. infestans* AVR3a effector, highlighting the role of dynamin GTPases in immunity-related subcellular trafficking. The finding that ligand-induced FLS2 at least transiently localizes to TGN compartments (Choi et al., 2013) raises the possibility that membrane trafficking regulators associated with this compartment are involved in FLS2 endocytosis (1.2 Figure 1A). DN-ARA7/RabF2b abolishes flg22-induced FLS2 endocytosis in *Arabidopsis* (Beck et al., 2012c). In addition, DN-RabA4c reduces the localization of activated FLS2 receptors at SYP61-positive TGN, whereas this is increased by DN-RabA6a in *N. benthamiana* (Choi et al., 2013). These results position one Rab5 and two Rab11

GTPase family members at distinct steps in the regulation of FLS2 trafficking to subcellular compartments. Rab GTPases switch between a GDP-bound inactive and a GTP-bound active conformation, which is catalysed by GDP/GEFs. Yet, a GEF has not been identified in PRR endocytosis. Stomatal cytokinesis-defective 1 (SCD1) is a vesicle trafficking protein with putative Rab GEF activity (McMichael et al., 2013) and associates with FLS2, although in an flg22-independent manner (Korasick et al., 2010). Additional experiments are needed to elucidate a role for SCD1 in FLS2 subcellular trafficking. Furthermore, several effectors seem to target Rab GTPases and their interactors, the prenylated RAB acceptor 1 (PRA1) proteins (Mukhtar et al., 2011, Wessling et al., 2014), which suggests that pathogens can interfere with host membrane trafficking at this regulatory level.

Transport of activated FLS2 from the PM into LE/MVBs is likely required to ultimately degrade flg22-activated receptors by delivery to the vacuole. In agreement, treatment with Wortmannin (Wm), which affects MVB-to-vacuole trafficking and impedes internalization from the plasma membrane (Emans et al., 2002, Wang et al., 2009), decreased FLS2-GFP endosomal numbers and enlarged these endosomes (Beck et al., 2012c). Using either prolonged Wm treatment or transient overexpression of ARA7/RabF2b, activated FLS2 was identified inside the lumen of MVBs (Spallek et al., 2013). Thus, flg22-induced FLS2 is transported to the lumen of MVBs destined for vacuolar degradation.

### **Links between PRR Degradation and Endocytosis**

Receptor-mediated endocytosis offers a pathway for vacuolar degradation of activated PRRs, but mechanisms pointing to proteasomal degradation have also been reported. FLS2 protein levels decrease upon flg22 stimulation, which is correlated with enhanced ubiquitination of FLS2 (Gohre et al., 2008, Lu et al., 2011a). Two plant U-box (PUB) E3 ubiquitin ligases, PUB12 and PUB13, are recruited to FLS2 receptors via BAK1, and phosphorylated to mediate ubiquitination of FLS2 (Lu et al., 2011a). Inhibition by MG132 and the ability of PUB12/PUB13 to ubiquitinate the FLS2 PEST-motif mutant variant provide evidence that ubiquitination triggers FLS2 for degradation by the

proteasome (Lu et al., 2011a). Nevertheless, the mechanisms by which the proteasome can degrade transmembrane proteins, like FLS2, are not understood. It is possible that this is assisted by membrane-localized proteases, for instance the membrane-associated protease M1 (APM1) (Peer et al., 2009). However, there are alternative explanations for the observed effects of MG132 inhibition and FLS2 PEST-motif mutation. Considering that activated FLS2 is internalized into the late endocytic pathway by ESCRT-mediated sorting, which requires ubiquitination for cargo recognition, it is equally conceivable that FLS2 ubiquitination by PUB12/PUB13 is required for vacuolar degradation of the receptor. This notion is supported by Wm inhibition of both flg22-induced FLS2 degradation and its endocytosis (Smith et al., 2014, Beck et al., 2012c).

A second group of U-box E3 ubiquitin ligases has been implicated in the regulation of FLS2-induced defences. PUB22, PUB23, and PUB24 negatively regulate the amplitude and duration of both early and late events elicited by flg22 (Trujillo et al., 2008). Although recent work reported a role for PUB22 in the degradation of Exo70B2, a subunit of the exocyst complex that tethers secretory vesicles (Stegmann et al., 2012), and no direct link between FLS2 and PUB22, PUB23, and PUB24 is known to date, some similarities between the *pub12 pub13* and *pub22 pub23 pub24* mutant phenotypes are noticeable. For example, their enhanced flg22-induced ROS production may suggest that FLS2 degradation could involve both groups of E3 ligases. However, it may be that PUB12/PUB13 trigger the degradation of PM-derived endosomal FLS2, whereas PUB22, PUB23, and PUB24 could have implications in the regulation of FLS2 secretion.

Ubiquitination of host targets is a prominent process utilized by pathogens to promote infection success (Spallek et al., 2009). The bacterial effector AvrPtoB has similarities to eukaryotic E3 ligases and when secreted into host cells is able to interact with and ubiquitinate plant targets, including FLS2 (Gohre et al., 2008, Rosebrock et al., 2007). A recent study that examined the interaction between beneficial bacteria and *Arabidopsis* suggests that Nod factors, normally required for *Rhizobium* symbiosis in legume plants, trigger the degradation of FLS2 to suppress flg22-induced defence responses (Liang et al., 2013). In both cases, MG132 counteracts AvrPtoB- and Nod factor-mediated FLS2 degradation, suggesting a role for proteasome activity (Liang et

al., 2013, Gohre et al., 2008). Nevertheless, it remains to be elucidated whether bacterial-mediated degradation of FLS2 involves its endocytosis.

### Links between PRR Responses and Subcellular Trafficking

The secretory pathways that deliver PRRs to the PM contribute to plant immunity. Indeed, the *rtnlb1 rtnlb2* mutants affected in ER exit are generally reduced in all flg22- and elf18-induced defences and consequently show enhanced susceptibility to bacterial infection (Lee et al., 2011). The contribution of endocytic pathways to immunity is, however, less clear, as PRRs primarily initiate defence signalling from the PM. Nevertheless, the finding that PM-resident PRRs relocalize to the endocytic route in an activation-specific manner has prompted studies to identify the significance of this pathway for plant immunity. The most notable feature of flg22-induced events and FLS2 endocytosis is their transient patterns. The early flg22-induced alkalinization and calcium and ROS bursts typically appear within 5 min of stimulation, reach their maxima at approximately 20 min, and decrease within 1 h to unstimulated levels (Boller and Felix, 2009). Activation of MAPKs occurs within 5 min, peaks at approximately 15 min, and decreases within 30 min of flg22 treatment. By contrast, robust endocytosis of activated FLS2 is detected within 30 min, is maximal at approximately 1 h, and decreases at around 2 h in flg22-treated leaves (Beck et al., 2012c). Although a comparison of different experimental systems is limited, overall these time-dependent differences suggest that flg22-induced endocytosis of FLS2 is unlikely to be involved in the activation of early defence events. In agreement, *drp2b* and *vps37-1* mutants have normal induction kinetics of early flg22-induced defences and MAPK activation (Smith et al., 2014, Spallek et al., 2013). This provides some evidence that FLS2 initiate signalling from the PM similar to BRI1 (Irani et al., 2012), but the fact that endocytosis is only partially impaired in *drp2b* and *vps37-1* could be sufficient for full induction of defence responses. However, *drp2b* and *pub12 pub13*, but not *vps37-1*, mutants enhance the ROS burst triggered by flg22 (Smith et al., 2014, Spallek et al., 2013, Lu et al., 2011b). Thus, the inability to efficiently remove activated FLS2 receptors from the PM could affect the amplitude and duration of flg22-induced defences. Differences between the *drp2b* and *vps37-1* mutant phenotypes could reflect

the distinct levels at which induced FLS2 endocytosis is impaired. It is important to note that the ROS producing NADPH oxidase RBOHD is regulated by endocytosis (Hao et al., 2014), which could be affected in *drp2b* mutants, and that the elevated SA levels in *pub13* mutants could potentiate the flg22-induced responses (Li et al., 2012).

The effect of chemical interference is a stronger, more robust inhibition of activated FLS2 removal, as it's the case of Wm and the protein phosphatase inhibitor Cantharidin (Smith et al., 2014, Beck et al., 2012c, Serrano et al., 2007). Wm appears to reduce the flg22-triggered ROS burst (Smith et al., 2014). By contrast, Cantharidin not only significantly enhances and prolongs the flg22-induced ROS burst but also inhibits its decrease (Serrano et al., 2007). It is however unclear to what extent these positive and negative regulations are linked with FLS2 endocytosis, as Wm could impact RBOHD localization, and Cantharidin is also known to interact with membrane lipids (Becsi et al., 2014, Honkanen, 1993). In addition, these studies suggest that the flg22-induced early events seem to be separated from activated PRR endocytosis.

FLS2 plays a prominent role in defence against *Pto* DC3000 bacterial infection at the level of stomatal immunity (Zeng and He, 2010). Robust flg22-induced stomatal closure requires late endosomal sorting by VPS37-1 (Spallek et al., 2013). The stomata of *vps37-1* mutants close normally in response to abscisic acid, suggesting that ESCRT-I subunits are specifically regulating stomatal immunity, yet the exact molecular mechanism is not understood.

### **Subcellular Transport of Other PRRs**

Localization along the secretory-endosomal trafficking routes has been reported for a range of RLK- and RLP-type PRRs. EFR and PEPR1 and 2, were demonstrated to undergo internalization in a ligand-specific manner (Mbengue et al., 2016). Upon elicitation, FLS2, EFR and PEPR1/2 converge to the same endosomal population (Mbengue et al., 2016). This demonstrates a common endocytic route for the transport of activated PRRs inside the plant cell. Recent works revealed that the PM-localized *S/Cf-4* enters the late endocytic route when activated with Avr4

(Postma et al., 2016). This is in agreement with the localization patterns of suppressor of BIR1-1/EVERSHERD (SOBIR1/EVR), an RLK that constitutively associates with *S/Cf-4* and other RLPs (Liebrand et al., 2013). SOBIR1 interacts with ERQC components, indicating presence at the ER, and localizes to the PM and endosomal vesicles (Leslie et al., 2010, Sun et al., 2014).

*OsXa21* is also present at the PM and vesicles that exhibit features of SCAMP1-positive compartments, suggesting endosomal localization (Chen et al., 2010). As *OsXa21* localization is sensitive to BFA, the receptor recycles via endocytosis. Similarly, the tomato ethylene-inducing xylanase 2 (*S/Eix2*) resides at the PM, and after activation with xylanase, shows increased localization at FYVE-positive endosomes (1.2 Figure 1B). This correlates with an enhanced velocity and directional movement of these FYVE-positive endosomes in *N. benthamiana* (Sharfman et al., 2011, Bar and Avni, 2009a). In agreement, interference of late endosomal trafficking by Wm and disruption of the actin cytoskeleton reduces *S/Eix2* endocytosis (Bar and Avni, 2009a). EPS15 homology domain 2 (EHD2) has been implicated in decreasing the bundling of actin filaments and impairs endocytosis of *S/Eix2* upon overexpression (Bar et al., 2009). This is correlated with a reduction in xylanase-triggered HR, ethylene production, and PR1 gene expression, and is consistent with reduced xylanase-induced HR upon chemical disruption of actin (Bar and Avni, 2009a). Because endosidin 1, a chemical inhibitor of endocytosis also known to stabilize actin (Toth et al., 2012), enhances xylanase-induced ROS production (Sharfman et al., 2011), the mechanism by which EHD2 reduces *S/Eix2* endocytosis and xylanase-induced defence responses could be related to its role in actin remodelling.

Interestingly, although actin is required for endocytosis of activated FLS2 (Beck et al., 2012c), EHD2 does not seem to affect flg22-induced PR1 gene expression (Sharfman et al., 2011) but can interfere with *S/Cf-4*- and *S/Cf-9*-mediated HR (Bar and Avni, 2009b). However, whether EHD2 also has the ability to inhibit *S/Cf-4*, and not FLS2, endocytosis remains to be addressed. This could be related to EHD2 associating with RLPs but not RLKs, as there is evidence that EHD2 interacts with *S/Eix2* through its coiled-coil domain (Bar and Avni, 2009a, Bar et al., 2009). Recent works suggest a role for sterols in *S/Eix2* endocytosis. Overexpression of tomato cyclopropyl isomerase

(*S/CPI*), an enzyme involved in sterol biosynthesis, accelerates the appearance of *S/Eix2* endosomes, whereas silencing its *N. benthamiana* homolog leads to a reduction (Sharfman et al., 2014). Furthermore, filipin, which binds to sterols (Grebe et al., 2003), negatively affects *S/Eix2* endocytosis. This is correlated with altered *S/Eix2* defences, as *S/CPI* overexpression enhances xylanase-induced HR and ethylene production, and filipin reduces ROS production and cell death triggered by xylanase. The effects of *S/CPI* overexpression and silencing on sterol contents as well as the significance of the interaction between *S/Eix2* and *S/CPI* is not understood, although this could point at a role for sterol-enriched PM microdomains in *S/Eix2* endocytosis.

Likewise, only indirect evidence exists for the involvement of clathrin and dynamin GTPases in *S/Eix2* endocytosis. First, a dominant negative variant of clathrin (DN-HUB) reduces xylanase-triggered cell death (Sharfman et al., 2011), and second, *S/Eix2* carries a canonical tyrosine-based Yxx $\phi$  endocytic motif associated with CME in animals (Ohno et al., 1996) that when mutated, abolishes its endocytosis and xylanase-induced HR (Ron and Avni, 2004). Whether the *S/Eix2* Yxx $\phi$  motif (where  $\phi$  is a bulky hydrophobic residue and x any amino acid residue) is indeed linked with the endocytic machinery or could be related to the phosphorylation/activation status of the receptor needs to be addressed. Third, chemical interference using Dynasore indicates that dynamin activity is required for *S/Eix2* endocytosis, xylanase-triggered HR, and ROS production (Sharfman et al., 2011), although the molecular effects of this chemical have not been validated in plants. Xylanase induces differential phosphorylation of DRP2B, indicating that this dynamin GTPase, similarly to its function in FLS2 trafficking, also plays a role in *S/Eix2* endocytosis.

Overall, it appears that activated *S/Eix2* and FLS2 traffic along the late endocytic route and potentially share some common regulatory components, including clathrin, dynamin GTPases, and actin (1.2 Figures 1A and B). However, there are also remarkable differences. Although interference with flg22-induced FLS2 endocytosis can have no effect or can enhance or reduce FLS2 defence responses, depending on the type of flg22-elicited events, *S/Eix2* endosomal localization is correlated with the activation of all defences by xylanase. These range from early to late xylanase-induced events. To fully demonstrate that activated *S/Eix2* signals from

endosomes and the significance of this process in infection with *T. viride*, additional work must be performed beyond the use of chemical inhibition and transient expression in a heterologous system.

Another interesting difference between the endocytosis of activated *S/Eix2* and *FLS2* is the regulation by *BAK1*. Both *S/Eix2* endocytosis and xylanase-induced HR are abolished by overexpression of the homologous *S/Eix1* receptor in *N. benthamiana* (Bar et al., 2010, Ron and Avni, 2004), which does not occur in the absence of *NbSERK3* (Bar et al., 2010). As *BAK1/SERK3* is required for endocytosis of not only activated *FLS2* but also *Cf-4* (Postma et al., 2016), it is surprising that *S/Eix2* endocytosis appears to be independent of *NbSERK3* (Bar et al., 2010). Possibly, *S/Eix1* preferentially depends on *BAK1/SERK3* for its decoy function, whereas activated *S/Eix2* could engage with another member of the SERK family. It would also be interesting to address the potential involvement of *SOBIR1/EVR*, as this receptor associates with *S/Eix2* (Liebrand et al., 2013).

### **BAK1 Coreceptor Localization**

*BAK1* is a prominent member of the SERK family of coreceptors. These coreceptors are involved in the activation of RLKs and RLPs (Kim et al., 2013) and the regulation of their endocytic trafficking (Beck et al., 2012c, Robatzek et al., 2006, Bar et al., 2010, Chinchilla et al., 2007). In the latter role, *Arabidopsis BAK1* and *SERK1* are present at the PM and can constitutively localize to endosomes as homo- or heterodimeric receptor complexes (Kwaaitaal et al., 2005, Russinova et al., 2004). Thus, *BAK1* has the ability to engage with receptors at endosomes upon ligand perception, possibly from preassembled complexes at the PM (Russinova et al., 2004, Bucherl et al., 2013). However, these localization patterns relate to the interaction of *BAK1* with *BRI1*, and its function in brassinosteroid signalling.

*BAK1* subcellular localization and trafficking with regard to PRRs remain to be understood, as visualization of *BAK1* by fluorescent fusion impedes its function in PTI (Ntoukakis et al., 2011).

Indirect evidence exists that endosomal BAK1 is present in complex with activated FLS2. First, flg22 binds irreversibly to FLS2 and is in contact with BAK1 (Bauer et al., 2001, Sun et al., 2013). Second, flg22-induced endocytosis is dependent on BAK1 (Beck et al., 2012c, Chinchilla et al., 2007). This raises the possibility that flg22-induced, internalized FLS2 is present as an active receptor complex that has the ability to signal from endosomes, for instance via phosphorylating regulators of subcellular transport, although to date no evidence of active, endosome-localized FLS2 has been provided.

### **PRR Tracing of Pathogen-Reprogrammed Trafficking**

As secretory and endocytic trafficking are redirected to haustoria of filamentous pathogens (Lu et al., 2012, Inada et al., 2016), PRRs would appear to be well suited inducible cargos to trace the trafficking pathways contributing to EHM formation (Bozkurt et al., 2014). Although not involved in immunity against oomycetes, FLS2 localizes around haustoria, specialized extended hyphae functioning in nutrient acquisition and effector delivery, of virulent *H. arabidopsis* in Arabidopsis (Lu et al., 2012). This is independent of flg22 stimulus. Haustoria of *H. arabidopsis* are separated from the host cell PM by a callose-rich neck (Meyer et al., 2009, Micali et al., 2011), which thus indicates that haustorial-localized FLS2 possibly originates from the delivery of newly secreted receptors or an endosomal pool recycled to the hyphal invasion site. In agreement, *H. arabidopsis* haustoriated host cells maintain the ability to perform endocytic recycling (Lu et al., 2012).

By contrast, FLS2 and EFR were not present at haustoria of *P. infestans* in *N. benthamiana* (Lu et al., 2012). These observations suggest host specialization in the recruitment of transport processes in a pathogen-specific manner. However, flg22 induces FLS2 localization at the *P. infestans* haustorial interface (Bozkurt et al., 2014). Colocalization with RabG3c, a Rab7 GTPase family member present at LE/MVBs and the tonoplast, and the EHM-associated AVRblb2 effector (Bozkurt et al., 2011) suggests that activated FLS2 localizes to both late endosomes clustered around haustoria and EHM compartments of *P. infestans* (Bozkurt et al., 2014). Using flg22-

activated FLS2 as a tracer thus showed that late endocytic trafficking destined for vacuolar degradation is redirected towards haustoria. This is intriguing because haustoriated cells would contain AVR3a to inhibit FLS2 endocytosis (Chaparro-Garcia et al., 2014). Furthermore, as activated FLS2 localizes inside the lumen of MVBs (Spallek et al., 2013), it is unclear whether the pool of EHM-localized FLS2 is resident to the EHM, due to incomplete ESCRT-mediated sorting of the receptor at MVBs, or delivered to the matrix between the EHM and haustorial hyphae.

In summary, endocytosis appears to be a pivotal mechanism governing both LRR RLK- and LRR LRP-type PRRs localization upon elicitation. This enables the regulation of the steady-state level of receptors and associated factors at the cell surface. Despite the numerous attempts to determine the specific contribution of PRR endocytosis in the regulation of immunity, no definite conclusions can be drawn so far. This is due to the difficulty in uncoupling these two mechanisms which requires a better understanding of the cargo determinants.

### **3. Post-translational Modifications (PTMs) as Regulators of Endocytosis**

Cells employ protein post-translational modifications (PTMs) to rapidly and specifically respond to endogenous and exogenous stimuli, thus avoiding time- and energy- consuming *de novo* protein synthesis (Colby et al., 2006). PTMs can involve either small molecules attached to proteins such as methyl, phosphate and acetyl groups, or polypeptide-like modifiers encoded in the genome such as SUMO and ubiquitin. Although sharing only 18% amino acid identity, SUMO and ubiquitin have very similar three-dimensional structures (Colby et al., 2006). Covalent attachment of these polypeptides to a lysine residue in the target proteins involves mechanistically similar ATP-dependent reaction cascades of an E1 activating enzyme and an E2 conjugating enzyme. An additional E3 ligating enzyme is often required in the case of ubiquitination.

SUMOylation may act by masking and/or adding interaction surfaces, or by inducing conformational changes that alter the interactome of the targeted protein. Consequently,

subcellular localization, enzymatic activity or stability of the SUMOylated protein may be affected. In mammals, SUMOylation was shown to regulate receptor endocytosis (Wilkinson et al., 2012). This doesn't seem to be the case for the plant PM-localised PRRs, since the SUMO enzymes were shown to localise exclusively to the plant nucleus, though an indirect involvement of the SUMO machinery in the regulation of membrane trafficking cannot be ruled out.

Ubiquitination can also form distinct signals and hence regulate a broad range of signalling pathways. This depends on the nature of the ubiquitin linkage and the choice of the lysine residue used to form ubiquitin chains (Weissman, 2001). In particular, monoubiquitination and K63-linked polyubiquitin chains regulate endocytosis in mammalian cells (Ikeda and Dikic, 2008, Hochstrasser, 2009, Goh et al., 2010, Borgne et al., 2005). Accordingly, in-frame fusion of ubiquitin results in constitutive receptor internalization and enhanced degradation of the chimeric protein (Haglund et al., 2003, Mosesson et al., 2003). The involvement of ubiquitination in endocytosis of plant RLKs has only been documented for BRI1 (Martins et al., 2015). Indeed, K63-polyubiquitination of BRI1 promotes receptor internalisation and vacuolar degradation (Martins et al., 2015). Whether this is the case for its counterparts in immunity remains to be shown. Though not linked to their localisation patterns, ubiquitination has been shown to regulate the protein turn-over of several key components of PTI. In addition to the PUB12/PUB13-dependent ubiquitination of FLS2, fine-tuning of the protein levels of the central immune regulator BIK1 is achieved via ubiquitination and proteasome degradation, but the E3 ligase involved is yet to be determined (Monaghan et al., 2014).

Phosphorylation is a PTM that targets serine, threonine or tyrosine residues. It is known to modify PRR complexes and can regulate protein activity, subcellular localization, or degradation (Peck, 2006). In particular, tyrosine (Y) phosphorylation regulates endocytosis of receptors in mammals (Chowdhury et al., 2013). It often involves tyrosine-based endocytic motifs, specific sequences in the cytoplasmic domains of endocytosed RLKs which are recognized by components of the clathrin machinery to trap the endocytic cargo into CCVs (Su et al., 2016). Known motifs determining cargo internalization include the dileucine D(E)xxxLL(I) motif, the NPxY motif, the

YxNxxF motif, and the Yxxφ motif (Su et al., 2016). In plants however, the role of such internalization motifs is poorly understood. Indirect evidence points to a role of phosphorylation in endocytosis. For instance, phosphorylation of the auxin transporter PIN2 is essential for its polar PM localization in root epidermis, a process dependent on its intracellular trafficking (Zhang et al., 2010). In addition, mutation of a putative threonine phosphosite in FLS2 inhibits its endocytosis (Robatzek et al., 2006), suggesting an involvement of phosphorylation in plant PRR endocytosis.

## 4. Prologue

Significant progress was made during the last decade towards understanding the mechanisms that govern plant disease resistance as well as the strategies developed by microbes to overcome plant defence responses. Furthermore, a line of evidence points to an important role of the host subcellular trafficking machinery in the establishment of plant immunity. However, biochemical and mechanistic data addressing the involvement of PRR trafficking in PTI signalling remain sparse, and most approaches addressing this question so far were based on genetic interference with general trafficking regulators, and thus lacked specificity to PRRs.

The presence of different combinations of PTMs on target proteins is thought to act as a molecular barcode, particularly in the case of cell surface-localised receptors, that can regulate multiple responses and dynamic localisations. The leading model of receptor-mediated endocytosis in animals presumes that ligand binding to the extracellular domain leads to the activation of the kinase and autophosphorylation of residues in the cytoplasmic domain, which serve as interaction sites for proteins mediating receptor ubiquitination. Ubiquitinated receptors are then recruited into CCVs by interacting with endocytic regulatory proteins.

Within this scientific context, and with the knowledge that post-translational modifications of PRRs provides dynamically regulated responses with highly specific cellular outputs, I decided to dissect the molecular changes that may act as intrinsic endocytic signals within FLS2 and EFR receptors, with a focus on ubiquitination and phosphorylation.

My objectives were to:

1. Determine whether FLS2 trafficking is mediated by the ESCRT machinery, that specifically binds to ubiquitinated proteins
2. Determine the E3 ligase(s) that could be involved in the regulation of FLS2 subcellular trafficking.

3. Identify the ubiquitination sites of the activated FLS2 receptor.
4. Test FLS2 endocytosis in the E3 ligase *pub12 pub13* mutants and address the requirement of receptor endocytosis for flg22-mediated signalling.
5. Study the contribution of tyrosine phosphorylation in the endocytosis of activated PRRs, with a focus on EFR.
6. Address the requirement of EFR endocytosis in *elf18*-triggered immunity.

In summary, my PhD aimed at unveiling the importance of PTMs in the control of receptor endosomal trafficking in plants, and shedding new insights into the role of this process during the initiation of PTI. The emerging results are presented in the following chapters in manuscript format followed by a brief discussion and outlook chapter.

## Chapter 2: Involvement of Ubiquitination in FLS2 Subcellular Trafficking

### 1. ESCRT-I Mediates FLS2 Endosomal Sorting; From (Spallek et al., 2013)

#### 1.1 Introduction

The metazoan and plant immune systems deploy pattern recognition receptors (PRRs) at the cell surface to sense a wide range of potentially pathogenic microbes through the presence of distinct pathogen-associated molecular patterns (PAMPs), conserved molecules displayed by microbes (Boller and Felix, 2009). In plants, perception of the bacterial PAMP flagellin (or its eliciting epitope flg22) by the PRR flagellin-sensing 2 (FLS2) leads to the activation of immune signalling cascades and the internalization of the receptor (Robatzek et al., 2006). Following uptake from the plasma membrane (PM), endocytosed FLS2 traffics via the *trans*-Golgi network (TGN)/ early endosomal (EE) compartment before being delivered to late endosomes /multivesicular bodies (LE/MVBs), from where it can be sorted for degradation (Beck et al., 2012c, Choi et al., 2013). This latter step, and more precisely cargo delivery into intraluminal vesicles (ILVs) of MVBs, is known to be mediated in mammalian cells by the endosomal sorting complex required for transport (ESCRT)-0, -I, -II, and -III (Raiborg and Stenmark, 2009). The subunits of the ESCRTs are referred to as vacuolar protein sorting (VPS), and with the exception of ESCRT-0, are highly conserved in plants (Leung et al., 2008, Reyes et al., 2011, Richardson et al., 2011, Richardson and Mullen, 2011, Shahriari et al., 2011, Spitzer et al., 2009, Winter and Hauser, 2006). However, surprisingly little is known about ESCRT-I-mediated cargo sorting and their function in plant processes. Here, using live cell imaging, I showed that FLS2 is present at VPS37-1 positive compartments and that these two proteins form inducible complexes upon flg22 elicitation.

## 1.2 Activated FLS2 associates and co-localizes with VPS37-1 at endosomes

To determine if VPS37-1 is involved in FLS2 endosomal trafficking, I performed in planta co-localization experiments following flg22 elicitation. Endosomal FLS2-GFP partially colocalized with RFP-VPS37-1 (2.1 Figure 1), a similar pattern compared to the partial co-localization of FLS2-GFP with ARA7/Rab2Fb- and ARA6/RabF1-positive endosomes at early time points after flg22 treatment in *Arabidopsis* (Beck et al., 2012c). This suggests that activated FLS2 traffics via ESCRT-I-positive compartments along its endocytic route. Additionally, I performed co-immunoprecipitation analysis with VPS37-1. In the absence of flg22, FLS2-GFP was detected only in minor amounts of immunoprecipitated RFP-VPS37-1 (2.1 Figure 2B). By contrast, the levels of FLS2-GFP were significantly increased in immunoprecipitated RFP-VPS37-1 upon flg22 elicitation. These results indicate that FLS2 forms an inducible complex with the ESCRT-I subunit VPS37-1 coinciding with their shared endosomal localization.

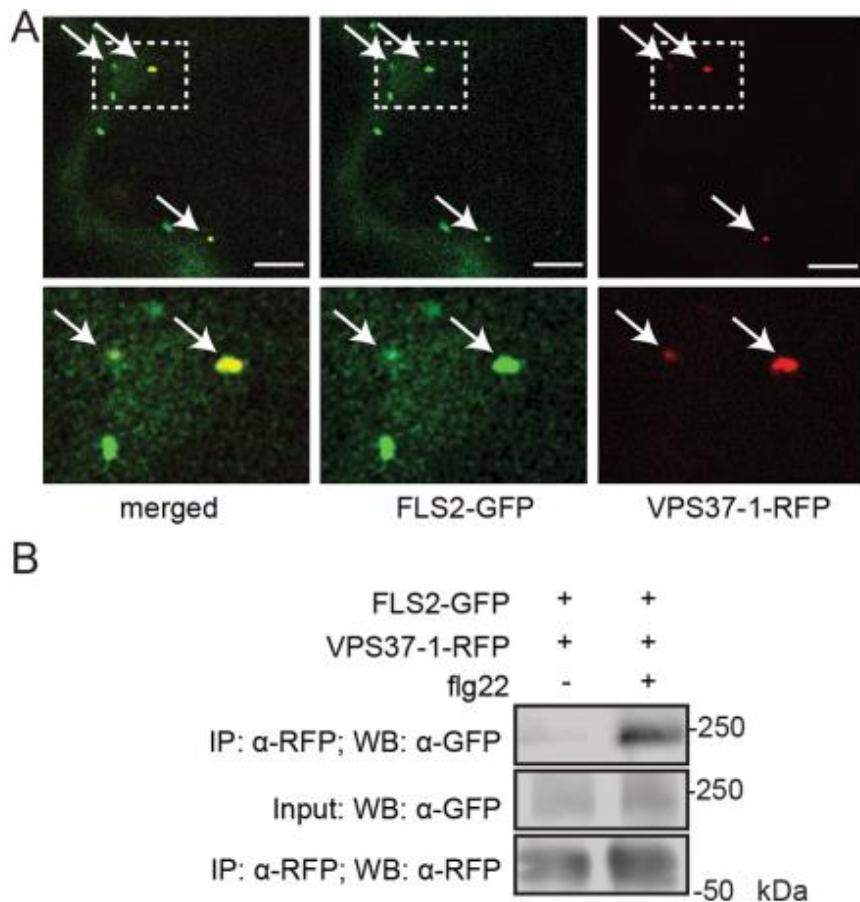
## 1.1 Materials and Methods

### Confocal microscopy and image analysis

Standard confocal microscopy was performed using the Leica SP5 microscope (Leica, Germany).

### Immunoblot analysis and co-immunoprecipitation

Immunoblot analysis with the indicated antibodies was performed as described before (Gohre et al., 2008). Pull-down experiments were carried out as previously reported (Albrecht et al., 2012) with the following modifications: Transiently transformed *N. benthamiana* leaves were infiltrated with 100 µM flg22 solution, and subjected to protein extraction in 50 mM Tris-HCl, pH 7.5; 150 mM NaCl; 10% glycerol, 2 mM EDTA, 5 mM DTT, 1% Triton 6100; 1% (vol/vol) protease inhibitor mixture (Sigma). Following filtration through Miracloth (Calbiochem) and centrifugation at 8000 g and 16.000 g each for 15 min, 5 ml per g fresh weight of GFP-Trap coupled to agarose beads (Chromotek) were added to the supernatant and incubated for 2 hours, washed four times, boiled for 5 min at 65°C in extraction buffer, and subjected to immunoblot analysis.



## 2.1 Figure 1.

### FLS2 is present at ESCRT-I-positive compartments and forms an inducible complex with VPS37-1.

**(A)** Standard confocal micrographs show optical sections of *N. benthamiana* leaf epidermal cells transiently expressing FLS2-GFP and RFP-VPS37-1 treated with 100  $\mu$ M flg22 for 100 min. Upper panel represents overview image, lower panel shows detail image of co-localization between FLS2-GFP and RFP-VPS37-1 at vesicles (indicated by arrows). Bars = 10  $\mu$ m. **(B)** Co-expressed FLS2-GFP and RFP-VPS37-1 were subjected for immunoprecipitation analysis. RFP-VPS37-1 was able to co-purify FLS2-GFP upon flg22 stimulus. These experiments have been done three times with similar results.

## 1.2 Discussion

Sorting of PM proteins into luminal vesicles of MVBs is a process mediated by the ESCRT machinery (Raiborg and Stenmark, 2009). Therefore, I sought to determine whether ESCRT components play a role in FLS2 endocytosis and trafficking. ESCRT-I is a heterotrimeric complex composed of the subunits VPS23/ELC, VPS28 and VPS37 (Spitzer et al., 2009). In *Arabidopsis*, the VPS28-1 subunit was shown to localize to the TGN/ EE, from which MVB maturation could be observed (Scheuring et al., 2011). As mutants in VPS23/ELC were in *Ws-0* background, which lacks a functional FLS2 gene (Spitzer et al., 2009, Zipfel et al., 2004), I focused on VPS37-1 (Shahriari et al., 2011). I showed that FLS2 colocalizes and forms inducible complexes with VPS37-1 upon flg22 elicitation. Additional work from Spallek and Beck demonstrated that this ESCRT-I subunit is required for FLS2 uptake into intraluminal vesicles of multivesicular bodies and that, when mutated, impairs FLS2 internalisation (Spallek et al., 2013). Thus, FLS2 trafficking to late endosomal compartments is regulated by the ESCRT machinery.

The ESCRT complex recognises ubiquitinated PM proteins. FLS2 was previously shown to be ubiquitinated upon flg22 perception (Lu et al., 2011a). However, the nature of this modification in planta and its involvement in FLS2 subcellular trafficking remained largely unknown. Therefore, I employed proteomic approaches to identify the E3 ligases that mediate FLS2 ubiquitination and the lysine residues targeted by this PTM.

## 2. Towards the Characterisation of the FLS2 Ubiquitin-Endocytic Trafficking Map

### 2.1 Introduction

Reversible protein ubiquitination plays crucial roles in plant growth and immunity. It is the product of a signalling cascade involving an activating E1, a conjugating E2 and a ligating E3 enzymes. E3 ubiquitin ligases are classified into different families depending on their structural

and functional features and they confer substrate specificity (Duplan and Rivas, 2014). In rice, the RING-type E3 ligase XB3 interacts with the receptor-like kinase (RLK) XA21, which confers resistance to bacterial blight caused by *Xanthomonas oryzae* pv. *oryzae* (*Xoo*) (Wang et al., 2006). XB3 is required for XA21 accumulation and XA21-mediated resistance to *Xoo* (Wang et al., 2006).

In Arabidopsis, the plant U-box 22 (PUB22) acts in concert with PUB23 and PUB24 to negatively regulate PTI responses, as the *pub22 pub23 pub24* triple mutants display enhanced early signalling responses to several PAMPs (Trujillo et al., 2008). Additionally, PUB22 targets Exo70B2, an exocyst complex subunit involved in vesicle tethering during exocytosis (Stegmann et al., 2012). PUB22 is stabilized in response to flg22 treatment (possibly via attenuation of its autocatalytic ubiquitination activity), which leads to Exo70B2 ubiquitination and proteasomal degradation. Since Exo70B2 is required for both early and late PTI responses (Stegmann et al., 2012), it is possible that Exo70B2 contributes to recycling of PM proteins involved in PTI, including NADPH oxidases, ion channels or RLKs such as FLS2. PUB22-mediated degradation of Exo70B2 would therefore attenuate the recycling pathway, redirecting positive signalling components towards the vacuolar degradation pathway (Stegmann et al., 2012).

Another pair of U-box E3 ligases, PUB12 and PUB13, has also been involved in the attenuation of PTI responses triggered by bacterial flagellin. In response to flg22, PUB12 and PUB13 form a BAK1-dependent complex with FLS2 and are able to ubiquitinate FLS2 and mediate its degradation (Lu et al., 2011a). Accordingly, flg22-dependent signalling is enhanced in *pub12 pub13* mutant plants (Lu et al., 2011a). This is consistent with the fact flg22 trigger leads to FLS2 endocytosis and degradation (Robatzek et al., 2006, Gohre et al., 2008, Beck et al., 2012c, Choi et al., 2013). However, whether PUB12 and PUB13 regulate FLS2 endocytosis, and whether stabilization of FLS2 in *pub12 pub13* plants is due to receptor accumulation at the PM or within endocytic compartments remains to be determined.

Nevertheless, the finding that FLS2 trafficking is regulated by the endosomal complex required for transport (ESCRT), which specifically sorts ubiquitinated cargoes into multivesicular bodies

(MVBs), led us to undertake a without a priori approach to investigate the involvement of E3 ligases and ubiquitination processes in the regulation of ligand-dependent endocytosis of FLS2.

## 2.2 Results and Discussion

### 2.2.1 Identification of Novel E3 ligases as Potential Regulators of flg22-Induced FLS2 Trafficking

To identify E3 ligases that interact with FLS2 upon flg22 perception, we employed protein immunoprecipitation coupled with mass spectrometry. As we were primarily interested in the identification of E3 ligases that regulate the uptake of FLS2 from the PM, rather than regulators of downstream trafficking processes, we decided to focus on interactors at 30 min upon flg22 treatment. Col-0/*FLS2p::FLS2-GFP* transgenic seedlings were incubated for 4 hours in 100  $\mu$ M proteasome inhibitor MG132, which not only inhibits the function of the proteasome, but also several proteases. This was followed by immunoprecipitation of FLS2-GFP upon treatment with mock or 10  $\mu$ M flg22 for 30 min. FLS2-interacting proteins were identified using liquid chromatography-tandem mass spectrometry (LC-MS/MS). Several known flg22-induced FLS2-interacting partners, such as BAK1, were detected in this analysis, highlighting the sensitivity of the approach (2.2 Table 1). Additionally, we identified several key regulators of endocytic trafficking such as clathrin, TPLATE and actin (2.2 Table 1). However, of the previously reported FLS2-interacting E3 ligases, PUB12 and PUB13, only PUB12 was detected in one technical replicate. Since Lu et al. (2011) showed that PUB12 and PUB13 interact with FLS2 30 seconds after flg22 perception, it is possible that these E3 ligases dissociate from the receptor before 30 min or the abundance of PUB12 and PUB13 in complex with FLS2 is lower at this time point. Further characterisation of PUB12 and PUB13 will be addressed in the next section.

Interestingly, we identified three novel E3 ligase interactors: the HECT-type ubiquitin protein ligase 3 (UPL3, also known as KAKTUS or KAK), the RING E3 ligase keep on going (KEG), and an unknown U-box E3 ligase (AT5G58410).

UPL3 is involved in trichome development by regulating their ploidy level (Downes et al., 2003, El Refy et al., 2003). However, the involvement of such processes in PTI is still unknown.

KEG is a 200 kDa RING E3 ligase, previously reported to have an *in vitro* ubiquitin ligase activity. In *Arabidopsis*, KEG localizes mainly to the *trans*-Golgi network (TGN)/early endosomes (EE), where FLS2 is found upon flg22 perception, suggesting a possible role of this E3 ligase in FLS2 sorting towards the late endocytic route. KEG contains a RING finger E3 ligase domain and nine ankyrin (ANK) repeats, which are hypothesized to function as a versatile protein–protein interaction module (Sedgwick and Smerdon, 1999). In contrast to other RING-ANK family members, KEG contains an additional serine/threonine kinase domain and is terminated by twelve HERC2-like repeats. This E3 ligase was implicated in the regulation of ABA signalling via degradation of the transcription factor abscisic acid insensitive 5 (ABI5) (Stone et al., 2006, Liu and Stone, 2010). In addition, KEG plays a central role in vacuolar biogenesis and the endomembrane trafficking system, including regulation of protein secretion and targeting of RLKs for vacuolar degradation (Gu and Innes, 2012).

Taken together, this approach identified three ubiquitin E3 ligases not previously linked to FLS2, along with several novel interacting partners previously linked to PTI, vesicle trafficking and vacuolar degradation.

## 2.2 Table 1.

### Overview of identified FLS2 interacting proteins.

C-terminally GFP-tagged FLS2 proteins were isolated using GFP-Trap beads (Chromotek). Immunoprecipitated proteins were eluted, digested with trypsin, and analysed by LC-MS/MS. Each protein pool represents a biological replicate. Two technical replicates were conducted for each pool. Spectral counts for each protein identification are indicated. Previously reported FLS2 interactors are given in bold.

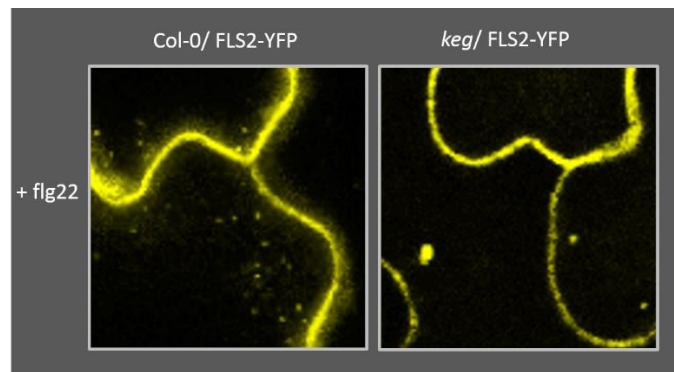
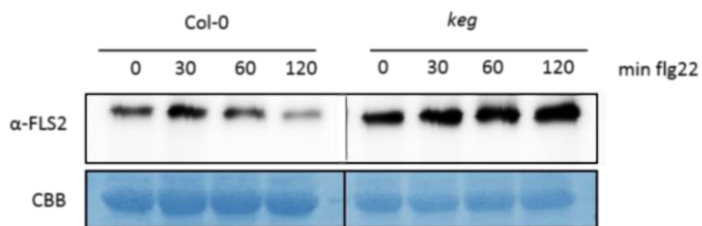
Protein identity	Untreated samples	flg22 treated samples				proteins involved in immunity	protein involved in trafficking	E3 ligases	other
		pool A		pool B					
<b>BAK1</b>	0	26	0	0	7				
MIN7	7	9	2	21	4				
CPK3	0	17	3	7	3				
MAPKKKK7	1	6	1	4	2				
<b>TPLATE</b>	0	7	0	0	0				
<b>RBOHD</b>	0	0	0	0	5				
clathrin heavy chain	54	60	45	67	53				
<b>SPK1 (ER GEF)</b>	0	40	26	34	43				
Actin 7	3	27	5	17	0				
Tubulin	1	24	5	7	7				
Myosin X1 A	0	12	0	0	1				
Sac9	0	4	3	6	2				
ACT2 (actin 2)	0	8	0	0	0				
DRP4C	0	1	2	1	1				
VLN4 (actin filament bundling protein)	0	0	0	3	0				
VTI12 (v-SNARE)	0	0	0	2	0				
VLN2	0	1	0	0	1				
KAK/UPL3	0	20	15	20	17				
U-box	2	8	4	7	0				
KEG	0	5	1	4	3				
<b>PUB12</b>	0	0	0	5	0				
PUB26	0	2	0	0	0				
PUB24	0	0	1	0	0				
OST2	18	38	11	43	16				
PPI2 (protein that interacts with AHA1)	2	8	3	4	19				
WAK1	0	14	3	8	5				
AHA2	0	8	3	0	3				

### 2.2.2 Endocytic Trafficking of Activated FLS2 is Altered in *keg* Mutants

To determine if KEG is involved in FLS2 vacuolar trafficking, we tested *keg-1* mutants expressing FLS2-YFP (kindly provided by Roger Innes) for flg22-induced receptor-mediated endocytosis. Surprisingly, in *keg* mutants, activated FLS2-YFP was not observed at distinct intracellular mobile vesicles but aggregated at larger intracellular bodies (2.2 Figure 1A). Accordingly, FLS2 protein levels were unaltered in the *keg* mutant, while they reduced in WT seedlings over a time course of flg22 treatment (2.2 Figure 1B, experiments performed by Katarzyna Rybak). Altogether our results show that KEG associates with FLS2 in a flg22-dependent manner and is required for proper endocytic trafficking and degradation of activated receptors. Considering the TGN localisation of this E3 ligase, and the observed FLS2-positive enlarged structures in the *keg* mutant (2.2 Figure 1A), it is likely that KEG is involved in the regulation of post-TGN trafficking of activated FLS2. This is in agreement with the previously reported involvement of KEG in the vacuolar sorting of BRI1, suggesting a broader role in RLK trafficking.

In order to investigate the possibility that KEG regulates vacuolar transport of FLS2, it is important to determine whether FLS2 is sorted to LE/MVBs in the *keg-1* mutant and whether it is properly located inside the ILVs of MVBs. Since this step is known to be mediated by the ESCRT complex, and in particular the FLS2-interacting component VPS37-1 (Spallek et al., 2013), it will be interesting to test whether this interaction is disrupted in the *keg* mutants.

Overall, to determine the specificity of the FLS2 ubiquitination by the identified E3 ligases, in vitro ubiquitination assays can be performed using KEG, PUB12/PUB13, UPL3, and the novel U-box ligase. In addition, the lysine (K) residues targeted by each one of these E3 ligases can be performed by differential mass spectrometry analysis.

**A****B**

## 2.2 Figure 1.

### KEG regulates flg22-induced FLS2 trafficking and degradation.

(A) Confocal microscopy images of Arabidopsis leaf epidermal cells in Col-0 and *keg* mutant expressing *35Sp::FLS2-YFP*. Seedlings were imaged 60 min after treatment with 10  $\mu$ M flg22. (B) Degradation of FLS2 in Col-0 or *keg* mutant was analysed by western blot using anti-FLS2 antibody. Seedlings were treated with 10  $\mu$ M flg22 for the indicated time points.

#### 2.2.3 Identification of FLS2 Ubiquitination Sites

As FLS2 is ubiquitinated upon flg22 perception (Lu et al., 2011a), we sought to identify which residues are targeted by this PTM. To determine the FLS2 ubiquitination sites, we analysed by LC-MS/MS FLS2 proteins immunoprecipitated from Col-0/*FLS2p::FLS2-GFP* transgenic seedlings treated with mock or flg22 for 30 min (the samples used in this analyses are derived from the same experiments as 2.2 Table 1). Upon trypsin digest, which usually cuts after an arginine residue, ubiquitin leaves on the ubiquitinated K a so-called ubiquitin footprint, which can be either GG or LRGG. Based on this, we identified a total of eight candidate *in vivo* ubiquitination

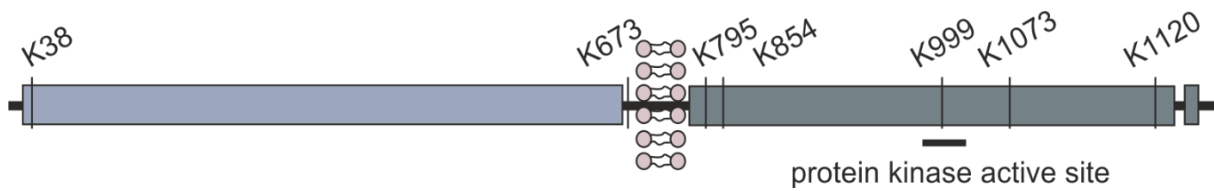
sites of FLS2: K38, K673, K795, K854, K999, K1073, K1120, and K1130 (2.2 Figure 2) (2.2 Table 2). Notably, K854, K999, K1073, K1120, and K1130 are in the intracellular domain, indicating that they might be involved in subcellular trafficking rather than ER quality control processes.

It is important to note however, that several of these lysine residues might be false positives. The sensitivity of the LC-MS/MS for identification of ubiquitination sites is rather limited. Indeed the peptide identification probability was below the threshold level for several peptides, which led us to manually inspect the spectrum at the residues identified. To obtain a better confidence and more conclusive results, we are currently performing further quantitative analysis with triple quadrupole mass spectrometry.

Additionally, we complemented our proteomic approaches by carrying out site-directed mutagenesis, whereby we replaced each of the five K residues present in FLS2 cytoplasmic domain with an Alanine residue.

Confocal analysis of *N. benthamiana* plants transiently expressing FLS2<sup>K854A</sup> showed no alteration in the trafficking of this FLS2 mutant variant (Spallek et al., personal communication). K854 is located in the K-rich region of the FLS2 juxtamembrane domain. Importantly, this region was shown to be involved in the regulation of ubiquitin-mediated BRI1 endocytosis (Martins et al., 2015) and is required for FLS2 ubiquitination by the E3 ligases PUB12 and PUB13 (Li et al., 2014). Additionally, Spallek et al. (personal communication) showed that K854 is ubiquitinated by the *Pto* DC3000 effector AvrPtoB. However, mutation of this residue and the two adjacent lysines, K856 and K861, did not affect FLS2 endocytosis (Spallek et al., unpublished). This result was expected since mutation of an ubiquitination site usually leads to the ubiquitination of adjacent lysines. Accordingly, in the case of BRI1, abolishment of receptor endocytosis was observed when 25 K residues were mutated (Martins et al., 2015). It is therefore possible that only mutation of all K832, K833, K834, K836, K837, K854, K856, and K861 would enable the determination of the effect of FLS2 ubiquitination in this domain.

In the following, I addressed the involvement of K1120 in FLS2 endocytosis, while the analyses of the three other cytoplasmic K candidates was taken over by a post-doc from our group.



## 2.2 Figure2.

### Schematic representation of the FLS2 showing the location of the candidate ubiquitinated Ks.

The LRR domain is shown in blue and the intracellular domain in green. The protein kinase active site is indicated.

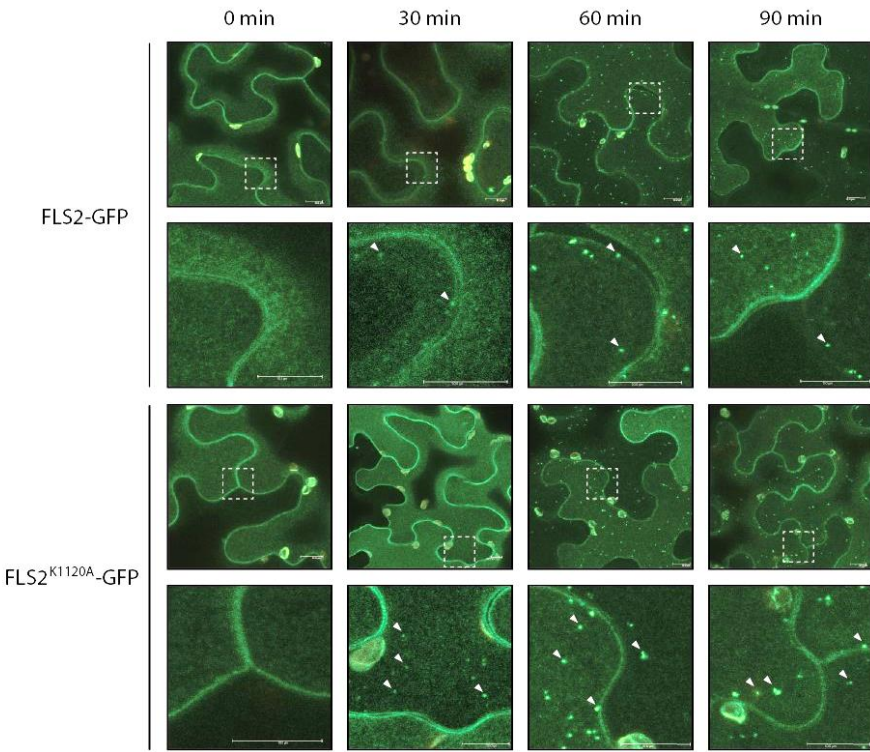
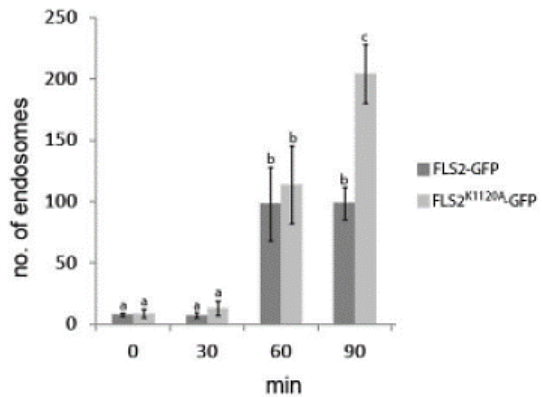
## 2.2 Table 2.

### Summary of identified candidate *in vivo* FLS2 ubiquitination sites by LC-MS/MS analysis.

Treatment	Ubiquiti- nation site	Peptide sequence	Best		
			Best probabi- lity	Number of Spectra	Masco t Score
	K38	(A)KQSFEPEIEALKSF <b>K</b> NGIS(N)	92%	2	50.3
	K38	(A)KQSFEPEIEALKSF <b>K</b> NGIS(N)	94%	4	50.2
		(?)SLQACKNVFTL(?)	21%	9	33.6
	K673	(?)SLQACK(?)	50%	19	34.1
	K795	(?)KPLKPCT <b>I</b> K(?)	17%	19	42.3
		(?)DSALKLKRFEPEK <b>E</b> LEQAT(?)	18%	9	44.3
	K854	(?)IENSSESSLPD <b>L</b> DSALK(?)	28%	19	45.5
	K999	(?)DLKPANILLSDRVAHVSDFGTAR(?)	40%	19	50.2
		(A)DVFSFGIIMM <b>E</b> LM <b>T</b> TKQRPTSL(N)	73%	4	50.1
		(A)DVFSFGIIMM <b>E</b> LM <b>T</b> TKQRPTSL(N)	65%	4	50.5
		(?)ADVFSFGIIMM <b>E</b> LM <b>T</b> K(?)	39%	19	33.2
	K1073	(A)DVFSFGIIMM <b>E</b> LM <b>T</b> TKQRPTSL(N)	66%	2	50.7
flg22 for 30 min	K1120	VLDMELGDSIVSL <b>K</b> QEEAIEDFLK	13%	19	50.3
	K1130	VLDMELGDSIVSL <b>K</b> QEEAIEDFLK	13%	19	50.3

#### 2.2.4 Mutation of K1120 Induces an Increase in FLS2-Labelled Vesicles

In order to determine the involvement of K1120 in FLS2 subcellular trafficking, we performed virus-induced gene silencing (VIGS) in *N. benthamiana* to silence the endogenous *NbFLS2*. Transient expression of FLS2<sup>K1120A</sup> mutant in the VIGSed plants showed similar PM localisation and expression pattern as WT FLS2 (2.2 Figure 3A, 0 min). Upon flg22 treatment, FLS2<sup>K1120A</sup> translocated into intracellular mobile vesicles, likely endosomes. Notably, we observed a marked increase of endosomal numbers of this mutant variant at later time points (2.2 Figure 3A, 90 min). Using quantitative imaging, we showed that the endosomal numbers of this mutant variant are similar to those of WT FLS2 for up to 60 min, but increase over time (2.2 Figure 3A and B). This suggests that K1120 is involved in vacuole sorting rather than endocytic uptake from the PM. Additional characterisation of Arabidopsis *fls2* mutants complemented with FLS2<sup>K1120A</sup>, as well as colocalization experiments with endocytic markers will allow a better understanding of the role of this K residue in FLS2 subcellular trafficking.

**A****B**

## 2.2 Figure 3.

### **FLS2<sup>K1120A</sup>-GFP exhibits altered flg22-induced receptor-mediated trafficking.**

(A) Confocal microscopy images of *N. benthamiana* leaf epidermal cells expressing FLS2-GFP and FLS2<sup>K1120A</sup>-GFP. A time course series was performed from 0 to 90 min after flg22 treatment. Squares indicate the area depicted in detail. Arrowheads point to GFP-labelled endosomes. Bars = 10  $\mu$ m. (B) Quantification of endosomal numbers at each time point. Student's t test showed a significant ( $p \leq 0.03$ ) increase of the number (no.) of endosomes at 90 min after flg22 treatment for the FLS2<sup>K1120A</sup>-GFP mutant in comparison to WT FLS2-GFP.

These experiments were carried out with the help of Stephanie Solle, a master student that I supervised.

## 2.3 Material and Methods

### Plant Materials and Growth Conditions

Plant materials and growth conditions have been previously described (Albrecht et al., 2012, Schwessinger et al., 2011). Selection of the *keg-1* mutants was performed by growing seedlings on plates containing Murashige–Skoog (MS) medium without sugar (including vitamins) (Duchefa, Haarlem, The Netherlands), supplemented with 0.8% agar, at 22°C and with a 16 h photoperiod. After five days, the stunted seedlings corresponding to the *keg* mutant are recovered on MS plates with sugar.

### Chemicals

Elicitors and treatments have been described before (Albrecht et al., 2012). Proteasome inhibitors MG132 (Merck Chemicals/ Calbiochem) was used at 100 µM to pre-treat plant tissues for 4h before PAMP treatment. The inhibitor was applied by floating seedlings in the inhibitor solution and was additionally added to the extraction buffer at 50 µM for immunoprecipitation assays. Furthermore, N-Ethylmaleimide (Sigma) was added to the extraction buffer at 2 µM.

### Protein Extractions, Immunoprecipitations, and Immunoblot Analyses

Protein extractions, immunoprecipitations, and immunoblots were performed as previously described (Schwessinger et al., 2011, Albrecht et al., 2012). Two-week-old *Arabidopsis* seedlings were used for protein extractions. Plant materials were ground in liquid nitrogen, and then extracted with buffer [150 mM Tris-HCl, pH 7.5; 150 mM NaCl; 5mM EDTA; 1% Igepal; 1% (vol/vol) protease inhibitor mixture, phosphatase inhibitor 2 and 3 (Sigma)] added at 1.5 mL/g powder. Samples were centrifuged 15 min at 4 °C and 21,000 g. Supernatants were adjusted to 3 mg/mL protein and incubated 4 h at 4 °C with 100 µL GFP-Trap coupled to agarose beads (Chromotek) with gentle agitation. Following incubation, the beads were collected and washed four times with the extraction buffer. For western blot, SDS loading buffer was then added to the beads, which were boiled for 10 min. Proteins were separated by SDS/PAGE 10%.

### **Identification of E3 ligases and ubiquitination sites by LC-MS/MS**

Proteins were separated by SDS-PAGE (NuPAGE®, Invitrogen) and after staining with Coomassie brilliant Blue G-250 CBB (SimplyBlue™ stain, Invitrogen), the proteins were cut out and digested by trypsin as described previously (Ntoukakis et al., 2009). LC-MS/MS analysis was performed using a LTQ-Orbitrap massspectrometer (Thermo Scientific) and a nanoflow-HPLC system (nanoAcuity; Waters) as described previously (Ntoukakis et al., 2009). The entire TAIR10 database was searched ([www.Arabidopsis.org](http://www.Arabidopsis.org)) using Mascot (v 2.3.02, Matrix Science) (with the inclusion of sequences of common contaminants, such as keratins and trypsin). Parameters were set for 5 ppm peptide mass tolerance and allowing for Met oxidation and two missed tryptic cleavages. Carbamidomethylation of cysteine residues was specified as a fixed modification, and oxidized methionine and ubiquitination of K residues were allowed as variable modifications. Scaffold (v3; Proteome Software) was used to validate MS/MS-based peptide and protein identifications and annotate spectra. The position and quality of spectra for ubiquitinated peptides were also manually examined.

### **Cloning**

Arabidopsis full-length FLS2 cloned into pCambia vector (Robatzek et al., 2006) was used as a template for amplification with Phusion High-Fidelity DNA Polymerase (New England Biolabs) using primers where the original sequence has been modified to generate the K to A substitution at the desired position. The primer sequences are available in Table 1. Resulting plasmids were sequenced to verify specific mutations and lack of additional mutations. Recombinants were transformed into *Agrobacterium tumefaciens* GV3101pMP90 by electroporation and FLS2<sup>K1120A</sup>-GFP was used for transient expression in *N. benthamiana*.

### **Virus-induced gene silencing of *NbFLS2***

*NbFLS2* VIGS was performed as described previously (Lu et al., 2003). *Agrobacterium tumefaciens* GV3101 strains carrying pBINTRA6 (RNA1) or pTV00 containing the kinase domain sequence of *NbFLS2* (RNA2) were grown overnight in Luria-Bertani (LB) medium supplemented with appropriate antibiotics. Cultures were spun down and re-suspended in buffer containing 10 mM

MgCl<sub>2</sub>, 10 mM MES pH 5.6 and 100 µM acetosyringone to OD600=1 and incubated overnight at room temperature. A mixture of both strains was infiltrated into *N. benthamiana* seedlings (4-leaf stage).

### **Confocal Microscopy**

Subcellular localization of FLS2-YFP in Col-0 or *keg* mutant backgrounds, as well the FLS<sup>K1120A</sup> variant in *N. benthamiana*, was determined by confocal laser-scanning microscopy with a DM6000B/TCS SP5 microscope (Leica) using standard settings for YFP detection provided by the manufacturer. Five-week-old *N. benthamiana* plants silenced for *NbFLS2* were used for transient expression assays as described before (Mbengue et al., 2016).

Quantification of FLS2-GFP endosomal numbers was performed using the image processing software Acapella (version 2.0; Perkin-Elmer) with an algorithm previously described (Beck et al., 2012c).

### **Statistical Analysis**

Statistical significances based on t test analyses were performed with Prism 5.01 software (GraphPad Software).

### **3. Ubiquitin-Mediated FLS2 Endocytosis is Required for Maintaining Responsiveness to Flagellin**

#### **3.1 Abstract**

Following activation by bacterial flagellin, the receptor flagellin-sensing 2 (FLS2), a key regulator of plant immunity, is internalized into endosomes and transported for degradation. Late endocytic trafficking depends on ubiquitination of the cargo and represents the major pathway of degrading plasma membrane-localized proteins. Here we demonstrate, using live-cell imaging, that the two redundant plant U-box (PUB) 12 and PUB13 E3 ligases mediated endocytosis of liganded FLS2. We found ligand-induced mono-ubiquitination of FLS2, for which PUB12 and PUB13 were essential. PUB12 and PUB13 accumulated at vesicles in a flagellin-dependent fashion that did not co-localize with endosomal FLS2, suggesting separation into the endocytic recycling and the late endocytic route. FLS2 endocytosis induced by flagellin is uncoupled from canonical defence responses, as the transient oxidative burst, activation of MAP kinases, and initial stages of inhibited seedling growth remained unchanged in *pub12 pub13* mutants. Under long-term flagellin exposure, *pub12 pub13* mutants recovered seedling growth. This correlated with an over-accumulation of FLS2, reduced MAP kinase activation and impaired flg22-induced resistance to bacterial infection. Our findings demonstrate that PUB12 and PUB13 ubiquitinate FLS2 to remove liganded receptors from the plasma membrane. This would preserve responsiveness to continuous exposure of flagellin in long-life associations of plants with their surrounding bacteria, and suggests a model by which endocytosis of activated receptors is coupled with the delivery of newly synthesized ones in a cargo-specific manner.

#### **3.2 Introduction**

Plants have evolved a sophisticated immune system to fight off invading microbes. The efficiency of the activation of plant immunity highly relies on its ability to engage the endomembrane system to deploy immune receptors and defence-related compounds (Ben Khaled et al., 2015).

Accordingly, mutation of key regulators of subcellular trafficking results in a significantly higher susceptibility to microbes (Ben Khaled et al., 2015). A key aspect of plant immunity is the perception of pathogen-associated molecular patterns (PAMPs) by surface-localized pattern-recognition receptors (PRRs) (Dodds and Rathjen, 2010). The *Arabidopsis* PRRs, flagellin-sensing 2 (FLS2) and EF-TU receptor (EFR), form an inducible complex with the coreceptor BRI1-associated kinase 1 (BAK1) upon perception of their respective ligands, flagellin and EF-Tu (Couto and Zipfel, 2016). This leads to a series of immune signalling responses such as production of reactive oxygen species (ROS), phosphorylation of mitogen-activated protein kinases (MAPK), stomata closure, transcriptional regulation, and growth arrest (Couto and Zipfel, 2016). Ligand perception is also associated with a dynamic change in FLS2 and EFR subcellular localisations from the plasma membrane (PM) to intracellular vesicles, in a BAK1-dependent manner (Couto and Zipfel, 2016, Mbengue et al., 2016). Although the subcellular trafficking routes of these receptor-like kinases (RLKs) have been extensively described (Beck et al., 2012c, Spallek et al., 2013) (Mbengue et al., 2016), the exact molecular mechanism underlying their endocytosis, and the requirement of their trafficking processes during the course of plant interaction with their surrounding microbes remain elusive.

In mammals, modification of transmembrane proteins by ubiquitination appears to serve as a signal sufficient to induce internalization and endocytic trafficking (Haglund and Dikic, 2012). Ubiquitination consists in the fixation of ubiquitin (Ub) monomers on a substrate lysine (K), and involves an activating enzymes (E1), a conjugating enzyme (E2) and a ligation enzyme (E3) (Komander and Rape, 2012). Ubiquitination may result in the attachment of single ubiquitin moieties (mono or poly-monoubiquitination), or ubiquitin chains (polyubiquitination). The choice of the lysine residue, within the Ub moieties forming the chain, influences the fate of the ubiquitinated protein (Komander and Rape, 2012). Poly-Ub chains linked via ubiquitin K48 or K11 mainly lead to degradation via the 26S proteasome (Komander and Rape, 2012). Mono-ubiquitin, multi-monoubiquitin and K63-linked polyubiquitin chains have always been associated with non-26S proteasome degradation processes, such as cargo endocytosis (Komander and Rape, 2012).

In plants, the contribution of ubiquitination in the regulation of cargo trafficking is much less understood, and the specificity of the Ub linkages involved has not been documented so far.

FLS2 is ubiquitinated by the two closely related plant U-box 12 and 13 (PUB12 and PUB13), which promote receptor ubiquitination and degradation (Lu et al., 2011a). However, it remains unclear whether PUB12/PUB13-mediated FLS2 degradation occurs by the proteasome or via the endocytic route. Here, we show that FLS2 is monoubiquitinated in planta upon perception of the flagellin-derived epitope flg22, and that this is dependent on PUB12/PUB13. Using live-cell imaging, we found that flg22-dependent FLS2 endocytosis is impaired in *pub12 pub13* mutants. We identify that inhibition of FLS2 endocytosis in *pub12 pub13* did not alter transient activation of flg22-mediated responses. Instead, lack of PUB12 and PUB13 affected plant responses to repeated and long-term flg22 exposures, leading to insensitivity towards this immune stimulus.

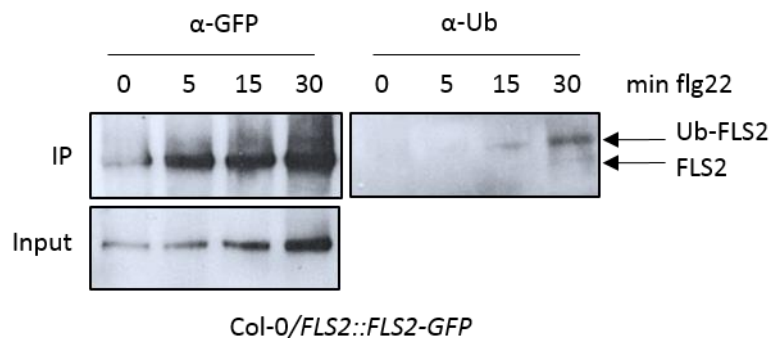
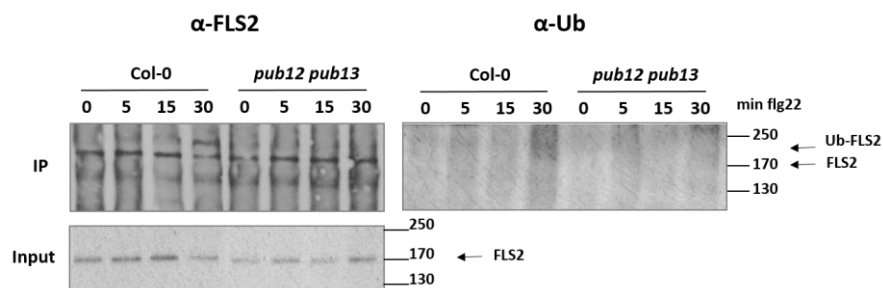
Taken together, our findings identify ubiquitination as a major regulator of flg22-induced FLS2 endocytosis. In addition, we propose that FLS2 trafficking plays a role in plant immunity, whereby receptor internalization sustains the cell's ability to sense immune stimuli during continuous microbial encounters.

### **3.3 FLS2 is Monoubiquitinated After flg22 Stimulation in a PUB12/PUB13-Dependent Manner**

The type of ubiquitination determines the fate of the substrate protein. To assess whether ubiquitination plays a role in regulating FLS2 endocytosis, we performed immunoblot analyses of immunoprecipitated FLS2-GFP using an antibody raised against *Arabidopsis* ubiquitin (2.3 Figure 1A). We observed a shift in the molecular weight of immunoprecipitated FLS2-GFP upon flg22 treatment that corresponded to a ubiquitinated form of FLS2 (2.3 Figure 1A). Ubiquitinated FLS2 predominantly occurred as a single sharp band, rather than higher molecular weight laddering or smear that are typical for poly-ubiquitinated proteins. To determine if poly-Ub chains were present in immunoprecipitated FLS2, we performed  $\alpha$ -K48 and  $\alpha$ -K63 immunoblots. While we

observed a clear signal for both antibodies on total protein extracts, we could not detect the presence of these modifications on immunoprecipitated FLS2 (2.3 Figure 1—figure supplement 1). This suggests that FLS2 is most likely mono- or poly-monoubiquitinated, and that ubiquitination might be mechanistically linked to receptor endocytosis.

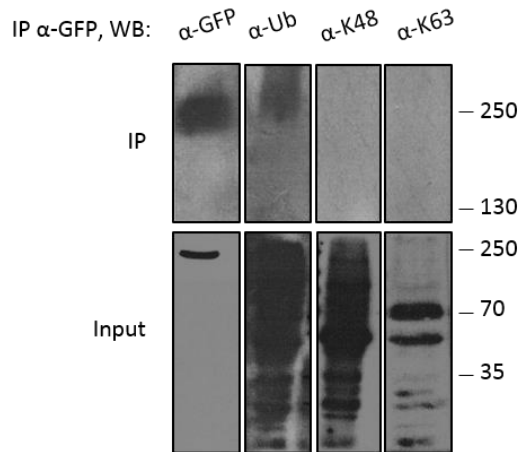
Previous work indicated a critical role for PUB12 and PUB13 in promoting FLS2 ubiquitination and degradation (Lu et al., 2011a). Therefore, we investigated whether PUB12/PUB13 contribute to the overall monoubiquitination of FLS2. Remarkably, we observed that flg22-dependent FLS2 ubiquitination was strongly impaired in the *pub12 pub13* mutant background, as compared to WT (Col-0) (2.3 Figure 1B).

**A****B**

### 2.3 Figure 1.

**flg22 induces monoubiquitination of FLS2 in vivo in a PUB12/PUB13-dependent manner.**

**(A)** *Col-0/FLS2p::FLS2-GFP* seedlings were treated or not (0) with 10  $\mu$ M flg22 for the indicated time points. Total proteins were subjected to immunoprecipitation with anti-GFP beads followed by immunoblot analysis with anti-GFP and anti-ubiquitin antibodies to check FLS2-GFP band shift. **(B)** *Col-0* or *pub12 pub13* seedlings were treated with 10  $\mu$ M flg22 at the indicated time points. Total proteins were subjected to immunoprecipitation with anti-FLS2 antibody followed by immunoblot analysis with anti-FLS2 and anti-ubiquitin antibodies to identify FLS2 band shift.



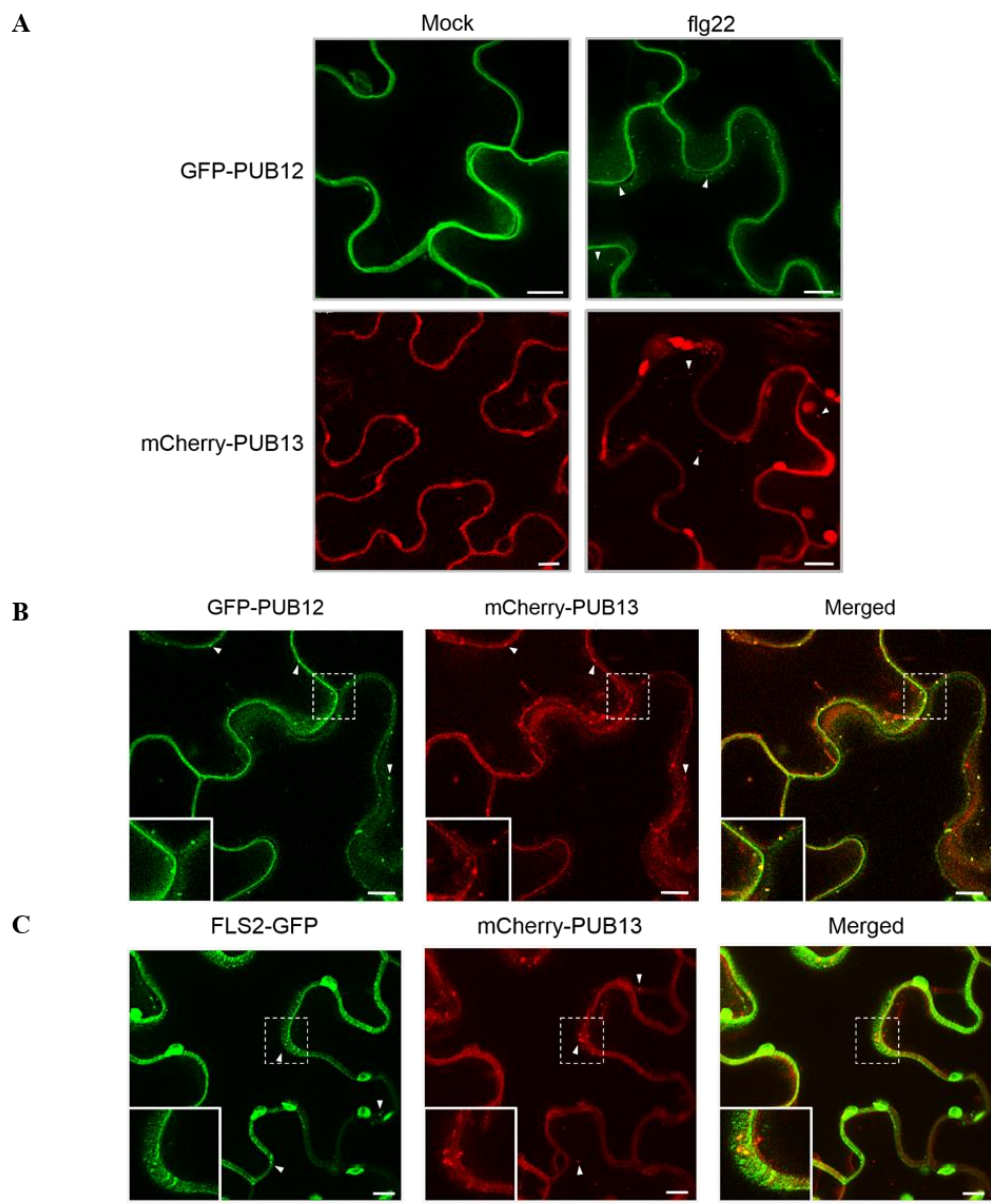
### 2.3 Figure 1 —figure supplement 1.

#### FLS2 is not targeted by K48 and K63 polyubiquitin chains.

Col-0/FLS2p::FLS2-GFP seedlings were treated with 10  $\mu$ M flg22 for 30 min. Total proteins were subjected to immunoprecipitation with anti-GFP beads followed by immunoblot analysis with anti-GFP, anti-ubiquitin, anti-K48, and anti-K63 polyubiquitin chains-specific antibodies to check the nature of FLS2-GFP band shift.

### 3.4 PUB12/PUB13-Mediated Ubiquitination of FLS2 Controls Early Endocytic Events in FLS2 Trafficking

PUB12- and PUB13-mediated monoubiquitination of FLS2 suggests a role for these ligases during ligand-induced receptor trafficking. To address this, we first determined the subcellular localization of PUB12 and PUB13. Fluorescent protein (FP)-fusions were generated and transiently expressed in *N. benthamiana*. Confocal microscopy analysis of GFP-PUB12 or mCherry-PUB13 expressed with untagged Arabidopsis BAK1 localized at the cytosol and cell periphery prior to flg22 elicitation (2.3 Figure 2A). Upon flg22 stimulation, a pool of PUB12 and PUB13 localised to intracellular vesicles (2.3 Figure 2A, white arrowheads). Colocalization experiments of GFP-PUB12 and mCherry-PUB13 showed a clear overlap in intracellular compartments upon flg22 treatment (2.3 Figure 2B). By contrast, flg22-elicited FLS2-GFP and mCherry-PUB13 were present in different pools of intracellular vesicles that rarely colocalized (2.3 Figure 2C).



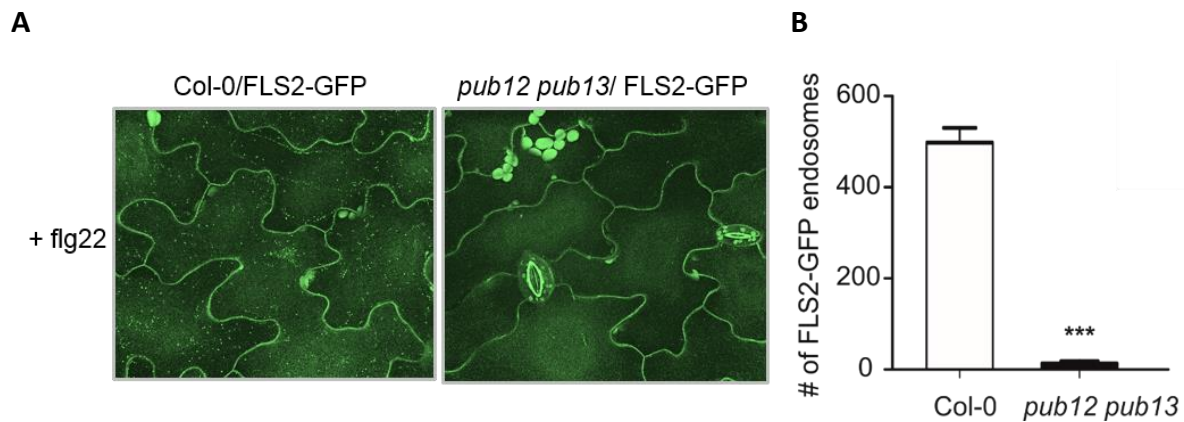
### 2.3 Figure 2.

**PUB12 and PUB13 translocate from the cytosol to intracellular vesicles upon flg22 stimuli.**

(A) Confocal microscopy images of *N. benthamiana* leaf epidermal cells expressing GFP-PUB12 or mCherry-PUB13 treated with mock or 100  $\mu$ M flg22. (B) Confocal images showing the overlap of GFP-PUB12 and mCherry-PUB13 upon elicitation with 100  $\mu$ M flg22 in *N. benthamiana* leaf epidermal cells. White arrowheads point at endosomes. Insets (dashed lines) are magnified in the bottom left corner of the corresponding image. Left, middle and right panels represent fluorescence signals recorded in the green (GFP), the red (mCherry) and the merged channels,

respectively. Bars = 10  $\mu$ m. (C) Colocalization images of internalized FLS2-GFP and mCherry-PUB13 after treatment with 100  $\mu$ M flg22.

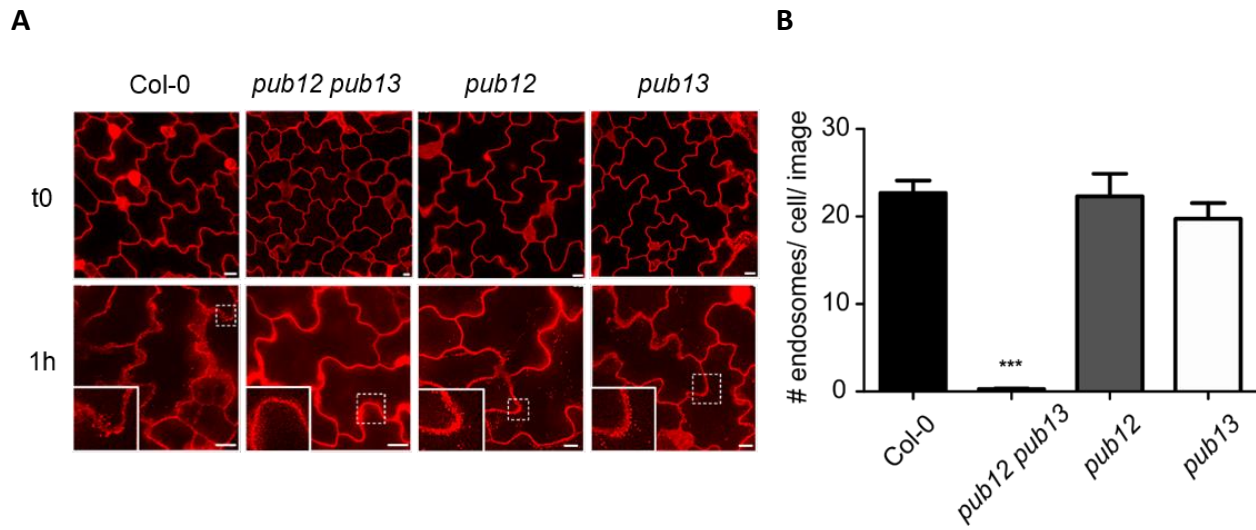
Next, we tested whether endocytosis of FLS2-GFP was affected in the *pub12 pub13* mutant background. Upon flg22 stimulation, FLS2 internalization was abolished in *pub12 pub13* as compared to WT (2.3 Figure 3A and B). In line with this, *pub12 pub13* seedlings were compromised in the internalisation of TAMRA-labelled flg22 (Underwood and Somerville, 2013) (2.3 Figure 4A and B, 2.3 Figure 4—figure supplement 1). This indicates that PUB12 and PUB13 are required for the uptake of FLS2 and its ligand flg22. Importantly, *pub12* and *pub13* single mutants showed WT-like uptake of TAMRA-flg22, although with delayed kinetics (2.3 Figure 4—figure supplement 1). This suggests that PUB12 and PUB13 act redundantly in the regulation of FLS2 endocytosis.



### 2.3 Figure 3.

#### PUB12 and PUB13 are required for FLS2 endocytosis.

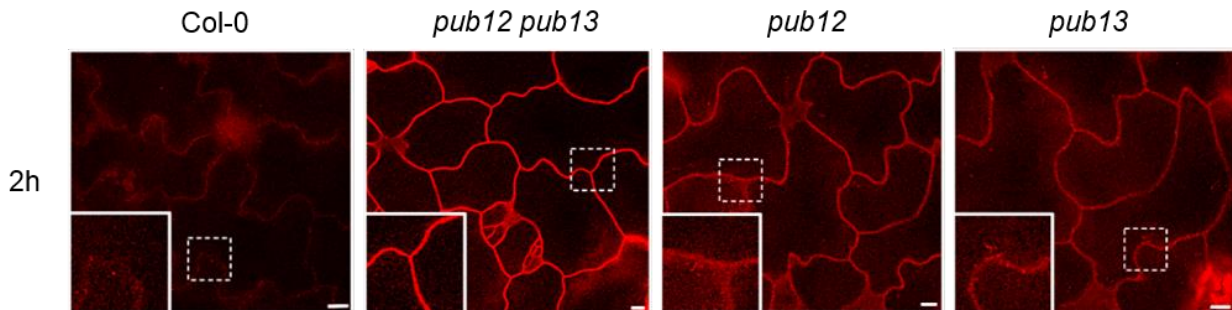
(A) Confocal micrographs of the indicated Arabidopsis lines expressing FLS2-GFP after treatment with 10  $\mu$ M flg22 for 45 min. (B) Quantification of FLS2-GFP positive puncta per image area analysed by one-way ANOVA. Values are shown as means  $\pm$  SEM. Asterisks indicate statistical significance of  $P$  value  $\leq 0.001$ .



### 2.3 Figure 4.

#### PUB12 and PUB13 are required for flg22 uptake.

(A) Confocal microscopy images of epidermal cells of the indicated genotypes after incubation with 20 $\mu$ M TAMRA-flg22 at t0 or 1h. Insets (dashed lines) are magnified in the bottom left corner of the corresponding images. Bars =10  $\mu$ m. (B) Quantification of TAMRA-flg22 endosomal numbers analysed by one-way ANOVA. Values are shown as means  $\pm$  SEM. Asterisks indicate statistical significance of P value  $\leq$  0.001.



### 2.3 Figure 4 —figure supplement 1.

#### *pub12* and *pub13* single mutants are delayed in TAMRA-flg22 internalization.

Epidermal cells 2h post-incubation with 20  $\mu$ M TAMRA-flg22 show stronger fluorescence intensity in *pub12* and *pub13* single mutants as compared to Col-0, indicating a delay in the internalization of flg22.

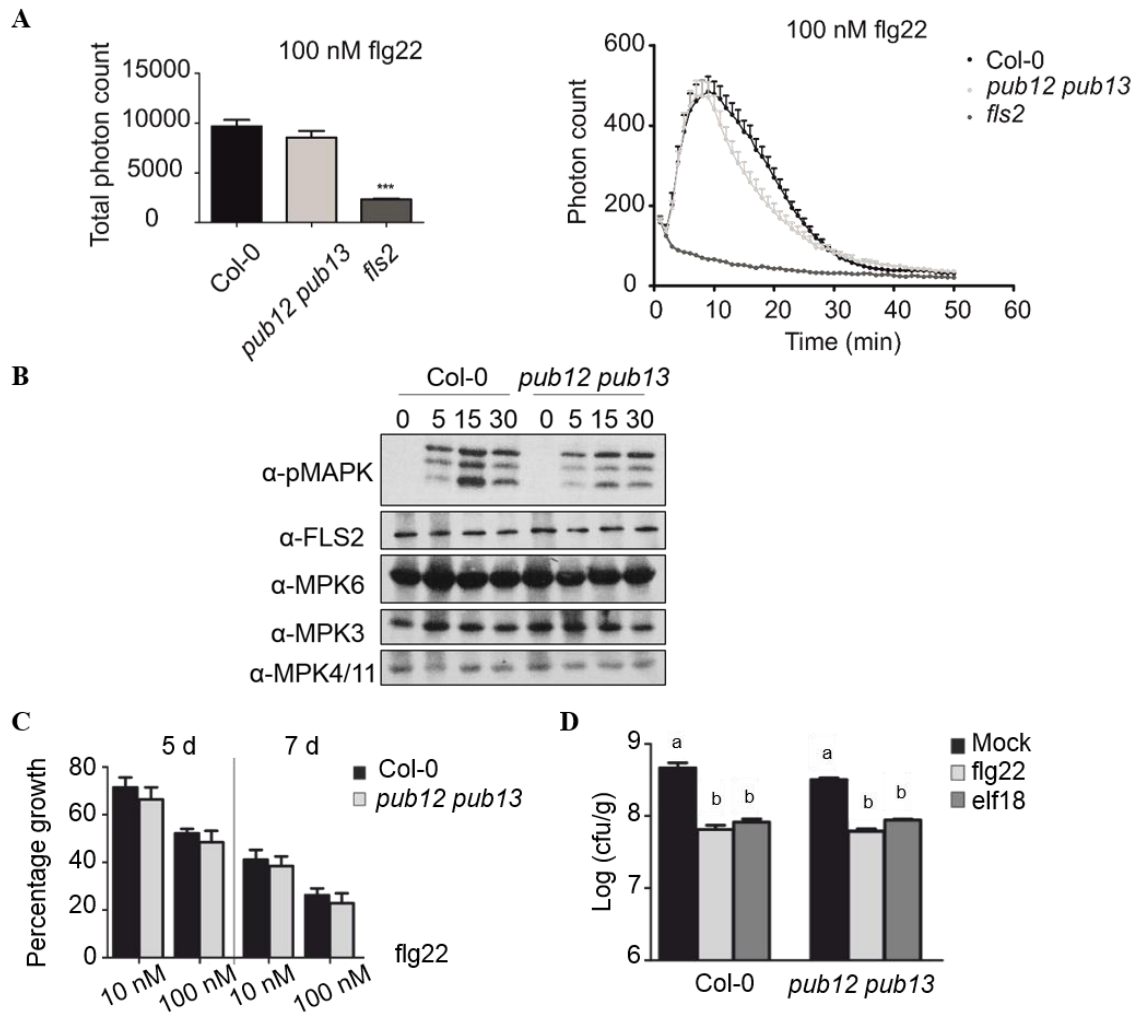
### 3.5 Inhibition of FLS2 Endocytosis in *pub12 pub13* Does Not Contribute to Sustaining or Restricting PTI Signalling

FLS2-mediated signalling was previously suggested to be regulated through receptor endocytosis (Waterman and Yarden, 2001), however the lack of molecular tools to specifically dissect FLS2-mediated signalling would not allow a strong conclusion on this matter. The identification of PUB12 and PUB13, which were previously shown to directly ubiquitinate FLS2 (Lu *et al.*, Science 2011), as critical regulators of ligand-dependent FLS2 endocytosis, provided us with a specific genetic tool to investigate the role of FLS2 endocytosis in PTI signalling.

We started by testing whether mutation of *PUB12* and *PUB13* alters the kinetics of FLS2-mediated signalling. Surprisingly, both flg22-triggered ROS burst and MAPK activation were similar in Col-0 and *pub12 pub13* plants (2.3 Figure 5A and B). These results contrasted with previously published data showing that the *pub12 pub13* mutants display enhanced flg22-induced MAPK activation and ROS production (Lu *et al.*, 2011a, Zhou *et al.*, 2015). Importantly, these studies used plants grown under different light conditions. To determine whether the conflicting results could be explained by the different growth conditions, we tested FLS2 protein accumulation and flg22-induced MAPK activation in seedlings grown under low ( $75 \mu\text{E m}^{-2} \text{s}^{-1}$ ), medium ( $110 \mu\text{E m}^{-2} \text{s}^{-1}$ ) or high ( $180 \mu\text{E m}^{-2} \text{s}^{-1}$ ) light (2.3 Figure 5—figure supplement 1). Strikingly, FLS2 protein accumulation was highly dependent on light conditions, correlating positively with the intensity of light (at least in the tested interval) (2.3 Figure 5—figure supplement 1). Importantly, under low light conditions, FLS2 protein levels were markedly lower in Col-0 as compared to *pub12 pub13*, which correlated with the observed enhanced MAPK activation in *pub12 pub13* seedlings. When grown under both medium and high light, FLS2 proteins accumulated to the same extend in *pub12 pub13* and Col-0 seedlings, and no differences in MAPK activation were detected (2.3 Figure 5—figure supplement 1). Thus, to avoid light-dependent FLS2 protein level variations, all our assays were performed with plants grown under  $110 \mu\text{E m}^{-2} \text{s}^{-1}$ , since  $180 \mu\text{E m}^{-2} \text{s}^{-1}$  is above the optimal light intensity for *Arabidopsis* growth (<https://abrc.osu.edu/seed-handling>). These results highlight the importance of light for the

establishment of PTI, especially regarding the protein levels of key signalling components, such as FLS2.

We then tested whether altering FLS2 endocytosis would have an effect on late PTI responses. Both WT and *pub12 pub13* seedlings showed similar flg22-induced growth inhibition (2.3 Figure 5C). In line with this, flg22- and elf18-induced resistance to *Pseudomonas syringae* pv. *tomato* (*Pto*) DC3000 in *pub12 pub13* seedlings were indistinguishable from those of Col-0 (2.3 Figure 5D). Although, as previously described by Lu et al. 2011, *pub12 pub13* adult plants exhibited enhanced resistance to *Pto* DC3000 (2.3 Figure 5—figure supplement 2), the flg22- and elf18-induced resistance was also to the same levels as WT. This demonstrated that the role of PUB12 and PUB13 in immunity is most likely uncoupled from FLS2 endocytosis and degradation, and could be related to their high endogenous SA levels (Li et al., 2012).

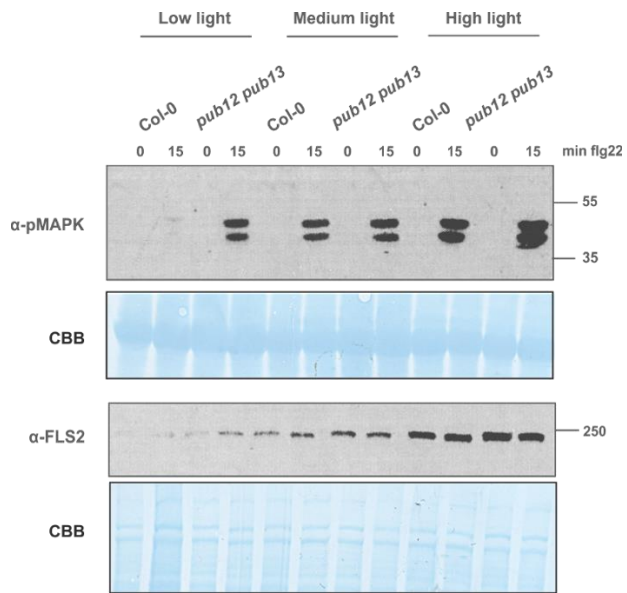


### 2.3 Figure 5.

#### FLS2 endocytosis is uncoupled from PTI signalling.

**(A)** ROS production was measured as relative luminescence units (RLU) in response to 100 nM flg22. Bar graph (left) is representative of two biological repeats. Values shown are means + SEM; n=24. Asterisks indicate statistical significant difference at p-value  $\leq 0.001$  after one-way ANOVA analysis and Tukey's multiple-comparison post-test.

**(B)** Phosphorylation of MAPKs after treatment with 10  $\mu$ M flg22 at the indicated time points. FLS2 protein levels analysed with anti-FLS2. Endogenous levels of MPK3, 4 and 6 were assessed using specific antibodies. **(C)** Seedling growth inhibition triggered by 10 nM and 100 nM flg22 in Col-0 and *pub12 pub13* seedlings for 5 and 7 days. Growth represented relative to mock. Data is mean + SEM, n = 8. **(D)** flg22- and elf18-induced resistance to *Pto* DC3000 in Col-0 and *pub12 pub13* seedlings. Seedlings were pre-treated with 10  $\mu$ M flg22, 10  $\mu$ M elf18 or water 24 hours prior to bacterial infection. Graph representative of three independent biological replicates analysed by one-way ANOVA and Tukey's multiple-comparison post-test. Values are shown as means  $\pm$  SEM, n=6. Letters indicate statistical significance at p-value  $\leq 0.001$ .



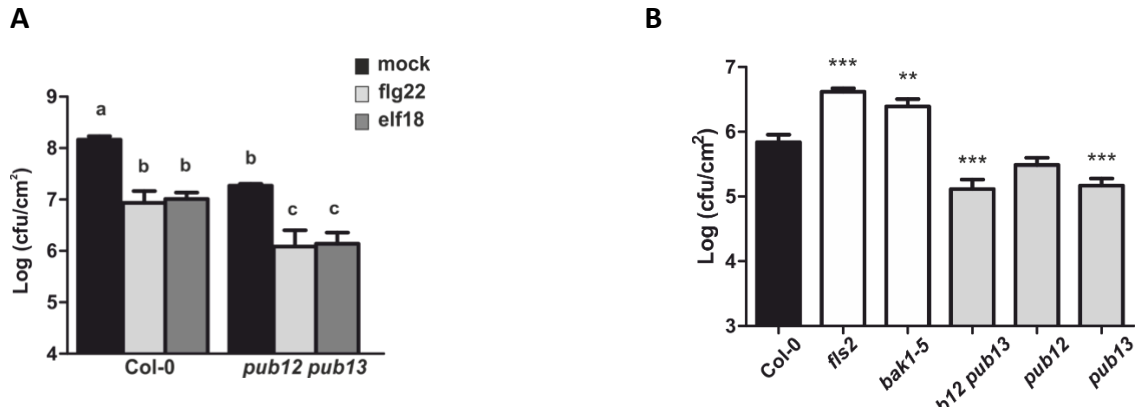
### 2.3 Figure 5—figure supplement 1.

#### Light intensity has an impact on flg22-induced MAPK activation and FLS2 accumulation

Phosphorylation of MAPKs after treatment with 10  $\mu$ M flg22 for the indicated time points. Anti-FLS2 antibody was used to show the levels of the receptor. Seedlings were grown under low ( $75 \mu\text{E m}^{-2} \text{s}^{-1}$ ), medium ( $110 \mu\text{E m}^{-2} \text{s}^{-1}$ ) or high ( $180 \mu\text{E m}^{-2} \text{s}^{-1}$ ) light intensity.

#### 3.6 FLS2 Endocytosis is Required for Maintaining flg22 Responsiveness after Repeated PAMP treatments

Our results show that ligand-mediated endocytosis is uncoupled from both PTI signalling activation and downregulation in the case of FLS2 (2.3 Figure 5). Yet this process is tightly regulated and highly conserved in plants (Mbengue et al., 2016), suggesting an important biological role. To address this, we tested the outcome of blocking endocytosis under conditions of prolonged or repeated ligand exposure, recurrent to the constant interaction of plants with their surrounding bacteria.



### 2.3 Figure 5—figure supplement 2.

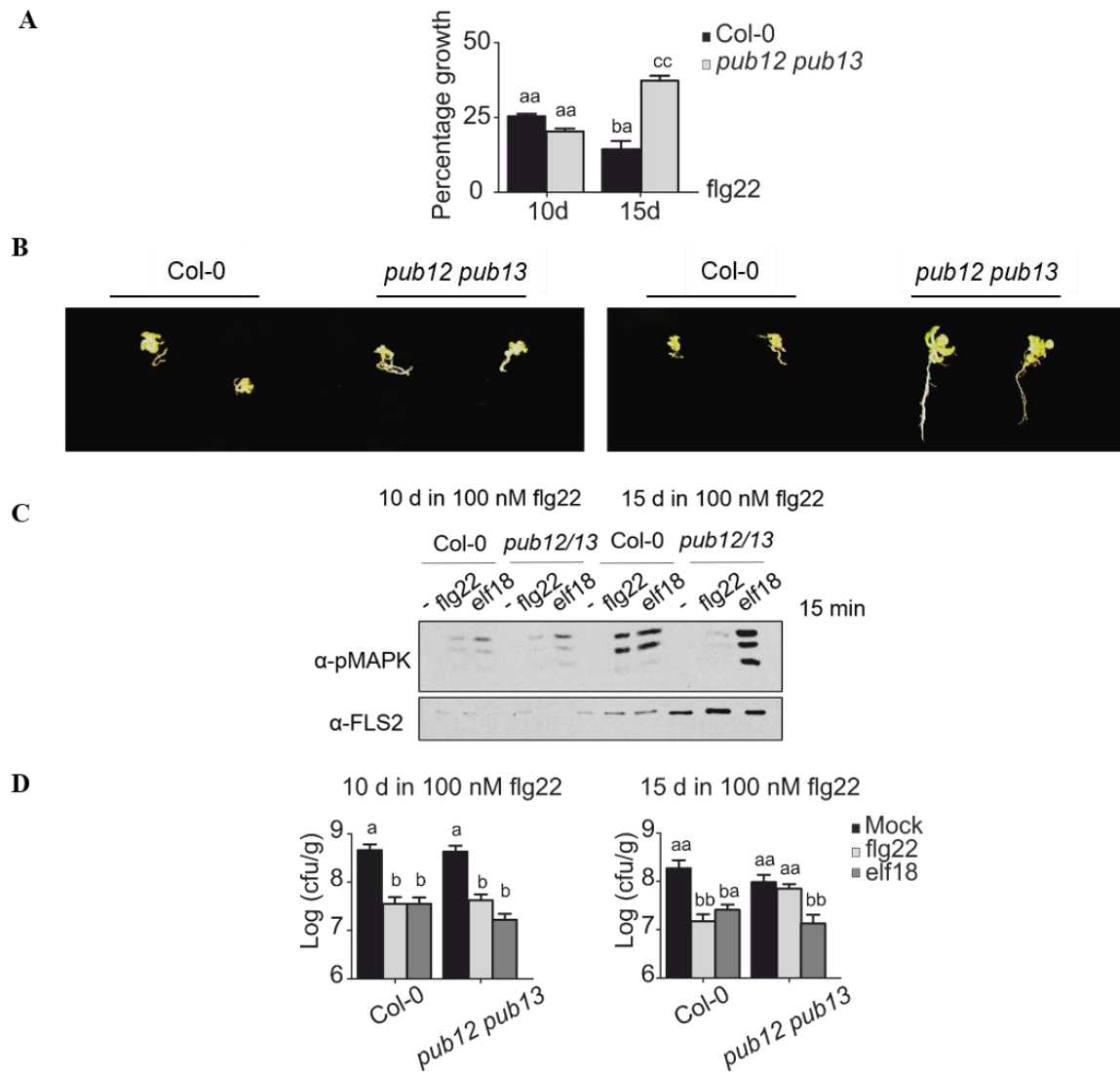
#### *pub12 pub13* adult plants show enhanced resistance to bacteria but similar flg22- and elf18-induced resistance to WT.

**(A)** flg22- and elf18-induced resistance to *Pto* DC3000 in Col-0 and *pub12 pub13* plants. Plants were pre-treated with 10  $\mu$ M flg22, 10  $\mu$ M elf18 or water 24 hours prior to bacterial infiltration. Graph representative of three independent biological replicates analysed by one-way ANOVA and Tukey's multiple-comparison post-test. Values are shown as means  $\pm$  SEM. Different letters indicate statistical significance of  $P$  value  $\leq 0.001$ ; bars represent SE,  $n=6$ . **(B)** Five-week-old Col-0, *fls2*, *bak1-5*, *pub12 pub13*, *pub12* and *pub13* plants were sprayed with *Pto* DC3000. Bacterial counts were assessed at 3 dpi. Values are shown as means  $\pm$  SEM ( $n=16$ ). Similar results were observed in at least three independent experiments and asterisks indicate  $P<0.001$  by one-way ANOVA and Tukey's multiple-comparison post-test.

As previously shown (Figure 5C), *pub12 pub13* mutants showed a WT-like inhibition of growth in response to 100 nM flg22 for up to 10 days of treatment (2.3 Figure 6A). Surprisingly, after 15 consecutive days of exposure to flg22, *pub12 pub13* seedlings restored growth as compared to Col-0 (2.3 Figure 6A and B). This phenotype correlated with a higher accumulation of FLS2 proteins in *pub12 pub13* mutants in comparison to Col-0 (2.3 Figure 6C), which is in agreement with the involvement of PUB12 and PUB13 in receptor degradation (Lu et al., 2011a). Importantly, although *pub12 pub13* seedlings accumulated more FLS2 receptor, their MAPK activation after 3 days of recovery (in the absence of flg22) was impaired in response to flg22 but not elf18, demonstrating that this effect is specifically due to the repeated exposure to flg22 and affects only FLS2-mediated responses (2.3 Figure 6C). In addition, this suggests that blocking endocytosis leads to an accumulation of a signalling-incompetent pool of FLS2 receptors.

To assess the impact of the above observations on plant immunity against virulent bacteria, we determined the responses of the recovered seedlings from long exposure to flg22 to the phytopathogenic bacteria *Pto* DC3000 in a disease protection assay induced by flg22 or elf18. The results showed that, although the bacterial growth in *pub12 pub13* seedlings exposed to flg22 for 15 days was not significantly different from that in Col-0, flg22- but not elf18-induced resistance was strongly reduced (2.3 Figure 6D). This finding shows the requirement of receptor endocytosis and degradation for maintaining the plant ability to provide a signalling-competent pool for FLS2, essential to establish plant immunity.

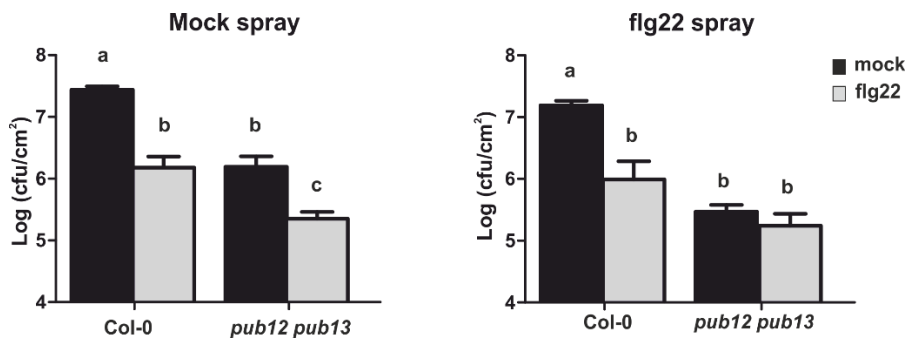
To determine whether this finding can also be confirmed in adult plants, we sequentially sprayed mock or 100 nM flg22 on 5 week old *Arabidopsis* plants prior to infiltration of flg22 and infection with virulent bacteria. In line with our observation in seedlings, flg22-induced resistance was altered in the *pub12 pub13* plants that were repeatedly sprayed with flg22 as compared to those sprayed with mock or to Col-0 (2.3 Figure 6—figure supplement 1).



### 2.3 Figure 6.

#### Ligand-dependent endocytosis and degradation of FLS2 is required for maintaining a signalling competent pool of FLS2.

**(A)** Seedling growth inhibition triggered with 100 nM flg22 in Col-0 and *pub12 pub13* seedlings for 10 and 15 days. Growth is represented relative to the untreated wild type. Results are average  $\pm$  se ( $n = 32$ ). **(B)** Representative phenotypes of randomly selected seedlings measured in **A**. **(C)** Phosphorylation of MAPKs after treatment with water (-), 10  $\mu$ M flg22 or 10  $\mu$ M elf18 for 15min in Col-0 and *pub12 pub13* seedlings recovered from **A**. anti-FLS2 antibody was used to show the levels of the receptor. **(D)** Seedlings from **A** were recovered for 3 days in liquid MS then treated with 10  $\mu$ M flg22, elf18 or water 24 hours prior to infection with *Pto* DC3000 (OD600 of 0.0002). Graph representative of at least three independent biological replicates analysed by one-way ANOVA and Tukey's multiple-comparison post-test. Values are shown as means  $\pm$  SEM. Different letters indicate statistical significance of  $P$  value  $\leq 0.001$ ; bars represent SE,  $n=12$ .



### 2.3 Figure 6—figure supplement 1.

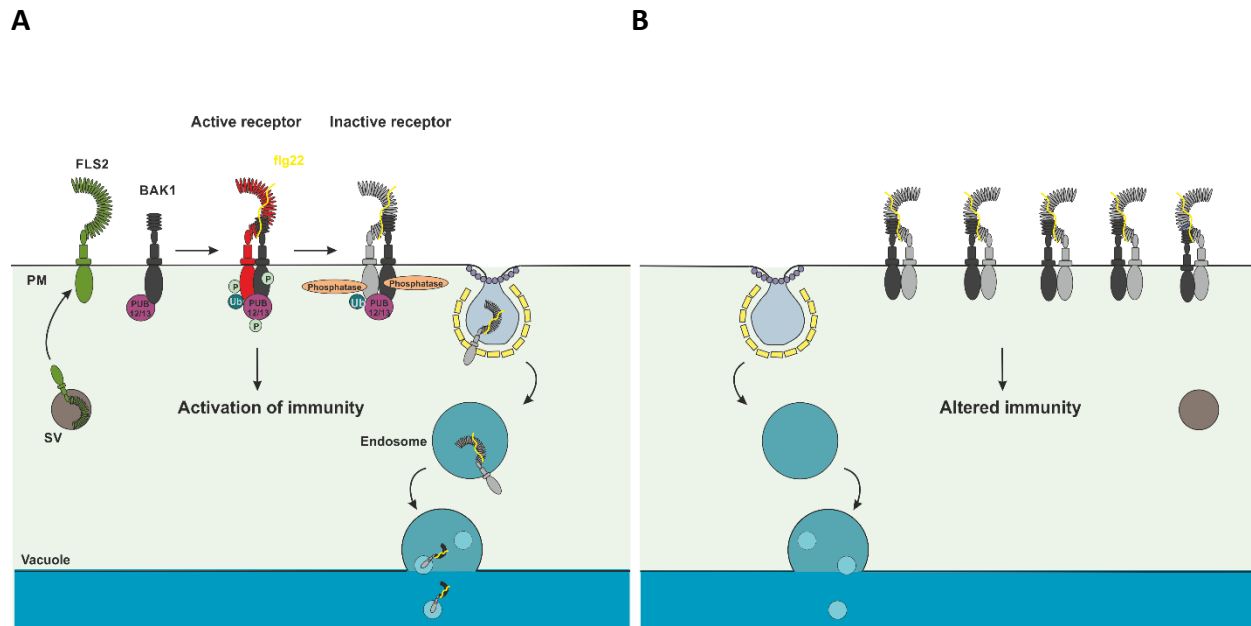
#### flg22-induced resistance is lost in *pub12 pub13* plants repeatedly sprayed with the PAMP.

5-week old plants were sprayed with water or 100 nM flg22 (supplemented with 0.04% Silwett L-77) twice a day for three days. Upon recovery, they were infiltrated with 10  $\mu$ M flg22 24 hours prior to infection with *Pto* DC3000. Graph representative of three independent biological replicates analysed by one-way ANOVA and Tukey's multiple-comparison post-test. Values are shown as means  $\pm$  SEM. Different letters indicate statistical significance of P value  $\leq 0.001$ ; bars represent SE, n=12.

### 3.6 Discussion

Ligand-mediated endocytosis of transmembrane receptors has emerged as a conserved mechanism in plant and mammalian cells (Mbengue et al., 2016, Goh and Sorkin, 2013). In the present study we identify, for the first time, a molecular mechanism required for PRR endocytosis in plants. The involvement of PUB12 and PUB13 in FLS2 degradation has already been documented (Lu et al., 2011a), but little information was available concerning the involvement of ubiquitination in receptor trafficking in response to PAMPs. Our results demonstrate that PUB12/PUB13-mediated FLS2 monoubiquitination drives receptor internalization upon ligand binding. To the contrary of previous approaches using mutants affected in general trafficking, we addressed the role of FLS2 endocytosis in *pub12 pub13* mutants. MAPK activation, ROS burst, SGI, and induced resistance assays revealed that FLS2 endocytosis is uncoupled from PTI activation as well as signal downregulation (2.3 Figure 5), demonstrating that FLS2 signalling is initiated exclusively at the PM. Moreover, we showed that inhibition of FLS2 internalisation and degradation results, after prolonged exposure to flg22, in growth recovery, altered MAPK

activation, and enhanced susceptibility to virulent bacteria (2.3 Figure 6). This is very likely resulting from a defective delivery of newly synthesised, signalling-competent FLS2 receptors to the PM. These findings shed a new light on our understanding of the importance of dynamic endocytosis and secretion of FLS2 upon flg22 stimulus for maintaining PAMP responsiveness (2.3 Figure 7).



### 2.3 Figure 7.

#### Model of regulation of FLS2 endocytosis by dynamic ubiquitination and its requirement for immunity after repeated PAMP stimulation.

(A) Upon flg22 perception, FLS2 forms an active complex with the co-receptor BAK1 and induces immune signalling. Once PTI is successfully initiated, PUB12 and PUB13 ligases monoubiquitinate FLS2. This triggers the endocytic trafficking of ligand-bound FLS2 towards vacuolar degradation, enabling the replenishment of the PM with newly synthesised receptors. (B) In *pub12 pub13* mutants, repeated or prolonged exposure to flg22 leads to an accumulation of signalling-incompetent receptors at the cell periphery. This might alter the ability of the cell to replenish the PM with new receptors, and ultimately result in insensitivity to flg22. Arrows indicate trafficking through the secretory pathways via secretory vesicles (SV), and endocytic pathways via endosomes. Colour coding of FLS2 is as following: Green indicates signalling competent receptors, red indicates ligand-bound receptors engaged in immune signalling, and grey indicates ligand-bound receptors that have been deactivated potentially by PM-associated phosphatases. P: phosphorylation. Ub: ubiquitination.

The approach undertaken in this work specifically assesses the effect of inhibiting PRR trafficking on PTI activation by identifying the molecular regulation underlying ligand-mediated endocytosis. Protein ubiquitination is an important post-translational modification enabling the cell to remodel its proteome, and thus rapidly respond to external stimuli (Behrends and Harper, 2011). It regulates key cellular functions, including protein degradation, endocytic trafficking, signal transduction, and DNA replication and repair (Grabbe et al., 2011). The fate of the modified substrate is determined by the nature of the Ub linkage (Komander and Rape, 2012). Therefore, determining the type of ubiquitination that targets FLS2 in vivo upon flg22 perception is an important indication to whether this PTM is involved in receptor internalisation. Using pull down assays and antibodies specific for K48- and K63-linked polyubiquitin chains, we showed that flg22-activated FLS2 is targeted by monoubiquitination in a PUB12/PUB13-dependent manner (2.3 Figure 1, 2.3 Figure1 —figure supplement 1). Conversely, in vitro ubiquitination assays previously showed that both PUB12 and PUB13 polyubiquitinate FLS2 (Lu et al., 2011a). E3 enzymes synergize with different E2s to adopt distinct catalytic architectures that define the kind of ubiquitination their substrate will receive (Hibbert et al., 2011, Brown et al., 2016). Hence, it is possible that PUB12 and PUB13 are capable of catalysing ubiquitin chains in vitro with UBC8, but have a preference for a different E2 enzyme in vivo to induce monoubiquitination of FLS2. However, we cannot rule out that FLS2 might be targeted by other types of ubiquitination. Indeed, misfolded FLS2 proteins are very likely to be K48-polyubiquitinated at the level of the endoplasmic reticulum (ER) and destined for proteasomal degradation (Liu and Li, 2014). Nevertheless, it appears that polyubiquitinated FLS2 is below our range of detection by immunoblot analysis of immunoprecipitated receptors.

Consistent with its importance in triggering FLS2 degradation, ubiquitination is employed by the *P. syringae* type III-secreted effector AvrPtoB, which is an active E3 ligase (Gohre et al., 2008). This leads to the removal of FLS2 from the cell periphery, supporting the virulence of *Pto* DC3000. AvrPtoB ubiquitination of FLS2 is further amplified after flg22 treatment. Whether AvrPtoB competes with PUB12 and PUB13 for the same ubiquitination sites remains to be showed. It is possible that PUB12/PUB13-mediated FLS2 ubiquitination and endocytosis could feedback to the

secretory machinery to replenish the PM with new receptors, whereas AvrPtoB-mediated FLS2 degradation doesn't lead to such feedback.

PUB12 and PUB13 constitutively interact with BAK1, which suggests that they are PM-associated (Lu et al., 2011a). Additionally, PUB13 was shown to interact with FLS2 10 seconds after flg22 perception (Lu et al., 2011a), whereas endocytosis of activated FLS2 was only observed after 15 min (Lu et al., 2011a, Robatzek et al., 2006, Beck et al., 2012b). This indicates that PUB12 and PUB13 are recruited to the FLS2 receptor complex prior to internalisation. PUB13 was reported to localise to the TGN and Golgi compartments (Antignani et al., 2015). Hence, we tested the localisation of PUB12 and PUB13 before and after PAMP treatment. Our results show that both E3 ligases are in the cytosol and cell periphery and relocalize to overlapping intracellular vesicles after flg22 perception (2.3 Figure 2). Surprisingly, PUB13-positive compartments did not colocalize with FLS2-GFP labelled endosomes. This suggests that PUB12 and PUB13 ligases dissociate from FLS2 upon internalisation and are recycled back to the cytoplasm, while FLS2 continues along the late endocytic trafficking route.

Sorting of FLS2 onto intraluminal vesicles (ILVs) of late endosomes/ multivesicular bodies (LE/MVBs) depends on its interaction with the vacuolar sorting protein (VPS) 37, a component of the endosomal sorting complex required for transport (ESCRT machinery) (Spallek et al., 2013). In the case of the human epidermal growth factor receptor (EGFR), the ESCRT machinery spatially segregates ligand-stimulated ubiquitinated receptors from the non-ubiquitinated ones that are retained at the MVB limiting membrane, before being recycled back to the PM. Once the recycling receptors have been removed, MVBs fuse with lysosomes and release the ILVs content, enabling the degradation of ligand-stimulated EGFR (Eden et al., 2012). This led us to hypothesise that blocking FLS2 ubiquitination could alter its recognition by the ESCRT machinery and result in its accumulation at the TGN or the MVB limiting membrane. This was not the case, as *pub12 pub13* mutants showed no formation of FLS2-positive vesicles (2.3 Figure 3, 2.3 Figure 4), suggesting that receptor ubiquitination is required for early endocytosis events. Yet it might be possible that our imaging techniques only allow us to detect late endosomes, but this is not likely

since we could previously image FLS2-GFP in the outer membrane of MVBs in the *yps37-1* mutants (Spallek et al., 2013).

Using *pub12 pub13* mutants, we showed that FLS2 endocytosis is uncoupled from flg22-triggered ROS burst, MAPK activation, seedling growth inhibition, and induced resistance to virulent bacteria. Notably, the duration of the responses was also not altered suggesting that signalling gets down-regulated despite of the PM accumulation of the FLS2 receptor (2.3 Figure 5). It is therefore possible that FLS2 inactivation occurs at the PM prior to endocytosis, suggesting that PRRs are only capable of “one round” signalling, or that deactivation mechanisms are recruited within minutes of receptor activation. Recently, three different groups have shown that mutation of *PUB13* results in enhanced resistance to virulent bacteria (Antignani et al., 2015, Li et al., 2012, Lu et al., 2011a, Zhou et al., 2015). The effects were predominantly dependent on salicylic acid (SA), since SA-responsive genes were elevated in the *pub13* mutants (Antignani et al., 2015, Li et al., 2012). The results are not necessarily contradictory with ours since: i) we confirmed that *pub12*, *pub13*, and *pub12 pub13* mutants show enhanced resistance to *Pto* DC300 (2.3 Figure 5—figure supplement 2A and B), but demonstrated that this is unlikely to be mediated by FLS2 (2.3 Figure 5—figure supplement 2A); ii) the aforementioned studies used light conditions that either affected the accumulation of the FLS2 receptor and therefore activation of MAP kinases or were beyond the optimal physiological growth conditions of *Arabidopsis*. The findings of all studies highlight the complexity of the mode of action of the U-box E3 ligases and suggest light-dependent receptor accumulation and MAPK activation, which will need to be further explored. It will be equally important to determine whether light conditions have a similar effect on other PTI outputs and whether their dysregulation contributes to pathology.

Plants are in constant interaction with their microbiome and our sporadic PAMP treatments might be insufficient to fully understand the impact of blocking endocytosis on PTI. Hence, we prolonged our seedling growth inhibition assay for up to 15 days. Strikingly, we observed that *pub12 pub13* mutants restore growth at 15 days as compared to Col-0, symptomatic of a defect in their responsiveness to flg22 (2.3 Figure 6A and B). This correlated with altered MAPK

activation and induced resistance to *Pto* DC3000 (2.3 Figure 6C and D), suggesting that ligand-dependent endocytosis is required for maintaining a signalling-competent pool of FLS2 at the PM. It was recently demonstrated that clathrin-mediated endocytosis is spatially synchronised with exocytosis (Yuan et al., 2015). Considering that proteins are hypothesised to be non-homogenously distributed along the PM, but rather in small islands or microdomains, it is logical to speculate that long-term inhibition of the removal of activated FLS2 would result in defective exocytosis of newly synthesised receptors, and therefore impaired responsiveness.

Additionally, it is still possible that alternative endocytic routes might compensate for the impaired FLS2 endocytosis in the absence of PUB12 and PUB13 E3 ligases. Our observed phenotypes might reflect the additional effects of impaired PUB12/PUB13-dependent endocytosis of FLS2 and alternative slower, possibly clathrin-independent pathways, although a recent study strongly challenges the contribution of clathrin-independent pathways in cargo uptake (Bitsikas et al., 2014).

The accumulation of significantly higher levels of FLS2 in the *pub12 pub13* seedlings as compared to Col-0 at 15 days (2.3 Figure 6C), and their inability to induce flg22-dependent MAPK activation, suggests that this pool of FLS2 is signalling incompetent. Added to our observation that ROS burst and MAPK activation are downregulated in the *pub12 pu13* mutants despite maintaining PM localisation of FLS2 (2.3 Figure 5), this indicates that deactivation of PRR signalling occurs at the level of the PM, prior to receptor endocytosis (2.3 Figure 7). This is reminiscent of the activation/deactivation mechanism of the G-protein-coupled receptors (GPCRs), whereby ligand-bound GPCRs deactivation precedes internalisation and is regulated via phosphorylation by the receptor kinases GRKs. The mechanism that negatively regulates signalling at the FLS2 receptor level is therefore still the missing piece of the puzzle; evidently, this doesn't exclude additional negative regulatory mechanisms at the levels of cytoplasmic kinases such as Botrytis-induced kinase 1 (BIK1) and MAPK kinase kinases (MAPKKKs).

In summary, our data demonstrate the requirement of the U-box E3 ligases for FLS2 endocytosis, corroborating previously established knowledge on the molecular mechanism underlying FLS2 degradation and unveiling the biological relevance of internalisation of FLS2 for maintaining plant responsiveness to bacteria.

### **3.7 Materials and Methods**

#### **Plant Materials and Growth Conditions**

Plant materials and growth conditions have been previously described (Albrecht et al., 2012, Schwessinger et al., 2011). Briefly, *Arabidopsis thaliana* ecotype Columbia (Col-0) was used as the wild-type control. Arabidopsis adult plants used in this study were grown as one plant per pot at 20-21°C with a 10 h photoperiod in environmentally controlled chambers. Seedlings were grown on plates containing Murashige–Skoog (MS) medium (including vitamins) (Duchefa, Haarlem, The Netherlands), 1% sucrose, supplemented or not (liquid) with 0.8% agar, at 22°C and with a 16 h photoperiod. Generation of *pub12 pub13*, *pub12* and *pub13* mutant plants has been described before (Lu et al., 2011a). *pub12 pub13* plants expressing *FLS2p::FLS2-GFP* were obtained by crossing. Primers for genotyping of this line are included in Table 1.

#### **Chemicals**

Elicitors and treatments have been described before (Albrecht et al., 2012). Proteasome inhibitor MG132 (Merck Chemicals/ Calbiochem) was used at 100 µM to pre-treat plant tissues for 4h before PAMP treatment. The inhibitor was applied by floating seedlings in the inhibitor solution and was additionally added to the extraction buffer at 50 µM for immunoprecipitation assays. Furthermore, N-Ethylmaleimide (Sigma) was added to the extraction buffer at 2 µM.

#### **Protein Extractions, Immunoprecipitations, and Immunoblot Analyses**

Protein extractions, immunoprecipitations, and immunoblots were performed as previously described (Schwessinger et al., 2011, Albrecht et al., 2012). Two-week-old Arabidopsis seedlings were used for protein extractions. Plant materials were ground in liquid nitrogen, and then

extracted with buffer [150 mM Tris-HCl, pH 7.5; 150 mM NaCl; 5mM EDTA; 1% Igepal; 1% (vol/vol) protease inhibitor mixture, phosphatase inhibitor 2 and 3 (Sigma)] added at 1.5 mL/g powder. Samples were centrifuged 15 min at 4 °C and 21,000 g. Supernatants were adjusted to 3 mg/mL protein and incubated 4 h at 4 °C with 100 µL GFP-Trap coupled to agarose beads (Chromotek) with gentle agitation or with 20 µL True Blot beads (eBioscience) previously incubated for 30min with 15 µL of anti-FLS2 antibody. Following incubation, the beads were collected and washed four times with the extraction buffer. For western blot, SDS loading buffer was then added to the beads, which were boiled for 10 min. Proteins were separated by SDS/PAGE 10% and analysed by Western blot. Immunodetection of FLS2 has been described before (Chinchilla et al., 2006). Ubiquitinated proteins were detected with anti-ubiquitin (Santa Cruz), anti-ubiquitin Lys48-specific (Millipore, UK) or anti-ubiquitin Lys63-specific (Millipore, UK) antibodies.

### **Cloning**

Arabidopsis PUB12 and PUB13 were synthesized as Golden Gate cloning-compatible level 0 modules. They were assembled with a digestion/ ligation reaction into pICH47761 level 1 vector to obtain Ub10::GFP-PUB12-NOS and Ub10::mCherry-PUB13-NOS. Resulting plasmids were sequenced (primers in Table 1) and transformed into *Agrobacterium tumefaciens* GV3101pMP90 by electroporation and used for transient expression in *N. benthamiana*.

### **Confocal Microscopy**

Subcellular localization of FLS2-GFP, GFP-PUB12 and mCherry-PUB13, transiently expressed in *N. benthamiana*, was determined by confocal laser-scanning microscopy with a DM6000B/TCS SP5 microscope (Leica) using standard settings for GFP and RFP detection provided by the manufacturer. Five-week-old *N. benthamiana* plants were used for transient expression assays as described before (Mbengue et al., 2016). TAMRA-flg22 was imaged in 5-days-old Arabidopsis seedlings as described before (Mbengue et al., 2016). In brief, seedlings were dipped in 20 µM TAMRA-flg22 solution in liquid MS then washed twice with liquid MS for one minute. Samples were imaged either immediately (t0) or 1 hour after treatment.

F2 seedlings from the cross between *pub12 pub13* and Col-0/FLS2-GFP were imaged using the

spinning disc high-throughput automated Opera microscope (Perkin-Elmer Cellular Technologies) as described (Beck et al., 2012c) and were analysed with the image processing software Acapella (version 2.0; Perkin-Elmer) with an algorithm previously described (Beck et al., 2012c) for quantification of endosomal numbers.

### **ROS Burst Assays**

ROS burst assays were performed as described previously (Albrecht et al., 2012). ROS was elicited with flg22 (100 nM). 24 leaf discs from 5-week-old plants were used for each condition. Luminescence was measured over 50 min using a High Resolution Photon Counting System (HRPCS218) (Photek, UK) coupled to an aspherical wide lens (Sigma Corp, Japan).

### **MAP Kinase Activation Assays**

MAP kinase activation assays were performed as described in (Schwessinger et al., 2011). Phospho-p44/42 MAPK (Erk1/2; Thr202/Tyr204) rabbit monoclonal antibodies (Cell Signaling Technologies, Hitchin, UK) were used according to the manufacturer's protocol.

### **Seedling Growth Inhibition Assay**

Seedling growth inhibition assays were performed as described in (Nekrasov et al., 2009). In brief, four-day-old *Arabidopsis* seedlings were grown in liquid MS medium containing 1% sucrose supplemented with flg22 and the appropriate chemicals. Seedlings were weighed between 5 and 15 days after treatment.

### **Bacterial Infections**

Induced resistance assays were performed as described previously (Zipfel et al., 2004). In brief, water, 10  $\mu$ M flg22 or 10  $\mu$ M elf18 solution were infiltrated with a needleless syringe into leaves of four-week-old *Arabidopsis* plants 24 hours prior to bacterial inoculation (*Pto* DC3000, OD600 of 0.0002). Bacterial growth was determined 2 days after inoculation by plating serial dilutions of leaf extracts. To test the effect of repeated stimulations, water or 100 nM of flg22 supplemented with 0.04% Silwet L-77 was sprayed twice a day for three days. Plants were then rested for three

days before performing the induced resistance assay.

Spray inoculation of *Pto* DC3000 0788-9 was performed as described in (Schwessinger et al., 2011). In brief, bacteria were grown in an overnight culture in LB medium, cells were harvested by centrifugation, and pellets were re-suspended to OD600 = 0.02 in 10 mM MgCl<sub>2</sub> with 0.04% Silwet L-77. Bacterial suspensions were sprayed onto leaf surfaces and plants were kept covered for the first 24 hours. Bacterial growth was determined 2 days after inoculation by plating serial dilutions of leaf extracts.

### **Statistical Analysis**

Statistical significances based on one-way ANOVA analyses were performed with Prism 5.01 software (GraphPad Software).

# **Chapter 3: Ligand-Dependent EFR Endocytosis is a Determinant of Long-Term Cellular Responsiveness to EF-Tu and is Regulated by Tyrosine Phosphorylation (PAPER2)**

## **1. Abstract**

Cell surface-localized pattern recognition receptors (PRRs) control key immune processes during infection by microbes. Upon ligand binding, the EF-Tu receptor (EFR) interaction with brassinosteroid insensitive 1 (BRI1)-associated kinase 1 (BAK1) leads to phosphorylation of specific tyrosine (Y) residues. This activation initiates downstream immune responses and the internalization of EFR from the plasma membrane into endosomes. The view of endocytosis as a way of propagating receptor kinase responses from intracellular compartments or attenuating signalling due to receptor removal is highly controversial. Here, using site-directed mutagenesis, we identified Y875 and Y877 as critical for EFR endocytosis, but uncoupled from forming signalling competent complexes. Both  $\text{EFR}^{\text{Y875F}}$  and  $\text{EFR}^{\text{Y877F}}$  variants exhibited wild type-like oxidative burst and mitogen-associated protein kinase (MAPK) activation stimulated by the EF-Tu derived peptide elf18, suggesting that EFR endocytosis is not required to regulate these elf18-induced responses. Plants establish long-life associations with microbiota, a condition of continuous exposure to EF-Tu. Long-term EF-Tu stimulation inhibited seedling growth, but with increasing time,  $\text{EFR}^{\text{Y875F}}$  and  $\text{EFR}^{\text{Y877F}}$  plants, not wild type, recovered growth. This correlated with a reduction in MAPK activation and failure to induce resistance to bacterial infection. Altogether, our results identify ligand-dependent EFR endocytosis as a determinant of long-term cellular signalling responsiveness during the continuous encounters between plants and their surrounding bacteria.

## 2. Introduction

Plants are sessile organisms that lack specialized immune cells. For their interaction with pathogens, plants rely heavily on a complex cell-autonomous defence network. The plant innate immune system detects invaders via recognition of non-host molecules such as pathogen-associated molecular patterns (PAMPs), or modified host molecules, by pattern recognition receptors (PRRs). PRRs are usually surface-localized receptor-like kinases (RLKs) or receptor-like proteins (RLPs). The best characterized plant PRRs are flagellin-sensing 2 (FLS2) and EF-Tu receptor (EFR), which perceive their respective ligands, flagellin and EF-Tu (Boller and Felix, 2009). This leads to the activation of PAMP-triggered immunity (PTI), comparable to the innate immune system of animals (Boller and Felix, 2009). PTI constitutes a basal immune status effective against a broad spectrum of pathogens. To fulfill their myriad functions, FLS2 and EFR need to associate with the co-receptor BRI1-associated kinase 1 (BAK1) (Roux et al., 2011). This is followed by a series of signalling events such as the production of reactive oxygen species (ROS), phosphorylation of mitogen-activated proteins kinases (MAPKs), stomata closure, callose deposition, transcriptional regulation, and plant growth arrest (Couto and Zipfel, 2016). EF-Tu comprises 5-10% of total bacterial proteins, making it the most abundant protein (Pel and Pieterse, 2013). Thus, maintaining responsiveness to EF-Tu by EFR might rely on tightly regulated host subcellular trafficking mechanisms, allowing the degradation of ligand-bound receptors and the replenishment of the plasma membrane (PM) with newly synthesized PRRs. We have previously shown that EFR undergoes endocytosis upon perception of the EF-Tu derived peptide elf18 (Mbengue et al., 2016). However, the requirement of ligand-mediated endocytosis for maintaining responsiveness to PAMPs has not been address so far.

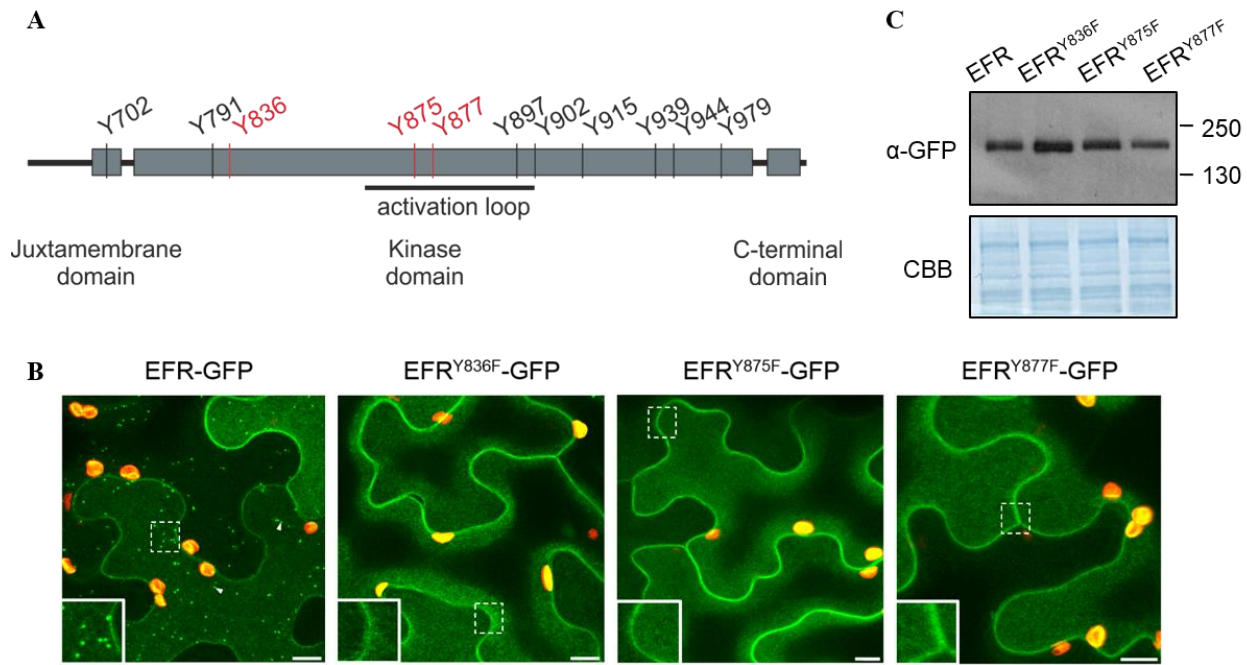
To gain insight into the biological function of ligand-induced endocytosis of EFR, we first dissected the molecular regulation underlying the PRR subcellular trafficking. Tyrosine phosphorylation regulates ligand-mediated endocytosis in mammals (Chowdhury et al., 2013). This is often enabled by the phosphorylation of tyrosine-based motifs within the cargo, which is recognized by endocytic adaptor proteins (Pandey, 2009, Su et al., 2016). Yet, no conclusive evidence have

validated the involvement of such motifs in endocytosis in plants. Using site-directed mutagenesis, we identified Y875 and Y877 as critical for ligand-dependent EFR internalization. Mutation of either one of these tyrosine residues did not alter the formation of signalling-competent complexes or the duration and intensity of PTI responses, uncoupling EFR endocytosis from both signalling activation and down-regulation. Instead, long-term and repeated elf18 stimulations in EFR<sup>Y875F</sup>- or EFR<sup>Y877F</sup>-expressing lines resulted in impaired signalling and abolished elf18-mediated protection to virulent bacteria. Thus, our results identify tyrosine-mediated EFR endocytosis as a mechanism for preserving the cell responsiveness to multiple stimuli of bacterial EF-Tu, as it exists in natural encounters of plants with their biotic environment.

### 3. Results

#### 3.1 Y875 and Y877 are Required for Ligand-Induced EFR Endocytosis and Degradation

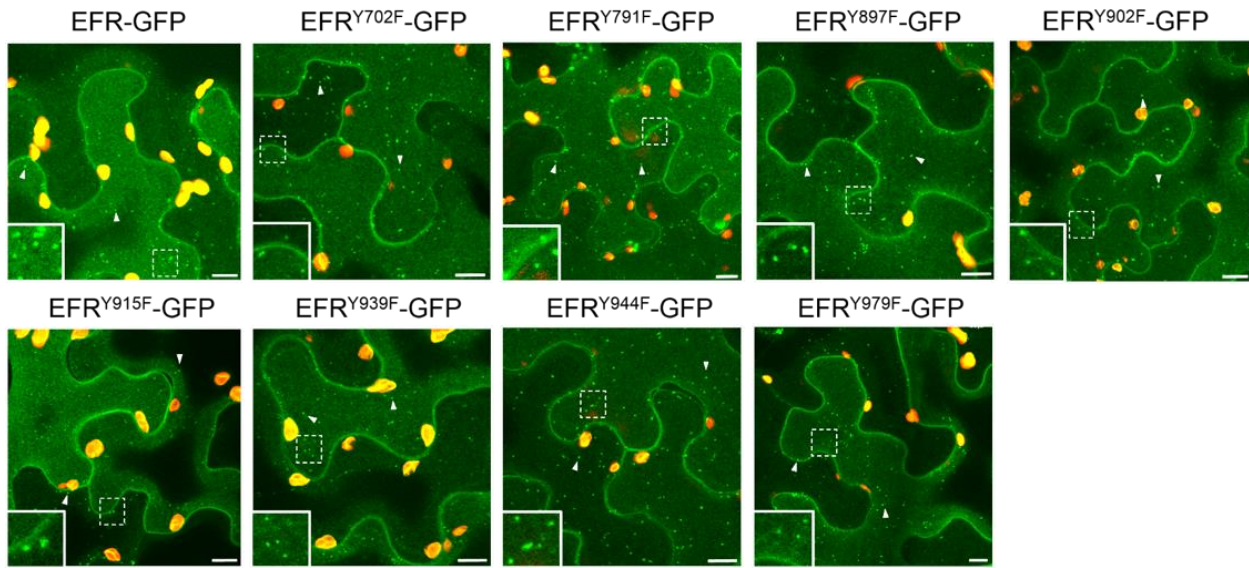
In order to determine whether tyrosine (Y) phosphorylation is involved in the regulation of EFR endocytosis, we screened for altered ligand-induced endocytosis EFR variants carrying individual point mutations in each one of the eleven Y residues present in the EFR cytoplasmic domain (3 Figure 1A). The point mutants were previously obtained by substitution of each tyrosine (Y) to a phenylalanine residue (F), lacking the phosphorylatable hydroxyl group (Macho et al., *Science* 2014). The resulting EFR variants were then transiently expressed in *N. benthamiana*, which lacks endogenous EFR but is otherwise capable of activating elf18-induced immune responses upon EFR expression (Zipfel et al., 2006). All variants accumulated to levels similar to wild-type EFR at the PM (3 Figure 1 B, 3 Figure1—figure supplement 1). Out of the eleven EFR tyrosine mutants, three were compromised in elf18-induced endocytosis: EFR<sup>Y836F</sup>, EFR<sup>Y875F</sup> and EFR<sup>Y877F</sup> (3 Figure 1B and C). This suggests a requirement of Y phosphorylation for ligand-mediated endocytosis of EFR. Since Y836 was previously reported to be essential for EFR function and elf18-triggered responses (Macho et al., 2014), we focused on Y875 and Y877 to investigate the role of ligand-induced PRR endocytosis in innate immunity.



**3 Figure1.**

**Mutational screen identifies Y residues in EFR cytoplasmic domain required for elf18-induced endocytosis.**

(A) Schematic representation of the EFR cytoplasmic domain showing the location of the tyrosine residues. Point mutants of the Y residues highlighted in red are imaged in B. (B) Confocal microscopy images of *N. benthamiana* leaf epidermal cells expressing EFR<sup>Y836F</sup>-GFP, EFR<sup>Y875F</sup>-GFP, and EFR<sup>Y877F</sup>-GFP upon treatment with 100 μM elf18 for 90 min. Insets (dashed lines) are magnified in the bottom left corner of the corresponding images. Bars =10 μm. (C) Western blot analysis showing the accumulation of the EFR variants expressed in B.



### 3 Figure1—figure supplement 1.

**Mutation of most Y residues in the EFR cytoplasmic domain did not affect ligand-induced endocytosis.**

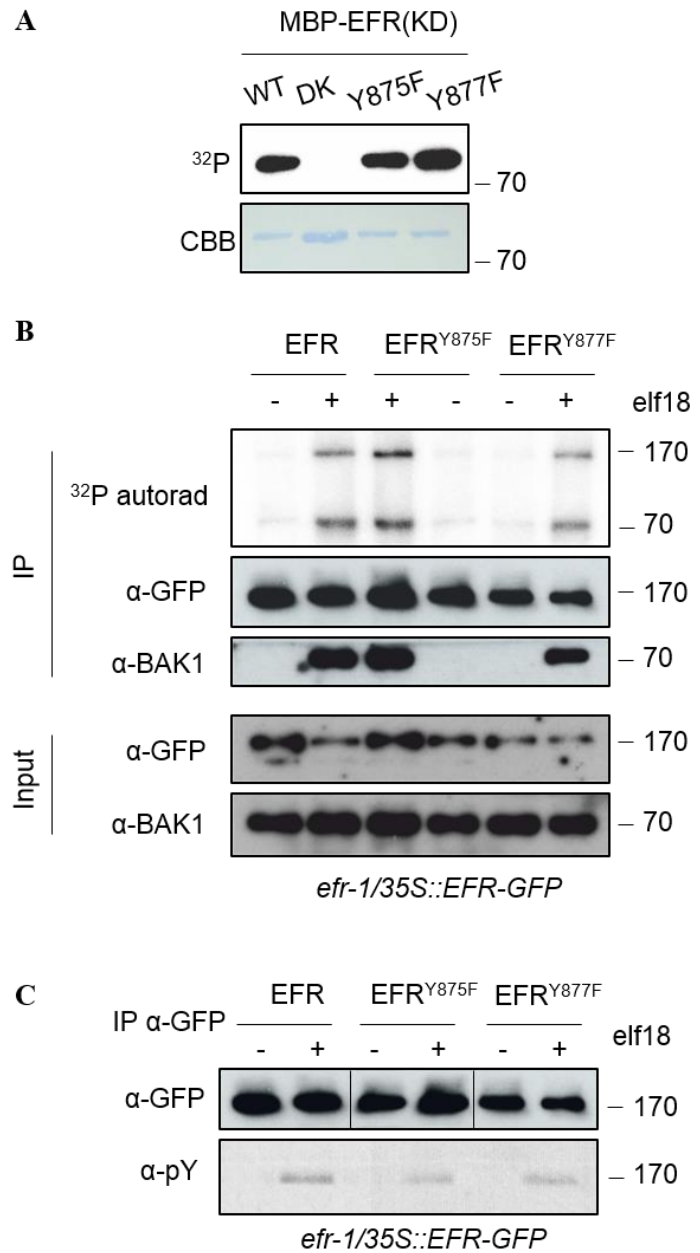
Confocal microscopy images of *N. benthamiana* leaf epidermal cells expressing the indicated constructs upon treatment with 100  $\mu$ M elf18 for 90 min. Insets (dashed lines) are magnified in the bottom left corner of the corresponding images. Bars = 10  $\mu$ m.

### 3.2 Y875- or Y877-mediated Internalization of EFR is Uncoupled from elf18-Triggered Immune Signalling

The Y875 and Y877 residues are positioned in the activation loop of EFR and are phosphorylated in vivo upon elf18 perception (3 Figure2—figure supplement 1A). Alignment of EFR with PRRs and other RLKs showed that these tyrosines are located in a highly variable region (3 Figure2—figure supplement 1B). The in vitro kinase activities of EFR<sup>Y875F</sup> and EFR<sup>Y877F</sup> are almost identical to WT EFR (3 Figure 2A). Using stable transgenic Arabidopsis lines expressing EFR<sup>Y875F</sup>-GFP or EFR<sup>Y877F</sup>-GFP in *efr* mutant background, we immunoprecipitated the EFR mutant variants and subsequently performed in vitro kinase assays using  $^{32}$ P-labelled ATP (3 Figure2—figure supplement 2A). Our results showed that both mutant variants associate with BAK1 in a ligand-dependent manner and are fully catalytic active (3 Figure 2B). The Y875F and Y877F mutations slightly reduced the overall ligand-induced tyrosine phosphorylation of EFR but did not abolish it

(3 Figure 2C), suggesting that Y875 and Y877 are not required for the phosphorylation of other EFR Y residues. Upon *elf18* treatment, a reduction in WT EFR protein levels was observed (Figure 2—figure supplement 2B). Consistent with the altered endocytic phenotype (3 Figure 1A), *elf18*-induced degradation of EFR<sup>Y875F</sup> and EFR<sup>Y877F</sup> was compromised (3 Figure 2—figure supplement 2B). This data provide a mechanistic link between phosphorylation of EFR in Y875 and Y877 and ligand-induced receptor endocytosis.

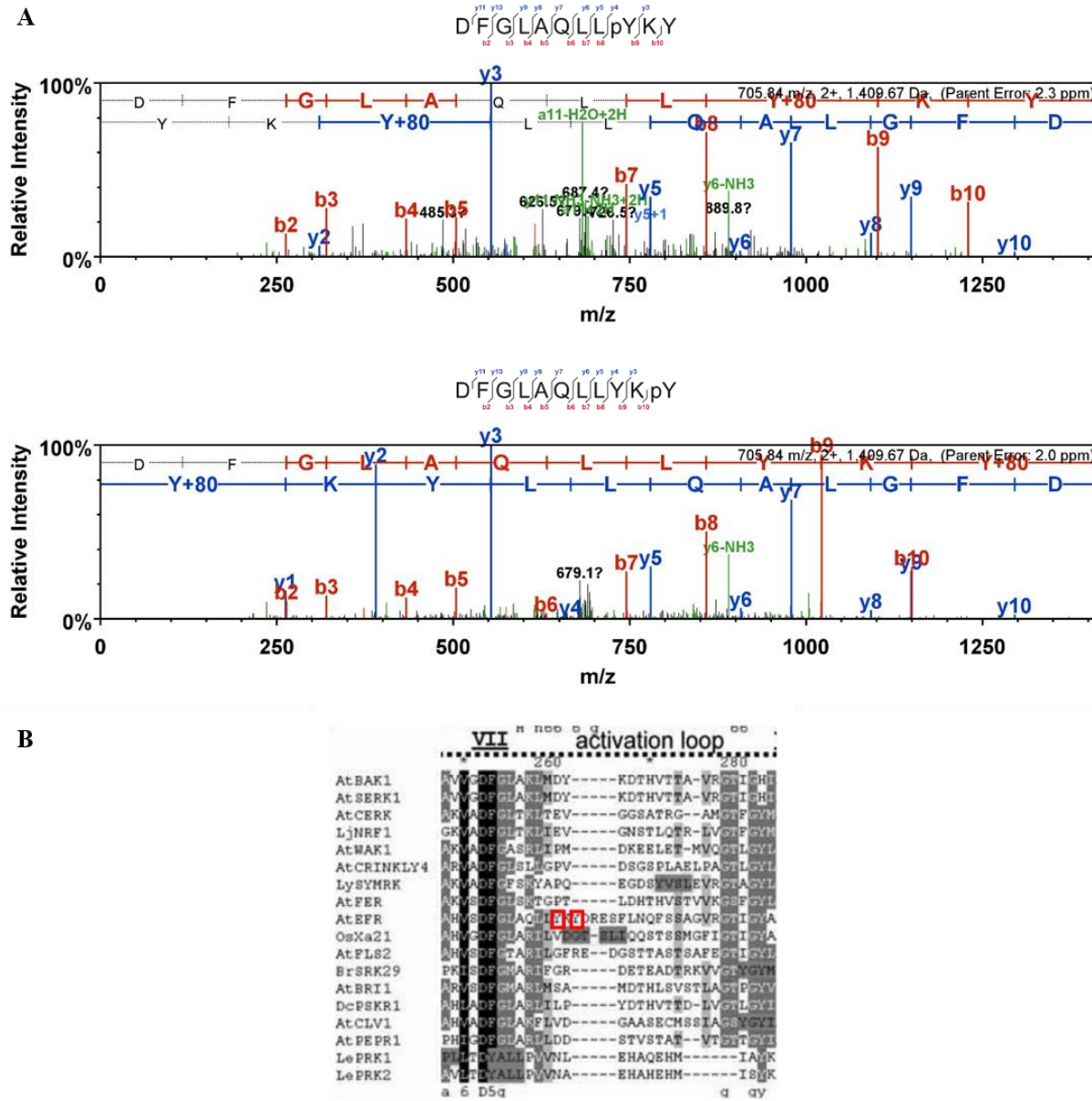
We next investigated whether inhibition of ligand-induced EFR endocytosis affects acute immune responses stimulated by *elf18*. The extracellular oxidative burst produced by the NADPH oxidase RBOHD as well as the phosphorylation of MAPKs remained similar to wild type in *Arabidopsis* transgenic lines expressing EFR<sup>Y875F</sup>-GFP or EFR<sup>Y877F</sup>-GFP (3 Figure 3A and B), supporting the observations in *N. benthamiana* (Macho et al. 2014, Figure 3—figure supplement 1A). Both lines also showed similar extent of growth inhibition in response to *elf18* as WT (3 Figure 3C), and were not significantly different from Col-0 in response to the phytopathogenic bacteria *Pseudomonas syringae* pv. *tomato* (*Pto*) DC3000 in a disease protection assay induced by *elf18* pre-treatment (3 Figure 3D, 3 Figure 3—figure supplement 1B). Additionally, the EFR<sup>Y875F</sup> and EFR<sup>Y877F</sup> lines had similar growth of surface-inoculated *Pto* DC3000 as Col-0 (3 Figure 3—figure supplement 1C). These results suggest that ligand-induced EFR endocytosis is not involved in positive or negative regulation of acute immune responses and resistance against bacterial infection induced by a single *elf18* treatment.



### 3 Figure 2.

#### Y875 and Y877 are not required for the formation of signalling-competent receptor complexes.

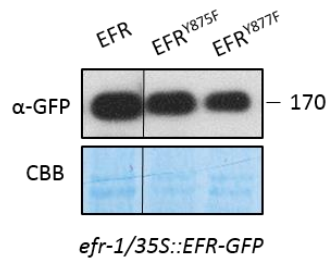
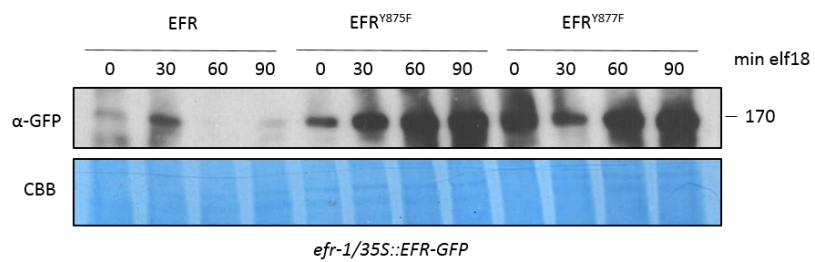
(A) Recombinant MBP-EFR kinase domain (KD) was incubated with [ $^{32}$ P] $\gamma$ -ATP. In vitro phosphorylation is revealed by autoradiography. CBB, Coomassie Brilliant Blue. DK: dead kinase. (B) Activation of EFR-GFP immunoprecipitated from *Arabidopsis* seedlings treated with water (-) or 100 nM elf18 (+) for 10 min. Immunoprecipitated EFR-GFP was incubated with [ $^{32}$ P] $\gamma$ -ATP. In vitro phosphorylation is revealed by autoradiography. (C) Y phosphorylation on EFR-GFP immunoprecipitated in B after treatment with water (-) or 100 nM elf18 (+) for 10 min. Immunoblots were analysed using anti-pTyr or anti-GFP antibody. Vertical bars indicates a separation of lanes within the same blot.



### 3 Figure2—figure supplement 1.

#### Detection of *in vivo* phosphorylation of EFR Y875 and Y877 by LC-MS/MS.

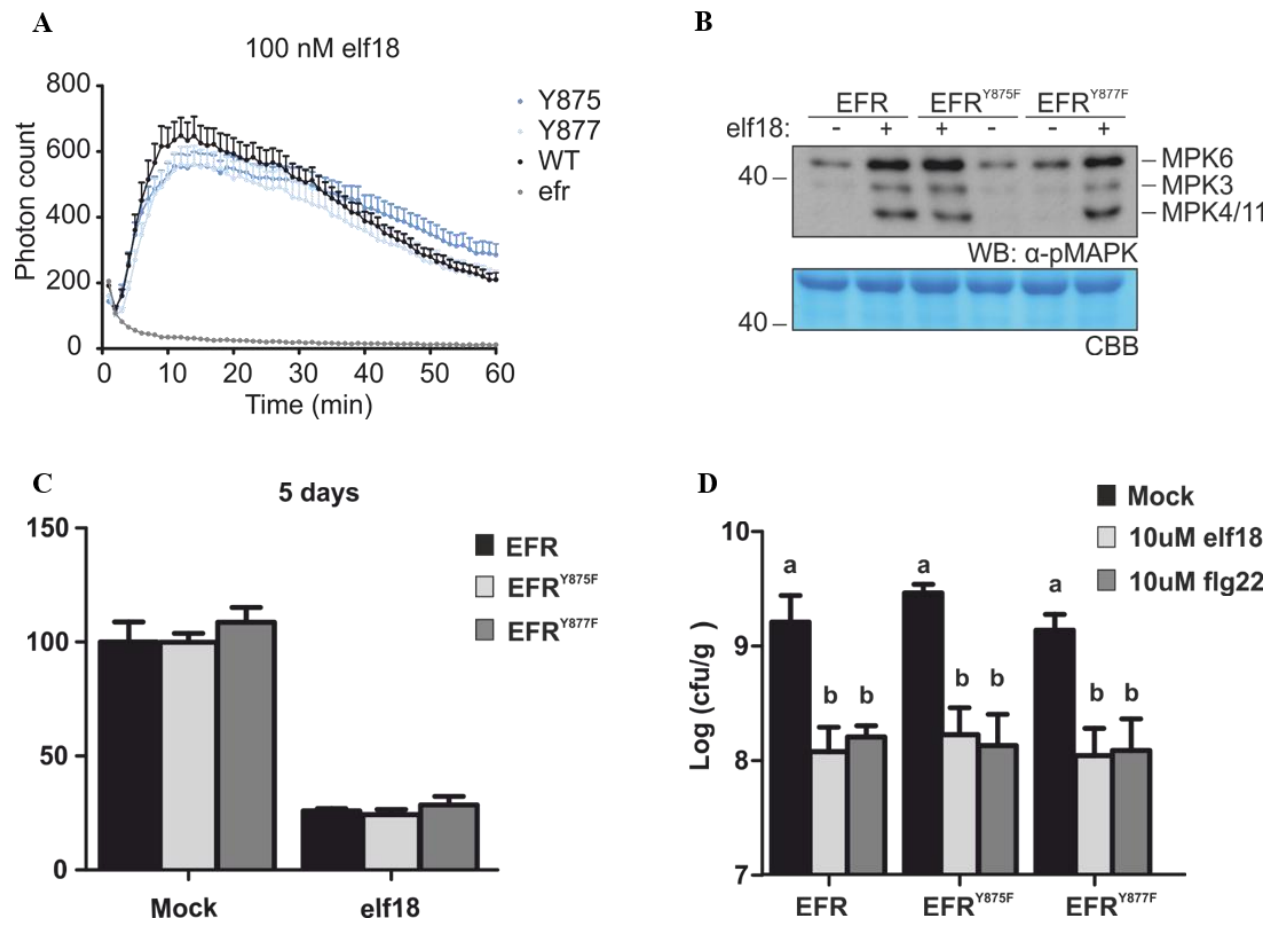
**(A)** LC-MS/MS analysis of immunoprecipitated EFR-GFP resulted in the identification of a doubly charged precursor ( $m/z$  705.84) with fragmentation pattern consisting of singly and doubly charged b- and y-ions. Modified peptide sequences and fragmentation patterns are shown above the spectra. **(B)** Conservation of EFR Y875 and Y877 in plant kinases. Alignment showing the activation loop containing EFR Y875 and Y877 (red rectangles) and conserved residues in kinases from different plant species.

**A****B**

### 3 Figure2—figure supplement 2.

#### Y875 and Y877 are required for ligand-mediated degradation of EFR.

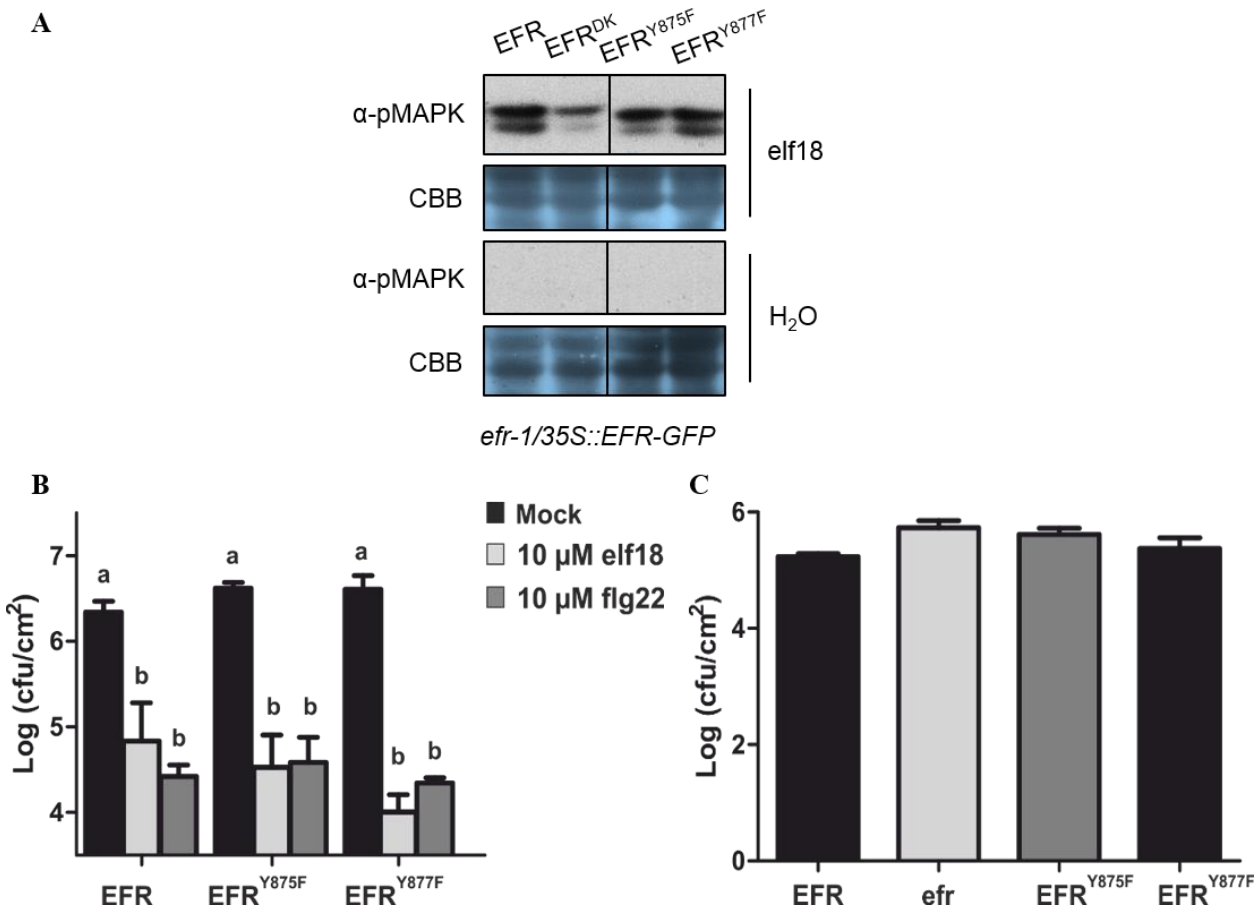
(A) Western blot analysis showing the accumulation of the different variants of EFR in the generated *Arabidopsis* stable transgenic lines. Vertical bar indicates a separation of lanes within the same blot. (B) Degradation of EFR $^{Y875F}$  and EFR $^{Y877F}$  was analysed by western blot. Seedlings were treated with 10  $\mu$ M elf18 for the indicated time points.



### 3 Figure 3.

#### Mutation of EFR Y875 or Y877 does not compromise elf18-triggered PTI responses.

(A) ROS production was measured as relative luminescence units (RLU) in response to 100 nM elf18. The graph is representative of two biological repeats; n=24. (B) Phosphorylation of MAPKs after treatment with 100 nM elf18 for 10 min. (C) Seedling growth inhibition triggered by 100 nM elf18 for 5 days in *efr* mutants complemented with WT EFR, EFR<sup>Y875F</sup>, or EFR<sup>Y877F</sup>. Growth is represented relative to mock. Results are average  $\pm$  SEM, n = 24. (D) flg22- and elf18-induced resistance to *Pto* DC3000 in lines expressing WT EFR, EFR<sup>Y875F</sup>, or EFR<sup>Y875F</sup>. Seedlings were pre-treated with 10  $\mu$ M elf18, 10  $\mu$ M flg22 or water (Mock) 24 hours prior to bacterial infection. Graph representative of two independent biological replicates analysed by one-way ANOVA and Tukey's multiple-comparison post-test. Values are shown as means  $\pm$  SEM. Different letters indicate statistical significance of P value  $\leq$  0.001; bars represent SE, n=8.



**3 Figure 3—figure supplement 1.**

**elf18-triggered responses are not affected by mutation of Y875 and Y877.**

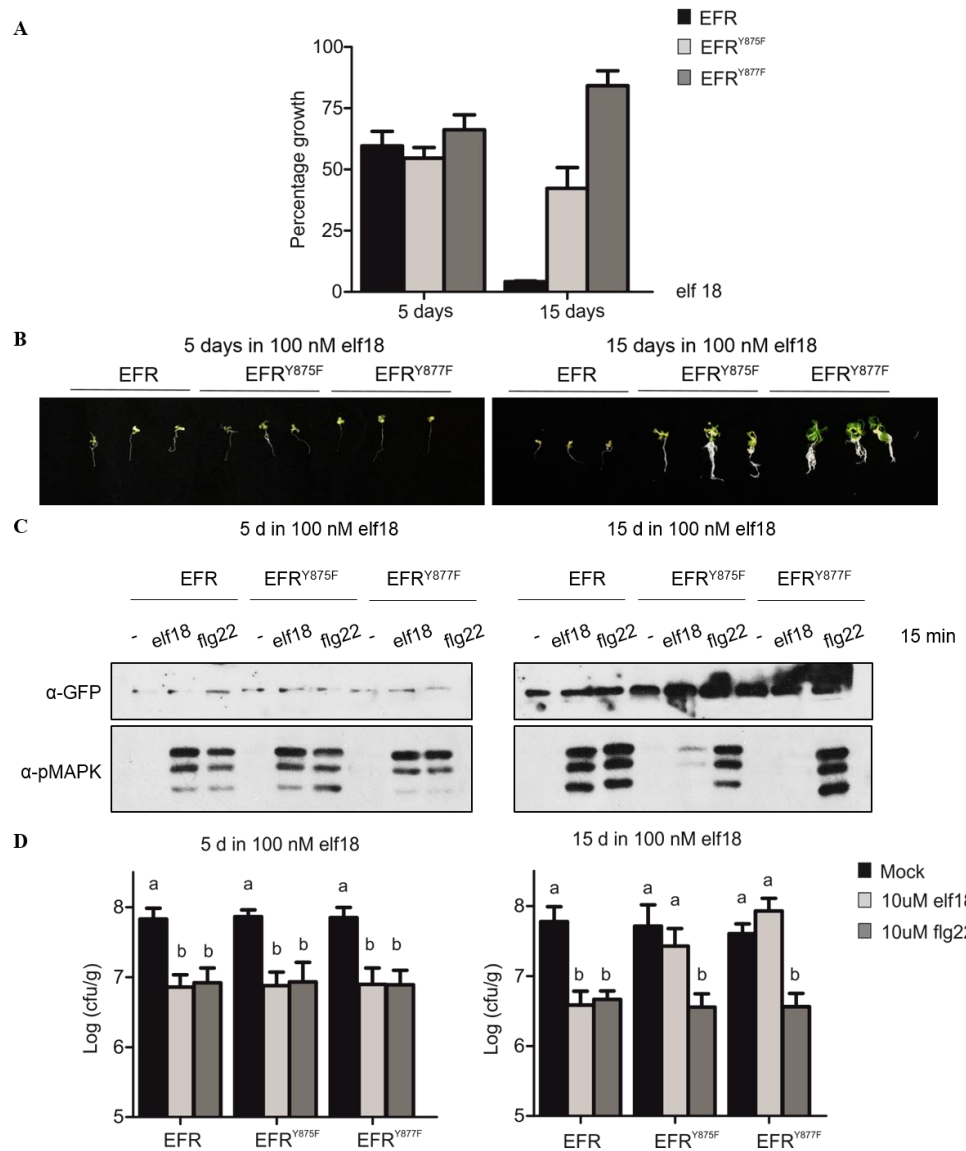
(A) The expression of EFR<sup>Y875F</sup> and EFR<sup>Y877F</sup> does not compromise elf18-triggered MAPK activation in *N. benthamiana*. Blot showing phosphorylation of MAPKs after treatment with water (H<sub>2</sub>O) or 100 nM elf18 for 10 min. Vertical bar indicates a separation of lanes within the same blot. (B) elf18- and flg22-induced resistance to *Pto* DC3000 in *efr* mutants expressing WT EFR, EFR<sup>Y875F</sup>, or EFR<sup>Y875F</sup>. Plants were pre-treated with 10 μM elf18, 10 μM flg22 or water 24 hours prior to bacterial infiltration. Graph representative of at least three independent biological replicates analysed by one-way ANOVA and Tukey's multiple-comparison post-test. Values are shown as means ± SEM. Different letters indicate statistical significance of P value ≤ 0.001; bars represent SE, n=8. (C) Five-weeks-old *efr* plants expressing the indicated constructs were sprayed with *Pto* DC3000 (OD600 of 0.2, supplemented with 0.04% Silwett L-77) and covered for 24 hours. Bacterial counts were assessed at 2 dpi. Values are shown as means ± SEM (n=12). Similar results were observed in two independent experiments.

### 3.3 Y-mediated EFR Endocytosis is Required to Maintain elf18 Responsiveness

Since EFR<sup>Y875F</sup> and EFR<sup>Y877F</sup> plants were not altered in acute immune responses stimulated by elf18, we focused on chronic immune responses observed as inhibition of growth when plants were incubated continuously with PAMPs for longer time points.

Our results showed that, although exhibiting WT-like growth inhibition at 5 days (3 Figure 3), the EFR<sup>Y875F</sup> and EFR<sup>Y877F</sup>-expressing lines recovered growth after 15 days of continuous exposure to elf18 (3 Figure 4A and B). This reflects a defective responsiveness to the PAMP, also revealed by the altered phosphorylation of MAPKs in response to elf18 but not flg22 (3 Figure 4C). Together, this suggests that inhibition of ligand-induced PRR endocytosis affects chronic immune responses. The altered elf18-induced MAPK activation correlated with a higher accumulation of EFR<sup>Y875F</sup> and EFR<sup>Y877F</sup> as compared to WT EFR at 15 days (3 Figure 4C), suggesting that inhibition of tyrosine-mediated endocytosis leads to an accumulation of a signalling incompetent pool of EFR receptors.

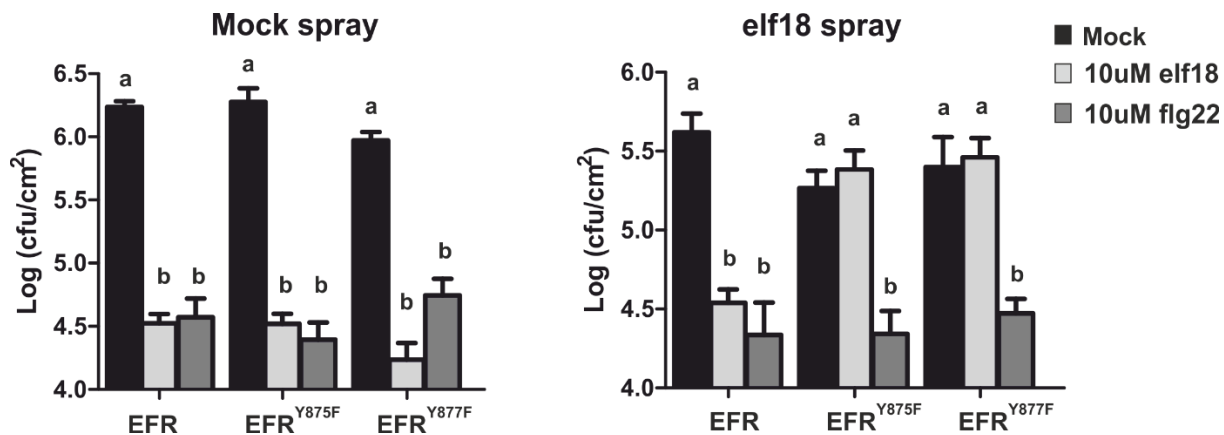
To determine the outcome of prolonged inhibition of ligand-mediated endocytosis of EFR on immunity, seedlings exposed to elf18 for 5 or 15 days were rescued on MS medium for three days then subjected to a *Pto* DC3000 disease protection assay induced by elf18 or flg22 pre-treatment. Plants exposed for 5 days to elf18 exhibited WT-like resistance to bacterial infection induced by both elf18 and flg22. However, EFR<sup>Y875F</sup> and EFR<sup>Y877F</sup> plants exposed for 15 days to elf18 showed strongly impaired resistance to bacterial infection when induced by elf18 but not by flg22 treatment (3 Figure 4D). Using an independent approach, in which we sequentially sprayed five-weeks-old plants with 100 nM elf18 twice a day for three days prior to inducing resistance against bacterial infection with elf18 and flg22, we observed similarly that in the EFR<sup>Y875F</sup> and EFR<sup>Y877F</sup> plants, elf18 but not flg22 treatment failed to induce resistance to bacterial infection (3 Figure 4—figure supplement 1). Together, these findings suggest that maintaining responsiveness to continuous PAMP stimulus, as it would occur in nature, is required for plant immunity and this is dependent on ligand-induced PRR endocytosis.



**3 Figure 4.**

**Ligand-dependent endocytosis is required for maintaining a signalling competent pool of EFR.**

(A) Seedling growth inhibition of *efr* seedlings expressing WT EFR, EFR<sup>Y875F</sup>, or EFR<sup>Y877F</sup> triggered with 100 nM elf18 for 5 and 15 days. Growth is represented relative to the untreated wild type. Results are average  $\pm$  se (n = 24). (B) Representative phenotypes of randomly selected seedlings measured in A. (C) Phosphorylation of MAPKs after treatment with water (0), 10  $\mu$ M elf18 or 10  $\mu$ M flg22 for 15 min in seedlings expressing the indicated constructs after recovery from A. anti-GFP antibody was used to show the levels of the receptor. (D) Seedlings from A were recovered for 3 days in liquid MS then treated with 10  $\mu$ M elf18, flg22, or water 24 hours prior to infection with *Pto* DC3000 (OD600 of 0.0002). Graph representative of two independent biological replicates analysed by one-way ANOVA and Tukey's multiple-comparison post-test. Values are shown as means  $\pm$  SEM. Different letters indicate statistical significance of P value  $\leq$  0.001; bars represent SE, n=8.



### 3 Figure4—figure supplement 1.

**elf18- but not flg22-induced resistance is lost in EFR<sup>Y875F</sup>- EFR<sup>Y875F</sup>-expressing plants repeatedly sprayed with elf18.**

Five-weeks-old plants were sprayed with 100 nM elf18 or mock (supplemented with 0.04% Silwett L-77) twice a day for three days. Upon recovery, they were infiltrated with 10  $\mu$ M elf18, 10  $\mu$ M flg22, or mock 24 hours prior to infection with *Pto* DC3000. Graph representative of at least three independent biological replicates analysed by one-way ANOVA and Tukey's multiple-comparison post-test. Values are shown as means  $\pm$  SEM. Different letters indicate statistical significance of P value  $\leq$  0.001; bars represent SE, n=8.

## 4. Discussion

Subcellular trafficking processes are conserved among all eukaryotic cells. Proper control of the secretory and endocytic membrane networks is crucial to the functioning of cells and organisms, and failures therein result in spontaneous signalling events (Baumdick et al., 2015), obstructed immune responses, and disease development (Ben Khaled et al., 2015). The involvement of ligand-mediated endocytosis in PRR signalling is however less clear, and conflicting results from both mammalian and plant fields are accumulating (Irannejad et al., 2015, Ben Khaled et al., 2015). Whereas viral pathogens of mammalian cells are perceived via endosomal receptors, the cell periphery-localised bacterial receptors are thought to signal exclusively from the plasma membrane (Wang et al., 2016, Asrat et al., 2014). Conversely, previous results from our lab and others suggest that ligand-dependent endocytosis of plant PRRs, such as FLS2, contributes to PTI

signalling (Mbengue et al., 2016). Here, we dissected the intrinsic biochemical determinants of PRR trafficking, using EFR as a model.

In mammalian systems, endocytic cargo determinants include tyrosine-based motifs, which are short linear sorting signals that mediate cargo entry into the endocytic route (Kozik et al., 2010). These motifs are recognized by the endocytic adaptors of PM-derived clathrin-coated vesicles (CCVs) (Kozik et al., 2010). However, it remains unclear whether such Y-based endocytic motifs play a role in endocytosis of plant PRRs. To assess this, we screened EFR variants comprising point mutations in each of the eleven intracellular tyrosines of EFR cytoplasmic domain for altered endocytosis. We showed that EFR<sup>Y836F</sup>, EFR<sup>Y875F</sup> and EFR<sup>Y877F</sup> were fully compromised in elf18-mediated internalization of the receptor (3 Figure 1). Y836 is a major EFR phosphosite and is required for receptor activation and downstream signalling (Macho and Zipfel, 2014). Given that the kinase inactive EFR variant is unable to undergo ligand-mediated internalisation (Mbengue et al., 2016), it stands to reason that the altered endocytosis of EFR<sup>Y836F</sup> is linked to the role of this residue in receptor complex activation. Hence, we focused in this work on the functional characterisation of Y875 and Y877 to specially assess the requirement of endocytosis for PTI signalling. Notably, the tyrosines 702 and 791, located within canonical Yxxφ endocytic motifs, were not required for elf18-triggered endocytosis of EFR (3 Figure 1—figure supplement 1). This suggests that this consensus type of motifs doesn't play a role in internalization of plant PRRs.

EFR Y875 and Y877 are located in the activation loop, a highly variable region among plant PRRs and RLKs (3 Figure2—figure supplement 1B). Hence, it could be possible that a strong negative charge within the activation loop of PRRs mediates ligand-triggered endocytosis. Alternatively, phosphorylation of these tyrosines might be required to induce other post-translational modifications necessary for EFR endocytosis, such as ubiquitination.

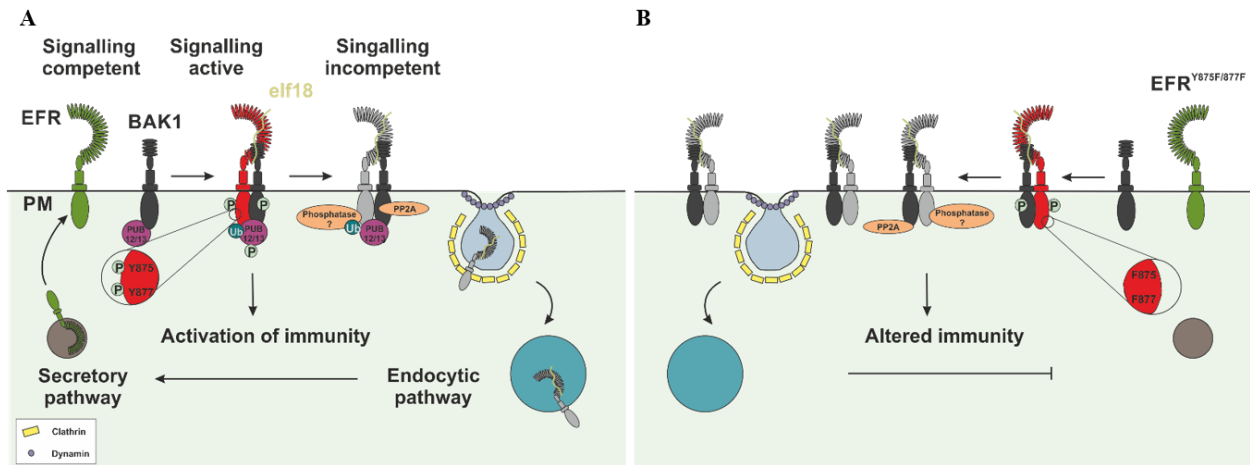
Endosomes have long been hypothesised to act as signalling platforms. To assess whether endosomal-located EFR receptors contribute to PTI signalling, we determined whether EFR<sup>Y875F</sup>- or EFR<sup>Y877F</sup>-expressing lines were altered in elf18-triggered immune signalling. We show that

receptor complex activation as well as all tested PTI outputs were not compromised by the Y875F and Y877F mutations (3 Figure 3, 3 Figure3—figure supplement 1). This uncouples Y-mediated EFR endocytosis from PTI signalling. Ligand-induced endocytosis is also thought to negatively regulate receptor signalling by physically reducing the amount of ligand-bound receptors at the cell periphery, and separating them from their downstream substrates (Sorkin and von Zastrow, 2009). Yet, our data showed that inhibiting EFR internalisation through the Y875F and Y877F mutations did not result in sustained PTI signalling (3 Figure 3). This suggests that attenuation of EFR activity occurs prior to endocytosis, at the level of the PM.

Though apparently uncoupled from PTI activation and downregulation, the requirement of subcellular trafficking processes for maintaining the plant responsiveness to its surrounding pathogens has not been explored so far. To shed light into this phenomenon, we exposed EFR<sup>Y875F</sup> and EFR<sup>Y877F</sup> lines to long term or repeated stimulations with elf18, and determined whether they are still able to induce EFR-mediated responses. Our results revealed that prolonged exposure to the peptide strongly affected elf18-triggered growth arrest, MAPK activation and induced immunity of lines abolished in Y-mediated endocytosis (3 Figure 4, 3 Figure4—figure supplement 1). This suggests that clearing the PM from ligand-bound receptors is required to replenish the cell surface with newly synthesised receptors, maintaining the plant responsiveness to the elf18 stimuli. This is supported by the recent discovery of plant-specific proteins that act at the crossroad of exocytic and endocytic trafficking routes (Sparks et al., 2016), suggesting the existence of a multilayered regulatory feedback between endocytosis and secretion of PRRs. Importantly, in our long-term elf18 treatment assays, we noticed that growth recovery of plants expressing EFR<sup>Y875F</sup> was slower as compared to those expressing EFR<sup>Y877F</sup> (3 Figure 4). This could indicate that Y877 is the major phosphosite underlying ligand-triggered endocytosis of EFR, and that mutation of Y875 might induce some conformational changes in the protein that reduce the phosphorylation of Y877.

Taken together, it is becoming increasingly clear that the endomembrane trafficking of ligand-activated EFR is a determinant of long-term cellular signalling responsiveness (3 Figure 5). The

sheer dependency of EFR trafficking on phosphorylation on tyrosine residues provides a mechanistic link between tyrosine phosphorylation and ligand-mediated endocytosis. This is gleamed from our observations on defects in EFR internalization when the phosphosites Y875 and Y877 are mutated. Furthermore, as a long-term outcome of restrained uptake of ligand-bound EFR receptors, sensitivity to EF-Tu is lost, rendering the plant irresponsive to stimulation by its surrounding bacteria. This finding represents the first instance of uncoupling PRR signalling from ligand-mediated endocytosis in plants as well as a first documentation of the outcome of inhibiting PRR trafficking for a long term. The possible involvement of ubiquitination downstream of phosphorylation will certainly add layers of complexity of the endocytic signal, though the cross-talk between these two PTMs in plants just began to be explored. Our findings take a key step toward understanding how plant cells maintain their responsiveness to surrounding bacteria and unveil a new facet of molecular regulation of ligand-mediated endocytosis.



### 3 Figure 5.

#### Schematic overview of EFR subcellular trafficking regulation.

(A) Upon elf18 perception, EFR forms an active complex with the co-receptor BAK1 and induces immune signalling. Once PTI is successfully initiated, phosphorylation of EFR on Y875 and Y877 might facilitate receptor ubiquitination possibly by the U-box E3 ligases PUB12 and PUB13. This would trigger the endocytic trafficking of ligand-bound EFR towards vacuolar degradation, enabling the replenishment of the PM with newly synthesised receptors. (B) Repeated or prolonged exposure to elf18 of EFR carrying the Y875F or Y877F mutation leads to an accumulation of signalling incompetent receptors at the cell periphery. This might alter the ability of the cell to replenish the PM with new receptors, and ultimately results in insensitivity to elf18. Arrows indicate trafficking through the secretory pathways via secretory vesicles (SV), and endocytic pathways via endosomes. Colour coding of EFR is as following: Green indicates signalling competent receptors, red indicates ligand-bound receptors engaged in immune signalling, and grey indicates ligand-bound receptors that have been deactivated potentially by PM-associated phosphatases. P: phosphorylation. Ub: ubiquitination.

## 5. Materials and Methods

### Confocal Microscopy

Subcellular localization of WT EFR-GFP as well as all the GFP-tagged tyrosine mutant variants, transiently expressed in *N. benthamiana*, was determined by confocal laser-scanning microscopy with a DM6000B/TCS SP5 microscope (Leica) using standard settings for GFP detection provided by the manufacturer. Five-weeks-old *N. benthamiana* plants were used for transient expression assays as described before (Mbengue et al., 2016).

### **Plant Materials and Growth Conditions**

Plant materials and growth conditions have been previously described (Albrecht et al., 2012, Schwessinger et al., 2011). *Arabidopsis* adult plants used in this study were grown as one plant per pot at 20-21°C with a 10 h photoperiod in environmentally controlled chambers. Seedlings were grown on plates containing Murashige–Skoog (MS) medium (including vitamins) (Duchefa, Haarlem, The Netherlands), 1% sucrose, supplemented or not (liquid) with 0.8% agar, at 22°C and with a 16 h photoperiod. Generation of *efr-1*/EFRp:EFR-GFP-HA plants has been described before (Nekrasov et al., 2009). Expression of GFP-tagged EFR fully complemented the *efr-1* mutation (Nekrasov et al., 2009).

### **Cloning and Generation of Transgenic Plants**

Generation of the EFR tyrosine mutant variants has been described before (Macho et al., 2014). WT EFR, EFR<sup>Y875F</sup>, and EFR<sup>Y877F</sup> were transformed into *Arabidopsis efr-1* mutant plants using the floral dipping method (Clough and Bent, 1998). Transformants were selected by growing seedlings on agar plates supplemented with ppt (glufosinate-ammonium, PESTANAL) to select for BASTA resistance and by checking for accumulation of EFR-GFP by immunoblots.

### **Protein Extractions, Immunoprecipitations, Kinase Assays, and Immunoblot Analyses**

Protein extractions, purifications, immunoprecipitations, kinase assays, and immunoblots were performed as previously described (Schwessinger et al., 2011, Albrecht et al., 2012). Two-weeks-old *Arabidopsis* seedlings were used for protein extractions. Five-weeks-old *N. benthamiana* plants were used for transient expression assays as described before (Schwessinger et al., 2011) (Mbengue et al., 2016). Plant materials were ground in liquid nitrogen, and then extracted with buffer [150 mM Tris-HCl, pH 7.5; 150 mM NaCl; 5mM EDTA; 1% Igepal; 1% (vol/vol) protease inhibitor mixture, phosphatase inhibitor 2 and 3 (Sigma)] added at 1.5 mL/g powder. Samples were centrifuged 15 min at 4 °C and 21,000 g. Supernatants were adjusted to 3 mg/mL protein and incubated 4 h at 4 °C with 100 µL GFP-Trap coupled to agarose beads (Chromotek) with gentle agitation. Following incubation, the beads were collected and washed four times with the extraction buffer. For western blot, SDS loading buffer was then added to the beads, which were

boiled for 10 min. Immunoprecipitations used for subsequent kinase assays were washed three times with the extraction buffer and once with kinase buffer (50mM Tris-HCl, pH 7.4, 5mM MnCl<sub>2</sub>, 1mM DTT). Immunoprecipitates were finally incubated 30 min at 30 °C and under vigorous shaking with 30 µL of the kinase buffer supplemented with 1µM ATP and radioactive [<sup>32</sup>P]γ-ATP (183 kBq; Perkin-Elmer). The reactions were stopped by addition of SDS loading buffer and denatured for 10 min at 70 °C. Proteins were separated by SDS/PAGE 10% and analysed by Western blot. Radioactive membranes were analysed using a FLA5000 PhosphorImager (Fuji). Densitometry measurements were carried out with the AIDA software (Raytest), normalized to the elf18-treated EFR wild-type sample and shown as percentages. Epitope-tagged proteins were detected with anti-GFP (Santa Cruz) or anti-HA (Roche) conjugated to Horseradish peroxidase, following the manufacturer's instructions. Immunodetection of BAK1 has been described before (Schwessinger et al., 2011). Phosphotyrosine was detected with anti-pY99 (Santa Cruz) as described before (Macho et al., 2014).

### **Identification of proteins and phosphopeptides by LC-MS/MS**

Proteins were separated by SDS-PAGE (NuPAGE®, Invitrogen) and after staining with Coomassie brilliant Blue G-250 CBB (SimplyBlue™ stain, Invitrogen), the proteins were cut out and digested by trypsin as described previously (Ntoukakis et al., 2009). LC-MS/MS analysis was performed using a LTQ-Orbitrap massspectrometer (Thermo Scientific) and a nanoflow-HPLC system (nanoAcuity; Waters) as described previously (Ntoukakis et al., 2009). The entire TAIR10 database was searched ([www.Arabidopsis.org](http://www.Arabidopsis.org)) using Mascot (v 2.3.02, Matrix Science) (with the inclusion of sequences of common contaminants, such as keratins and trypsin). Parameters were set for 5 ppm peptide mass tolerance and allowing for Met oxidation and two missed tryptic cleavages. Carbamidomethylation of cysteine residues was specified as a fixed modification, and oxidized methionine and phosphorylation of serine, tyrosine or threonine residues were allowed as variable modifications. Scaffold (v3; Proteome Software) was used to validate MS/MS-based peptide and protein identifications and annotate spectra. The position and quality of spectra for phosphopeptides were also manually examined before acceptance.

### **ROS Burst Assays**

ROS burst assays were performed as described previously (Albrecht et al., 2012). ROS was elicited with 100 nM elf18. 24 leaf discs from five-weeks-old plants were used for each condition. Luminescence was measured over 50 min using a High Resolution Photon Counting System (HRPCS218) (Photek, UK) coupled to an aspherical wide lens (Sigma Corp, Japan).

### **MAP Kinase Activation Assays**

MAP kinase activation assays were performed as described in (Schwessinger et al., 2011). Phospho-p44/42 MAPK (Erk1/2; Thr202/Tyr204) rabbit monoclonal antibodies (Cell Signaling Technologies, Hitchin, UK) were used according to the manufacturer's protocol.

### **Seedling Growth Inhibition Assay**

Seedling growth inhibition assays were performed as described in (Nekrasov et al., 2009). In brief, four-days-old *Arabidopsis* seedlings were grown in liquid MS medium containing 1% sucrose supplemented with elf18 and the appropriate chemicals. Seedlings were weighed between 5 and 15 days after treatment.

### **Bacterial Infections**

Induced resistance assays were performed as described previously (Zipfel et al., 2004). In brief, water, 10  $\mu$ M elf18 or 10  $\mu$ M flg22 solution were infiltrated with a needleless syringe into leaves of four-weeks-old *Arabidopsis* plants 24 hours prior to bacterial inoculation (*Pto* DC3000, OD600 of 0.0002). Bacterial growth was determined 2 days after inoculation by plating serial dilutions of leaf extracts. To test the effect of repeated stimulations, water or 100 nM of elf18 supplemented with 0.04% Silwet L-77 was sprayed twice a day for three days. Plants were then rested for three days before performing the induced resistance assay.

Spray inoculation of *Pto* DC3000 0788-9 was performed as described in (Schwessinger et al., 2011). In brief, bacteria were grown in an overnight culture in LB medium, cells were harvested by centrifugation, and pellets were re-suspended to OD600 = 0.02 in 10 mM MgCl<sub>2</sub> with 0.04% Silwet L-77. Bacterial suspensions were sprayed onto leaf surfaces and plants were kept covered

for the first 24 hours. Bacterial growth was determined 2 days after inoculation by plating serial dilutions of leaf extracts.

### **Statistical Analysis**

Statistical significances based on t test and one-way ANOVA analyses were performed with Prism 5.01 software (GraphPad Software).

**Table 1.****List of primers used in the thesis.**

Primer name	Sequence	Purpose
K1120A_F	GGACTCTATTGTTCTGGCACAGGAAGAGGGCTATTG	Lysine point mutagenesis
K1120A_R	CAATAGCCTTCCCTGTGCCAGAGAAACAATAGAGTCC	Lysine point mutagenesis
GFP_F	ATGGTGAGCAAGGGCGAGGAGCTGTTG	Genotyping GFP in <i>pub12 pub13</i>
GFP_R	CAGCTCGTCCATGCCAGAGTGATCATG	Genotyping GFP in <i>pub12 pub13</i>
pub12-2_F	TAACCACAGCTACCCAAAACG	Genotyping
pub12-2_R	ACGTGCTTGTTTGCTATGG	Genotyping
pub13_F	AAGAGGTATGGCTCCAGCTTC	Genotyping
pub13_R	ACGTGCTTGTTTGCTATGG	Genotyping
PUB12_CC9F	GCCTGAAGACCGAAGATCTGC	Sequencing synthesized PUB12
PUB12_CC9R	CCCGTCCGGATGACTCGATAG	Sequencing synthesized PUB12
PUB13_CC9F	GGTGGACACTCGACATGTCC	Sequencing synthesized PUB13
PUB13_CC9R	GAGGTATGGCTCCAGCTTCGG	Sequencing synthesized PUB13

## Chapter 4: General Discussion and Outlook

The endomembrane trafficking is a pivotal aspect of the cell responsiveness to endogenous and exogenous stimuli in all eukaryotes. Yet despite its importance, knowledge of its requirement for PTI in plants is still sparse.

Without a priori proteomics approaches have emerged in the past few years as key tools to study the protein composition of the successive stations along the endocytic route (Heard et al., 2015). While these methods provide a global understanding of the various endomembrane compartments and their regulatory proteins, well-characterised receptor models are key to unravel the cargo determinants behind the distinct sorting steps. In chapter 3 section 2, we attempted to characterise the ubiquitin code underlying FLS2 trafficking from the PM to the lytic vacuole. While PUB12 and PUB13 seem to ubiquitinate FLS2 and destine it for endocytosis at the PM, KEG appears to act at level of the TGN. Accordingly, FLS2 accumulates in enlarged vesicles in the *keg* mutant, though the specificity of this E3 ligase for regulating FLS2 sorting from the TGN as well as its direct ubiquitination of FLS2 have not been addressed in this work. Additionally, it is still unclear which ubiquitination processes are recognised by the ESCRT machinery for sorting into ILVs of MVBs. Notably, ubiquitination seems to be also involved in sorting downstream of TGN-to-MVB trafficking. The K1120 residue that has been identified by mass spectrometry approach as a ubiquitination site, seems to be essential for the vacuolar sorting of endosomal-localised FLS2. However, more work needs to follow to identify the E3 ligase behind this PTM, as well as the nature of the compartments in which the FLS2<sup>K1120A</sup> mutant accumulates.

It is currently thought that the branching of signalling cascades downstream of ligand perception is determined by specific phosphosites within the receptor. Though initially not applied to study EFR trafficking, proteomics approaches identifying EFR phosphosites were key to establish the link between Y phosphorylation and endocytosis in plants. Y875 and Y877 in EFR specifically regulate ligand-mediated endocytosis, without affecting immune signalling. The location of these residues on the receptor activation loop suggests that a strong negative charge in this region is

required to trigger endocytosis. Similar mutations on other PRRs or RLKs might help elucidate this question.

Using two independent approaches, results from chapter 3 section 3 and chapter 4 merged to demonstrate the requirement of ligand-mediated PRR endocytosis for preserving chronic immune responsiveness during the continuous interaction of plants with bacteria. These findings shed a new light on our understanding of the host cellular dynamics in response to pathogens. To our knowledge, this represents the first instance of characterising the molecular regulation underlying PRR trafficking in plants. While unravelling the post-translational code of ligand-induced endocytosis of FLS2 and EFR, our findings provide an additional layer of complexity to the unremitting arms race between plants and their surrounding pathogens. A key aspect that emerged from our approach is the gap between stimuli under lab condition and the constant and repeated exposure of plants to microbes in nature. It is therefore critical to expand our perception and analyses of results beyond single treatments.

Our current working hypothesis suggests a multilayered regulatory feedback between endocytosis and secretion of PRRs (2.3 Figure 7, 3 Figure 5). In fact, the accumulation of non-internalized FLS2 and EFR receptors was coupled with impaired responsiveness under repeated PAMP treatment conditions. This points towards a defective secretion of signaling-competent receptors to their destined locations within the PM islands or microdomains. The irreversible nature of PAMP binding to these PRRs (Sun et al., 2013) is likely to inhibit second rounds of stimulation and activation of immune signaling. It is however unclear at which level the crosstalk between endocytic and secretory trafficking of immune receptors is regulated. One strategy of addressing this would be to assess the transcriptional regulation of non-internalized PRRs versus endocytosis ones. If the negative feedback is not at the transcriptional level (possibly under regulation of hormones), it would be interesting to address the subcellular localization and trafficking routes of newly synthesized receptors upon saturation of the PM with signaling incompetent receptors (after long-term PAMP treatment). This could be achieved using transgenic *Arabidopsis* lines expressing two variants of the EFR Y mutants, one tagged with GFP and the other with RFP under an inducible promoter. Once the PM is saturated with EFR<sup>Y875/877F</sup>

GFP, induction of the RFP-labelled version would help determine whether its trafficking is inhibited at a secretory station, or rerouted towards vacuolar degradation before reaching the PM.

Beyond the theory of signalling endosomes, our field needs now to direct its attention to the contenders and their strategies to target PTMs of host components or subvert the plant endomembrane trafficking pathways, thereby inadvertently contributing to pathogenesis and disease outcome. For instance, the finding that the *P. infestans* effector AVR3a targets and stabilizes the plant U-box CMPG1 unveiled the molecular mechanism underlying AVR3a-mediated negative regulation of INF1-triggered cell death (ICD) (Bos et al., 2010). During the biotrophic phase of *P. infestans* infection, AVR3a interferes with CMPG1 activity, impeding normal proteasomal degradation of both CMPG1 and its host targets (Bos et al., 2010). Another aspect of microbial manipulation of the host ubiquitin/ proteasome system is the ability to use effectors that act themselves as E3 ligases inside the plant cell. In fact, Ub ligase-related domains have been reported in a diversity of pathogenic microbes including bacteria, fungi, oomycetes, viruses and nematodes (Marino et al., 2012). The best characterized example of microbial E3 ligases is certainly AvrPtoB from *Pseudomonas syringae* that has a C-terminal domain with a remarkable structural homology with RING and U-box E3 ligases (Janjusevic et al., 2006). AvrPtoB interacts and mediates the degradation of the PRRs FLS2 and CERK1, as well as the protein kinase Fen involved in ETI in response to *P. syringae* (Gohre et al., 2008, Gimenez-Ibanez et al., 2009, Rosebrock et al., 2007). Nonetheless, as degradation of integral PM proteins is mediated by the vacuole, the exact molecular mechanism of AvrPtoB-mediated degradation of FLS2 and CERK1 is not yet understood. In addition to acquiring E3 ligase activity, effector proteins can also act as phosphatases. One such effector conserved in several *P. syringae* pathovars is the protein tyrosine phosphatase HopAO1 (Bretz et al., 2003, Baltrus et al., 2011). HopAO1 targets the Tyr phosphorylation of EFR (and possibly FLS2), thereby inhibiting its ligand-induced activation and downstream immune signalling (Macho et al., 2014).

We have reviewed in the introduction that pathogens redirect cellular cargos to their invasion site and use effectors to coerce the plant subcellular trafficking processes (Nomura et al., 2006, Nomura et al., 2011, Bozkurt et al., 2011, Gu and Innes, 2012, Chaparro-Garcia et al., 2014). This pathogenic strategy is far from being restricted to plant invaders (Knodler et al., 2001). Indeed, whether the host genome is simple or complex, pathogens seem to have evolved the capacity to target key components of subcellular trafficking. Thus it is tempting to speculate that these processes are manipulated by core effectors conserved among pathogens of different kingdoms. Identifying some of these effector proteins in plants might expand our comprehension of the evolution itinerary that pathogens followed to maintain their pathogenicity.

Although the study of the involvement of plant subcellular trafficking processes in immunity spans over 20 years, it is only recently that we have begun to appreciate the intricate interactions and delicate balance that occurs inside the host endomembrane route. By being in contact with eukaryotes for millions of years, it is likely that phytopathogens have learned many tricks from plant molecules and turned them into virulence factors. As molecular studies progress on plant-microbe interactions, consideration of the dynamic aspect of all players within the battle field becomes imperative to understand pathogenic mechanisms. Hopefully this knowledge can be applied to develop novel strategies to fight against infectious diseases.

## References

ABRAMOVITCH, R. B., ANDERSON, J. C. & MARTIN, G. B. 2006. Bacterial elicitation and evasion of plant innate immunity. *Nat Rev Mol Cell Biol*, 7, 601-11.

AKIRA, S., UEMATSU, S. & TAKEUCHI, O. 2006. Pathogen recognition and innate immunity. *Cell*, 124, 783-801.

ALBRECHT, C., BOUTROT, F., SEGONZAC, C., SCHWESSINGER, B., GIMENEZ-IBANEZ, S., CHINCHILLA, D., RATHJEN, J. P., DE VRIES, S. C. & ZIPFEL, C. 2012. Brassinosteroids inhibit pathogen-associated molecular pattern-triggered immune signaling independent of the receptor kinase BAK1. *Proc Natl Acad Sci U S A*, 109, 303-8.

ALFANO, J. & COLLMER, A. 2003. Type III secretion system effector proteins: double agents in bacterial disease and plant defense. *Annu Rev Phytopathol*, 42, 385-414.

ALI, G. S., PRASAD, K. V., DAY, I. & REDDY, A. S. 2007. Ligand-dependent reduction in the membrane mobility of FLAGELLIN SENSITIVE 2, an arabidopsis receptor-like kinase. *Plant Cell Physiol*, 48, 1601-11.

AN, Q., EHLERS, K., KOGEL, K. H., VAN BEL, A. J. & HUCKELHOVEN, R. 2006a. Multivesicular compartments proliferate in susceptible and resistant MLA12-barley leaves in response to infection by the biotrophic powdery mildew fungus. *New Phytol*, 172, 563-76.

AN, Q., HUCKELHOVEN, R., KOGEL, K. H. & VAN BEL, A. J. 2006b. Multivesicular bodies participate in a cell wall-associated defence response in barley leaves attacked by the pathogenic powdery mildew fungus. *Cell Microbiol*, 8, 1009-19.

ANTIGNANI, V., KLOCKO, A. L., BAK, G., CHANDRASEKARAN, S. D., DUNIVIN, T. & NIELSEN, E. 2015. Recruitment of PLANT U-BOX13 and the PI4Kbeta1/beta2 phosphatidylinositol-4 kinases by the small GTPase RabA4B plays important roles during salicylic acid-mediated plant defense signaling in Arabidopsis. *Plant Cell*, 27, 243-61.

ASAI, T., TENA, G., PLOTNIKOVA, J., WILLMANN, M., CHIU, W., GOMEZ-GOMEZ, L., T BOLLER, AUSUBE, F. & SHEEN, J. 2002. MAP kinase signalling cascade in Arabidopsis innate immunity. *Nature*, 415, 977-983.

ASRAT, S., DE JESUS, D. A., HEMPSTEAD, A. D., RAMABHADRAN, V. & ISBERG, R. R. 2014. Bacterial pathogen manipulation of host membrane trafficking. *Annu Rev Cell Dev Biol*, 30, 79-109.

BALTRUS, D. A., NISHIMURA, M. T., ROMANCHUK, A., CHANG, J. H., MUKHTAR, M. S., CHERKIS, K., ROACH, J., GRANT, S. R., JONES, C. D. & DANGL, J. L. 2011. Dynamic evolution of

pathogenicity revealed by sequencing and comparative genomics of 19 *Pseudomonas syringae* isolates. *PLoS Pathog*, 7, e1002132.

BAR, M. & AVNI, A. 2009a. EHD2 inhibits ligand-induced endocytosis and signaling of the leucine-rich repeat receptor-like protein LeEix2. *Plant J*, 59, 600-11.

BAR, M. & AVNI, A. 2009b. EHD2 inhibits signaling of leucine rich repeat receptor-like proteins. *Plant Signal Behav*, 4, 682-4.

BAR, M., SHARFMAN, M., RON, M. & AVNI, A. 2010. BAK1 is required for the attenuation of ethylene-inducing xylanase (Eix)-induced defense responses by the decoy receptor LeEix1. *Plant J*, 63, 791-800.

BAR, M., SHARFMAN, M., SCHUSTER, S. & AVNI, A. 2009. The coiled-coil domain of EHD2 mediates inhibition of LeEix2 endocytosis and signaling. *PLoS One*, 4, e7973.

BAUER, Z., GOMEZ-GOMEZ, L., BOLLER, T. & FELIX, G. 2001. Sensitivity of different ecotypes and mutants of *Arabidopsis thaliana* toward the bacterial elicitor flagellin correlates with the presence of receptor-binding sites. *J Biol Chem*, 276, 45669-76.

BAUMDICK, M., BRUGGEMANN, Y., SCHMICK, M., XOURI, G., SABET, O., DAVIS, L., CHIN, J. W. & BASTIAENS, P. I. 2015. EGF-dependent re-routing of vesicular recycling switches spontaneous phosphorylation suppression to EGFR signaling. *Elife*, 4.

BECK, M., HEARD, W., MBENGUE, M. & ROBATZEK, S. 2012a. The INs and OUTs of pattern recognition receptors at the cell surface. *Curr Opin Plant Biol*, 15, 367-74.

BECK, M., ZHOU, J., FAULKNER, C., MACLEAN, D. & ROBATZEK, S. 2012b. Spatio-temporal cellular dynamics of the *Arabidopsis* flagellin receptor reveal activation status-dependent endosomal sorting. *Plant Cell*, 24, 4205-19.

BECSI, B., KISS, A. & ERDODI, F. 2014. Interaction of protein phosphatase inhibitors with membrane lipids assessed by surface plasmon resonance based binding technique. *Chem Phys Lipids*, 183, 68-76.

BEHREND, C. & HARPER, J. W. 2011. Constructing and decoding unconventional ubiquitin chains. *Nat Struct Mol Biol*, 18, 520-8.

BEN KHALED, S., POSTMA, J. & ROBATZEK, S. 2015. A moving view: subcellular trafficking processes in pattern recognition receptor-triggered plant immunity. *Annu Rev Phytopathol*, 53, 379-402.

BENSCHOP, J. J., MOHAMMED, S., O'FLAHERTY, M., HECK, A. J., SLIJPER, M. & MENKE, F. L. 2007. Quantitative phosphoproteomics of early elicitor signaling in *Arabidopsis*. *Mol Cell Proteomics*, 6, 1198-214.

BITSIKAS, V., CORREA, I. R., JR. & NICHOLS, B. J. 2014. Clathrin-independent pathways do not contribute significantly to endocytic flux. *Elife*, 3, e03970.

BOGDANOVA, A. J. & MARTIN, G. B. 2000. AvrPto-dependent Pto-interacting proteins and AvrPto-interacting proteins in tomato. *Proc Natl Acad Sci U S A*, 97, 8836-40.

BOHLENIUS, H., MORCH, S. M., GODFREY, D., NIELSEN, M. E. & THORDAL-CHRISTENSEN, H. 2010. The multivesicular body-localized GTPase ARFA1b/1c is important for callose deposition and ROR2 syntaxin-dependent preinvasive basal defense in barley. *Plant Cell*, 22, 3831-44.

BOLLER, T. & FELIX, G. 2009. A renaissance of elicitors: perception of microbe-associated molecular patterns and danger signals by pattern-recognition receptors. *Annu Rev Plant Biol*, 60, 379-406.

BOLLER, T. & HE, S. 2009. Innate immunity in plants: an arms race between pattern recognition receptors in plants and effectors in microbial pathogens. *Science*, 324, 742-744.

BOLTE, S., TALBOT, C., BOUTTE, Y., CATRICE, O., READ, N. D. & SATIAT-JEUNEMAITRE, B. 2004. FM-dyes as experimental probes for dissecting vesicle trafficking in living plant cells. *Journal of Microscopy*, 214, 159–173.

BORGNE, R. L., BARDIN, A. & SCHWEISGUTH, F. 2005. The roles of receptor and ligand endocytosis in regulating Notch signaling. *Development*, 132, 1751-1762.

BOS, J. I., ARMSTRONG, M. R., GILROY, E. M., BOEVINK, P. C., HEIN, I., TAYLOR, R. M., ZHENDONG, T., ENGELHARDT, S., VETUKURI, R. R., HARROWER, B., DIXELIUS, C., BRYAN, G., SADANANDOM, A., WHISSON, S. C., KAMOUN, S. & BIRCH, P. R. 2010. *Phytophthora infestans* effector AVR3a is essential for virulence and manipulates plant immunity by stabilizing host E3 ligase CMPG1. *Proc Natl Acad Sci U S A*, 107, 9909-14.

BOUDSOCQ, M., WILLMANN, M. R., MCCORMACK, M., LEE, H., SHAN, L., HE, P., BUSH, J., CHENG, S. H. & SHEEN, J. 2010. Differential innate immune signalling via  $\text{Ca}^{2+}$  sensor protein kinases. *Nature*, 464, 418-22.

BOZKURT, T. O., BELHAJ, K., DAGDAS, Y. F., CHAPARRO-GARCIA, A., WU, C. H., CANO, L. M. & KAMOUN, S. 2014. Rerouting of plant late endocytic trafficking towards a pathogen interface. *Traffic*.

BOZKURT, T. O., SCHORNACK, S., WIN, J., SHINDO, T., ILYAS, M., OLIVA, R., CANO, L. M., JONES, A. M., HUITEMA, E., VAN DER HOORN, R. A. & KAMOUN, S. 2011. *Phytophthora infestans* effector AVRblb2 prevents secretion of a plant immune protease at the haustorial interface. *Proc Natl Acad Sci U S A*, 108, 20832-7.

BRETT, J. R., MOCK, N. M., CHARITY, J. C., ZEYAD, S., BAKER, C. J. & HUTCHESON, S. W. 2003. A translocated protein tyrosine phosphatase of *Pseudomonas syringae* pv. *tomato* DC3000 modulates plant defence response to infection. *Mol Microbiol*, 49, 389-400.

BROWN, N. G., VANDERLINDEN, R., WATSON, E. R., WEISSMANN, F., ORDUREAU, A., WU, K. P., ZHANG, W., YU, S., MERCREDI, P. Y., HARRISON, J. S., DAVIDSON, I. F., QIAO, R., LU, Y., DUBE, P., BRUNNER, M. R., GRACE, C. R., MILLER, D. J., HASELBACH, D., JARVIS, M. A., YAMAGUCHI, M., YANISHEVSKI, D., PETZOLD, G., SIDHU, S. S., KUHLMAN, B., KIRSCHNER, M. W., HARPER, J. W., PETERS, J. M., STARK, H. & SCHULMAN, B. A. 2016. Dual RING E3 architectures regulate multiubiquitination and ubiquitin chain elongation by APC/C. *Cell*, 165, 1440-53.

BUCHERL, C. A., VAN ESSE, G. W., KRUIS, A., LUCHTENBERG, J., WESTPHAL, A. H., AKER, J., VAN HOEK, A., ALBRECHT, C., BORST, J. W. & DE VRIES, S. C. 2013. Visualization of BRI1 and BAK1(SERK3) membrane receptor heterooligomers during brassinosteroid signaling. *Plant Physiol*, 162, 1911-25.

BUTTNER, D. & BONAS, U. 2002. Getting across--bacterial type III effector proteins on their way to the plant cell. *The Embo Journal*, 21, 5313-5322.

CAAVEIRO, J. M., MOLINA, A., GONZALEZ-MANAS, J. M., RODRIGUEZ-PALENZUELA, P., GARCIA-OLMEDO, F. & GONI, F. M. 1997. Differential effects of five types of antipathogenic plant peptides on model membranes. *FEBS Lett*, 410, 338-42.

CAO, Y., LIANG, Y., TANAKA, K., NGUYEN, C. T., JEDRZEJCZAK, R. P., JOACHIMIAK, A. & STACEY, G. 2014. The kinase LYK5 is a major chitin receptor in *Arabidopsis* and forms a chitin-induced complex with related kinase CERK1. *Elife*, 3.

CARMONA, M. J., MOLINA, A., FERNANDEZ, J. A., LOPEZ-FANDO, J. J. & GARCIA-OLMEDO, F. 1993. Expression of the alpha-thionin gene from barley in tobacco confers enhanced resistance to bacterial pathogens. *Plant J*, 3, 457-62.

CHAPARRO-GARCIA, A., SCHWIZER, S., SKLENAR, J., YOSHIDA, K., BOS, J. I. B., SCHORNACK, S., JONES, A. M. E., BOZKURT, T. O. & KAMOUN, S. 2014. *Phytophthora infestans* RXLR-WY effector AVR3a associates with a Dynamin-Related Protein involved in endocytosis of a plant pattern recognition receptor. *bioRxiv*.

CHEN, L., HAMADA, S., FUJIWARA, M., ZHU, T., THAO, N. P., WONG, H. L., KRISHNA, P., UEDA, T., KAKU, H., SHIBUYA, N., KAWASAKI, T. & SHIMAMOTO, K. 2010. The Hop/Sti1-Hsp90 chaperone complex facilitates the maturation and transport of a PAMP receptor in rice innate immunity. *Cell Host Microbe*, 7, 185-96.

CHINCHILLA, D., BAUER, Z., REGENASS, M., BOLLER, T. & FELIX, G. 2006. The *Arabidopsis* receptor kinase FLS2 binds flg22 and determines the specificity of flagellin perception. *Plant Cell*, 18, 465-476.

CHINCHILLA, D., ZIPFEL, C., ROBATZEK, S., KEMMERLING, B., NURNBERGER, T., JONES, J. D., FELIX, G. & BOLLER, T. 2007. A flagellin-induced complex of the receptor FLS2 and BAK1 initiates plant defence. *Nature*, 448, 497-500.

CHOI, S. W., TAMAKI, T., EBINE, K., UEMURA, T., UEDA, T. & NAKANO, A. 2013. RABA members act in distinct steps of subcellular trafficking of the FLAGELLIN SENSING2 receptor. *Plant Cell*, 25, 1174-87.

CHOWDHURY, D., MARCO, S., BROOKS, I. M., ZANDUETA, A., RAO, Y., HAUCKE, V., WESSELING, J. F., TAVALIN, S. J. & PÉREZ-OTAÑO, I. 2013. Tyrosine phosphorylation regulates the endocytosis and surface expression of GluN3A-Containing NMDA receptors. *The Journal of Neuroscience*, 33, 4151-4164.

CLOUGH, S. J. & BENT, A. F. 1998. Floral dip: a simplified method for *Agrobacterium*-mediated transformation of *Arabidopsis thaliana*. *Plant J*, 16, 735-43.

COLBY, T., MATTHAI, A., BOECKELMANN, A. & STUIBLE, H. P. 2006. SUMO-conjugating and SUMO-deconjugating enzymes from *Arabidopsis*. *Plant Physiol*, 142, 318-32.

COLLINGS, D. A., GEBBIE, L. K., HOWLES, P. A., HURLEY, U. A., BIRCH, R. J., CORK, A. H., HOCART, C. H., ARIOLI, T. & WILLIAMSON, R. E. 2008. *Arabidopsis* dynamin-like protein DRP1A: a null mutant with widespread defects in endocytosis, cellulose synthesis, cytokinesis, and cell expansion. *J Exp Bot*, 59, 361-76.

COLLINS, N. C., THORDAL-CHRISTENSEN, H., LIPKA, V., BAU, S., KOMBRINK, E., QIU, J. L., HUCKELHOVEN, R., STEIN, M., FREIALDENHOVEN, A., SOMERVILLE, S. C. & SCHULZE-LEFERT, P. 2003. SNARE-protein-mediated disease resistance at the plant cell wall. *Nature*, 425, 973-7.

COLLMER, A. 1998. Determinants of pathogenicity and avirulence in plant pathogenic bacteria. *Curr Opin Plant Biol*, 1, 329-35.

COSTA, T. R., FELISBERTO-RODRIGUES, C., MEIR, A., PREVOST, M. S., REDZEJ, A., TROKTER, M. & WAKSMAN, G. 2015. Secretion systems in Gram-negative bacteria: structural and mechanistic insights. *Nat Rev Microbiol*, 13, 343-59.

COUTO, D. & ZIPFEL, C. 2016. Regulation of pattern recognition receptor signalling in plants. *Nat Rev Immunol*, 16, 537-52.

DE JONGE, R., VAN ESSE, H. P., MARUTHACHALAM, K., BOLTON, M. D., SANTHANAM, P., SABER, M. K., ZHANG, Z., USAMI, T., LIEVENS, B., SUBBARAO, K. V. & THOMMA, B. P. 2012. Tomato immune receptor Ve1 recognizes effector of multiple fungal pathogens uncovered by genome and RNA sequencing. *Proc Natl Acad Sci U S A*, 109, 5110-5.

DHONUKSHE, P., ANIENTO, F., HWANG, I., ROBINSON, D. G., MRAVEC, J., STIERHOF, Y. D. & FRIML, J. 2007. Clathrin-mediated constitutive endocytosis of PIN auxin efflux carriers in *Arabidopsis*. *Curr Biol*, 17, 520-7.

DODDS, P. N. & RATHJEN, J. P. 2010. Plant immunity: towards an integrated view of plant-pathogen interactions. *Nat Rev Genet*, 11, 539-48.

DOWNES, B. P., STUPAR, R. M., GINGERICH, D. J. & VIERSTRA, R. D. 2003. The HECT ubiquitin-protein ligase (UPL) family in *Arabidopsis*: UPL3 has a specific role in trichome development. *Plant J*, 35, 729-42.

DRAKAKAKI, G., VAN DE VEN, W., PAN, S., MIAO, Y., WANG, J., KEINATH, N. F., WEATHERLY, B., JIANG, L., SCHUMACHER, K., HICKS, G. & RAIKHEL, N. 2012. Isolation and proteomic analysis of the SYP61 compartment reveal its role in exocytic trafficking in *Arabidopsis*. *Cell Res*, 22, 413-24.

DUPLAN, V. & RIVAS, S. 2014. E3 ubiquitin-ligases and their target proteins during the regulation of plant innate immunity. *Front Plant Sci*, 5, 42.

EDEN, E. R., HUANG, F., SORKIN, A. & FUTTER, C. E. 2012. The role of EGF receptor ubiquitination in regulating its intracellular traffic. *Traffic*, 13, 329-37.

EL REFY, A., PERAZZA, D., ZEKRAOUI, L., VALAY, J. G., BECHTOLD, N., BROWN, S., HULSKAMP, M., HERZOG, M. & BONNEVILLE, J. M. 2003. The *Arabidopsis KAKTUS* gene encodes a HECT protein and controls the number of endoreduplication cycles. *Mol Genet Genomics*, 270, 403-14.

EMANS, N., ZIMMERMANN, S. & FISCHER, R. 2002. Uptake of a fluorescent marker in plant cells is sensitive to brefeldin A and wortmannin. *Plant Cell*, 14, 71-86.

EPEL, B. L. 1994. Plasmodesmata: composition, structure and trafficking. *Plant Mol Biol*, 26, 1343-56.

FARID, A., MALINOVSKY, F. G., VEIT, C., SCHÖBERER, J., ZIPFEL, C. & STRASSER, R. 2013. Specialized roles of the conserved subunit OST3/6 of the oligosaccharyltransferase complex in innate immunity and tolerance to abiotic stresses. *Plant Physiol*, 162, 24-38.

FAULKNER, C., PETUTSCHNIG, E., BENITEZ-ALFONSO, Y., BECK, M., ROBATZEK, S., LIPKA, V. & MAULE, A. J. 2013. LYM2-dependent chitin perception limits molecular flux via plasmodesmata. *Proc Natl Acad Sci U S A*, 110, 9166-70.

FELIX, G., DURAN, J., VOLKO, S. & BOLLER, T. 1999. Plants have a sensitive perception system for the most conserved domain of bacterial flagellin. *Plant J*, 18, 265-276.

FOTIN, A., CHENG, Y., SLIZ, P., GRIGORIEFF, N., HARRISON, S. C., KIRCHHAUSEN, T. & WALZ, T. 2004. Molecular model for a complete clathrin lattice from electron cryomicroscopy. *Nature*, 432, 573-579.

FUJIMOTO, M., ARIMURA, S.-I., UEDA, T., TAKANASHI, H., HAYASHI, Y., NAKANO, A. & TSUTSUMI, N. 2010. Arabidopsis dynamin-related proteins DRP2B and DRP1A participate together in clathrin-coated vesicle formation during endocytosis. *PNAS*, 107, 6094-6099.

FUJIMOTO, M., ARIMURA, S., NAKAZONO, M. & TSUTSUMI, N. 2008. Arabidopsis dynamin-related protein DRP2B is co-localized with DRP1A on the leading edge of the forming cell plate. *Plant Cell Rep*, 27, 1581-6.

GASPAR, Y. M., MCKENNA, J. A., MCGINNESS, B. S., HINCH, J., POON, S., CONNELLY, A. A., ANDERSON, M. A. & HEATH, R. L. 2014. Field resistance to *Fusarium oxysporum* and *Verticillium dahliae* in transgenic cotton expressing the plant defensin NaD1. *J Exp Bot*, 65, 1541-50.

GENDREA, D., OHA, J., BOUTTÉA, Y., BESTB, J. G., SAMUELSB, L., NILSSONA, R., UEMURAC, T., MARCHANTD, A., BENNETTE, M. J., GREBEF, M. & BHALERAOA, R. P. 2011. Conserved Arabidopsis ECHIDNA protein mediates trans-Golgi-network trafficking and cell elongation. *PNAS*, 108, 8048-8053.

GIMENEZ-IBANEZ, S., HANN, D. R., NTOUKAKIS, V., PETUTSCHNIG, E. & LIPKA, V. 2009. AvrPtoB targets the LysM receptor kinase CERK1 to promote bacterial virulence on plants. *Current Biology*, 19, 423-429.

GOH, L., HUANG, F., KIM, W., GYGI, S. & SORKIN, A. 2010. Multiple mechanisms collectively regulate clathrin-mediated endocytosis of the epidermal growth factor receptor. *J Cell Biol*, 189, 871-883.

GOH, L. K. & SORKIN, A. 2013. Endocytosis of receptor tyrosine kinases. *Cold Spring Harb Perspect Biol*, 5, a017459.

GOHRE, V., SPALLEK, T., HAWEKER, H., MERSMANN, S., MENTZEL, T., BOLLER, T., DE TORRES, M., MANSFIELD, J. W. & ROBATZEK, S. 2008. Plant pattern-recognition receptor FLS2 is directed for degradation by the bacterial ubiquitin ligase AvrPtoB. *Curr Biol*, 18, 1824-32.

GOMEZ-GOMEZ, L. & BOLLER, T. 2000. FLS2: an LRR receptor-like kinase involved in the perception of the bacterial elicitor flagellin in Arabidopsis. *Mol Cell*, 5, 1003-1011.

GOMEZ-GOMEZ, L., FELIX, G. & BOLLER, T. 1999. A single locus determines sensitivity to bacterial flagellin in *Arabidopsis thaliana*. *Plant J*, 18, 277-84.

GRABBE, C., HUSNJAK, K. & DIKIC, I. 2011. The spatial and temporal organization of ubiquitin networks. *Nat Rev Mol Cell Biol*, 12, 295-307.

GREBE, M., XU, J., MÖBIUS, W., UEDA, T., NAKANO, A., GEUZE, H. J., ROOK, M. B. & SCHERES, B. 2003. Arabidopsis sterol endocytosis involves actin-mediated trafficking via ARA6-positive early endosomes. *Curr Biol.*, 13, 1378–1387.

GU, Y. & INNES, R. W. 2012. The KEEP ON GOING protein of Arabidopsis regulates intracellular protein trafficking and is degraded during fungal infection. *Plant Cell*, 24, 4717-30.

GUST, A. A. 2015. Peptidoglycan perception in plants. *PLoS Pathog*, 11, e1005275.

HAGLUND, K. & DIKIC, I. 2012. The role of ubiquitylation in receptor endocytosis and endosomal sorting. *J Cell Sci*, 125, 265-75.

HAGLUND, K., SIGISMUND, S. & POLO, S. 2003. Multiple monoubiquitination of RTKs is sufficient for their endocytosis and degradation. *Nat Cell Biol*, 5, 461–466.

HANN, D. R. & RATHJEN, J. P. 2007. Early events in the pathogenicity of *Pseudomonas syringae* on *Nicotiana benthamiana*. *Plant J*, 49, 607-18.

HAO, H., FAN, L., CHEN, T., LI, R., LI, X., HE, Q., BOTELLA, M. A. & LIN, J. 2014. Clathrin and membrane microdomains cooperatively regulate RbohD dynamics and activity in Arabidopsis. *Plant Cell*, 26, 1729-1745.

HAWEKER, H., RIPS, S., KOIWA, H., SALOMON, S., SAIJO, Y., CHINCHILLA, D., ROBATZEK, S. & VON SCHAEWEN, A. 2010. Pattern recognition receptors require N-glycosylation to mediate plant immunity. *J Biol Chem*, 285, 4629-36.

HE, S., NOMURA, K. & TS WHITTAM, T. S. 2004. Type III protein secretion mechanism in mammalian and plant pathogens. *Biochim Biophys Acta*, 1694, 181-206.

HEARD, W., SKLENAR, J., TOME, D. F., ROBATZEK, S. & JONES, A. M. 2015. Identification of regulatory and cargo proteins of endosomal and secretory pathways in *Arabidopsis thaliana* by proteomic dissection. *Mol Cell Proteomics*, 14, 1796-813.

HENTY-RIDILLA, J. L., SHIMONO, M., LI, J., CHANG, J. H., DAY, B. & STAIGER, C. J. 2013. The plant actin cytoskeleton responds to signals from microbe-associated molecular patterns. *PLoS Pathog*, 9, e1003290.

HIBBERT, R. G., HUANG, A., BOELENS, R. & SIXMA, T. K. 2011. E3 ligase Rad18 promotes monoubiquitination rather than ubiquitin chain formation by E2 enzyme Rad6. *Proc Natl Acad Sci U S A*, 108, 5590-5.

HOCHSTRASSER, M. 2009. Origin and function of ubiquitin-like proteins. *Nature*, 458, 422–429.

HONKANEN, R. E. 1993. Cantharidin, another natural toxin that inhibits the activity of serine/threonine protein phosphatases types 1 and 2A. *FEBS Lett*, 330, 283-6.

HUANG, J., FUJIMOTO, M., FUJIWARA, M., FUKAO, Y., ARIMURA, S. & TSUTSUMI, N. 2015. *Arabidopsis* dynamin-related proteins, DRP2A and DRP2B, function coordinately in post-Golgi trafficking. *Biochem Biophys Res Commun*, 456, 238-44.

HUSS, M., INGENHORST, G., KONIG, S., GASSEL, M., DROSE, S., ZEECK, A., ALTENDORF, K. & WIECZOREK, H. 2002. Concanamycin A, the specific inhibitor of V-ATPases, binds to the V(o) subunit c. *J Biol Chem*, 277, 40544-8.

IKEDA, F. & DIKIC, I. 2008. Atypical ubiquitin chains: New molecular signals. 'Protein modifications: Beyond the usual suspects' review series. *EMBO Rep*, 9, 536–542.

INADA, N., BETSUYAKU, S., SHIMADA, T. L., EBINE, K., ITO, E., KUTSUNA, N., HASEZAWA, S., TAKANO, Y., FUKUDA, H., NAKANO, A. & UEDA, T. 2016. Modulation of plant RAB GTPase-mediated membrane trafficking pathway at the interface between plants and obligate biotrophic pathogens. *Plant Cell Physiol*.

IRANI, N. G., DI RUBBO, S., MYLLE, E., VAN DEN BEGIN, J., SCHNEIDER-PIZON, J., HNILIKOVA, J., SISA, M., BUYST, D., VILARRASA-BLASI, J., SZATMARI, A. M., VAN DAMME, D., MISHEV, K., CODREANU, M. C., KOHOUT, L., STRNAD, M., CANO-DELGADO, A. I., FRIML, J., MADDER, A. & RUSSINOVA, E. 2012. Fluorescent castasterone reveals BRI1 signaling from the plasma membrane. *Nat Chem Biol*, 8, 583-9.

IRANNEJAD, R., TSVETANOVA, N. G., LOBINGIER, B. T. & VON ZASTROW, M. 2015. Effects of endocytosis on receptor-mediated signaling. *Curr Opin Cell Biol*, 35, 137-43.

ITO, E., FUJIMOTO, M., EBINE, K., UEMURA, T., UEDA, T. & NAKANO, A. 2012. Dynamic behavior of clathrin in *Arabidopsis thaliana* unveiled by live imaging. *Plant J*, 69, 204-16.

JANJUSEVIC, R., ABRAMOVITCH, R., MARTIN, G. & STEBBINS, C. 2006. A bacterial inhibitor of host programmed cell death defenses is an E3 ubiquitin ligase. *Science*, 309, 222-226.

JARSCH, I. K., KONRAD, S. S., STRATIL, T. F., URBANUS, S. L., SZYMANSKI, W., BRAUN, P., BRAUN, K. H. & OTT, T. 2014. Plasma membranes are subcompartmentalized into a plethora of coexisting and diverse microdomains in *Arabidopsis* and *Nicotiana benthamiana*. *Plant Cell*, 26, 1698-1711.

JEHLE, A. K., LIPSCHIS, M., ALBERT, M., FALLAHZADEH-MAMAGHANI, V., FURST, U., MUELLER, K. & FELIX, G. 2013. The receptor-like protein ReMAX of *Arabidopsis* detects the microbe-associated molecular pattern eMax from *Xanthomonas*. *Plant Cell*, 25, 2330-40.

JONES, J. & DANGL, J. 2006. The plant immune system. *Nature*, 444, 323-329.

JONGSMA, M. L., BERLIN, I., WIJDEVEN, R. H., JANSSEN, L., JANSSEN, G. M., GARSTKA, M. A., JANSSEN, H., MENSINK, M., VAN VEELEN, P. A., SPAAPEN, R. M. & NEEFJES, J. 2016. An ER-associated pathway defines endosomal architecture for controlled cargo transport. *Cell*, 166, 152-66.

KAKU, H., NISHIZAWA, Y., ISHII-MINAMI, N., AKIMOTO-TOMIYAMA, C., DOHMAE, N., TAKIO, K., MINAMI, E. & SHIBUYA, N. 2006. Plant cells recognize chitin fragments for defense signaling through a plasma membrane receptor. *Proc Natl Acad Sci U S A*, 103, 11086-91.

KANG, B.-H., NIELSEN, E., PREUSS, M. L., MASTRONARDE, D. & STAHELIN, L. A. 2011. Electron tomography of RabA4b- and PI-4Kbeta1-labeled trans Golgi network compartments in *Arabidopsis*. *Traffic*, 12, 313–329.

KANG, Y., JELENSKA, J., CECCHINI, N. M., LI, Y., LEE, M. W., KOVAR, D. R. & GREENBERG, J. T. 2014. HopW1 from *Pseudomonas syringae* disrupts the actin cytoskeleton to promote virulence in *Arabidopsis*. *PLoS Pathog*, 10, e1004232.

KEINATH, N. F., KIERSZNIOWSKA, S., LOREK, J., BOURDAIS, G., KESSLER, S. A., SHIMOSATO-ASANO, H., GROSSNIKLAUS, U., SCHULZE, W. X., ROBATZEK, S. & PANSTRUGA, R. 2010. PAMP (pathogen-associated molecular pattern)-induced changes in plasma membrane compartmentalization reveal novel components of plant immunity. *J Biol Chem*, 285, 39140-9.

KIM, B. H., KIM, S. Y. & NAM, K. H. 2013. Assessing the diverse functions of BAK1 and its homologs in *Arabidopsis*, beyond BR signaling and PTI responses. *Mol Cells*, 35, 7-16.

KNODLER, L. A., CELLI, J. & FINLAY, B. B. 2001. Pathogenic trickery: deception of host cell processes. *Nat Rev Mol Cell Biol*, 2, 578-88.

KOMANDER, D. & RAPE, M. 2012. The ubiquitin code. *Annu Rev Biochem*, 81, 203-29.

KORASICK, D. A., MCMICHAEL, C., WALKER, K. A., ANDERSON, J. C., BEDNAREK, S. Y. & HEESE, A. 2010. Novel functions of Stomatal Cytokinesis-Defective 1 (SCD1) in innate immune responses against bacteria. *J Biol Chem*, 285, 23342-50.

KOZIK, P., FRANCIS, R. W., SEAMAN, M. N. J. & ROBINSON, M. S. 2010. A Screen for Endocytic Motifs. *Traffic*, 11, 843–855.

KWAAITAAL, M. A., DE VRIES, S. C. & RUSSINOVA, E. 2005. *Arabidopsis thaliana* Somatic Embryogenesis Receptor Kinase 1 protein is present in sporophytic and gametophytic cells and undergoes endocytosis. *Protoplasma*, 226, 55-65.

LAMA, S. K., SIUA, C. L., HILLMERB, S., JANGC, S., ANC, G., ROBINSONB, D. G. & JIANG, L. 2007. Rice SCAMP1 defines clathrin-coated, trans-golgi-located tubular-vesicular structures as an early endosome in tobacco BY-2 cells. *The Plant Cell* 19, 296-319.

LEE, A. H., HURLEY, B., FELSENSTEINER, C., YEA, C., CKURSHUMOVA, W., BARTETZKO, V., WANG, P. W., QUACH, V., LEWIS, J. D., LIU, Y. C., BORNKE, F., ANGERS, S., WILDE, A., GUTTMAN, D. S. & DESVEAUX, D. 2012a. A bacterial acetyltransferase destroys plant microtubule networks and blocks secretion. *PLoS Pathog*, 8, e1002523.

LEE, H., KHATRI, A., PLOTNIKOV, J. M., ZHANG, X. C. & SHEEN, J. 2012b. Complexity in differential peptide-receptor signaling: response to Segonzac et al. and Mueller et al. commentaries. *Plant Cell*, 24, 3177-85.

LEE, H. Y., BOWEN, C. H., POPESCU, G. V., KANG, H. G., KATO, N., MA, S., DINESH-KUMAR, S., SNYDER, M. & POPESCU, S. C. 2011. Arabidopsis RTNLB1 and RTNLB2 Reticulon-like proteins regulate intracellular trafficking and activity of the FLS2 immune receptor. *Plant Cell*, 23, 3374-91.

LESLIE, M. E., LEWIS, M. W., YOUN, J. Y., DANIELS, M. J. & LILJEGREN, S. J. 2010. The EVERSHED receptor-like kinase modulates floral organ shedding in Arabidopsis. *Development*, 137, 467-76.

LEUNG, K. F., DACKS, J. B. & FIELD, M. C. 2008. Evolution of the multivesicular body ESCRT machinery; retention across the eukaryotic lineage. *Traffic*, 9, 1698-716.

LI, B., LU, D. & SHAN, L. 2014. Ubiquitination of pattern recognition receptors in plant innate immunity. *Mol Plant Pathol*, 15, 737-46.

LI, J., ZHAO-HUI, C., BATOUX, M., NEKRASOV, V., ROUX, M., CHINCHILLA, D., ZIPFEL, C. & JONES, J. D. 2009. Specific ER quality control components required for biogenesis of the plant innate immune receptor EFR. *Proc Natl Acad Sci U S A*, 106, 15973-8.

LI, W., AHN, I. P., NING, Y., PARK, C. H., ZENG, L., WHITEHILL, J. G., LU, H., ZHAO, Q., DING, B., XIE, Q., ZHOU, J. M., DAI, L. & WANG, G. L. 2012. The U-Box/ARM E3 ligase PUB13 regulates cell death, defense, and flowering time in Arabidopsis. *Plant Physiol*, 159, 239-50.

LIANG, Y., CAO, Y., TANAKA, K., THIBIVILLIERS, S., WAN, J., CHOI, J., KANG, C., QIU, J. & STACEY, G. 2013. Nonlegumes respond to rhizobial Nod factors by suppressing the innate immune response. *Science*, 341, 1384-7.

LIEBRAND, T. W., VAN DEN BERG, G. C., ZHANG, Z., SMIT, P., CORDEWENER, J. H., AMERICA, A. H., SKLENAR, J., JONES, A. M., TAMELING, W. I., ROBATZEK, S., THOMMA, B. P. & JOOSTEN, M. H. 2013. Receptor-like kinase SOBIR1/EVR interacts with receptor-like proteins in plant immunity against fungal infection. *Proc Natl Acad Sci U S A*, 110, 10010-5.

LIU, H. & STONE, S. L. 2010. Abscisic acid increases Arabidopsis ABI5 transcription factor levels by promoting KEG E3 ligase self-ubiquitination and proteasomal degradation. *Plant Cell*, 22, 2630-41.

LIU, Y. & LI, J. 2014. Endoplasmic reticulum-mediated protein quality control in Arabidopsis. *Front Plant Sci*, 5, 162.

LU, D., LIN, W., GAO, X., WU, S., CHENG, C., AVILA, J., HEESE, A., DEVARENNE, T. P., HE, P. & SHAN, L. 2011b. Direct ubiquitination of pattern recognition receptor FLS2 attenuates plant innate immunity. *Science*, 332, 1439-1442.

LU, R., MARTIN-HERNANDEZ, A. M., PEART, J. R., MALCUIT, I. & BAULCOMBE, D. C. 2003. Virus-induced gene silencing in plants. *Methods*, 30, 296-303.

LU, X., TINTOR, N., MENTZEL, T., KOMBRINK, E., BOLLER, T., ROBATZEK, S., SCHULZE-LEFERT, P. & SAIJO, Y. 2009. Uncoupling of sustained MAMP receptor signaling from early outputs in an *Arabidopsis* endoplasmic reticulum glucosidase II allele. *Proc Natl Acad Sci U S A*, 106, 22522-7.

LU, Y. J., SCHORNACK, S., SPALLEK, T., GELDNER, N., CHORY, J., SCHELLMANN, S., SCHUMACHER, K., KAMOUN, S. & ROBATZEK, S. 2012. Patterns of plant subcellular responses to successful oomycete infections reveal differences in host cell reprogramming and endocytic trafficking. *Cell Microbiol*, 14, 682-97.

MACHO, A. P., SCHWESSINGER, B., NTOUKAKIS, V., BRUTUS, A., SEGONZAC, C., ROY, S., KADOTA, Y., OH, M. H., SKLENAR, J., DERBYSHIRE, P., LOZANO-DURAN, R., MALINOVSKY, F. G., MONAGHAN, J., MENKE, F. L., HUBER, S. C., HE, S. Y. & ZIPFEL, C. 2014. A bacterial tyrosine phosphatase inhibits plant pattern recognition receptor activation. *Science*, 343, 1509-12.

MACHO, A. P. & ZIPFEL, C. 2014. Targeting of plant pattern recognition receptor-triggered immunity by bacterial type-III secretion system effectors. *Curr Opin Microbiol*, 23C, 14-22.

MACNAB, R. M. 2003. How bacteria assemble flagella. *Annu Rev Microbiol*, 57, 77-100.

MARINO, D., PEETERS, N. & RIVAS, S. 2012. Ubiquitination during plant immune signaling. *Plant Physiol*, 160, 15-27.

MARTINS, S., DOHMANN, E. M., CAYREL, A., JOHNSON, A., FISCHER, W., POJER, F., SATIAT-JEUNEMAITRE, B., JAILLAIS, Y., CHORY, J., GELDNER, N. & VERT, G. 2015. Internalization and vacuolar targeting of the brassinosteroid hormone receptor BRI1 are regulated by ubiquitination. *Nat Commun*, 6, 6151.

MBENGUE, M., BOURDAIS, G., GERVASI, F., BECK, M., ZHOU, J., SPALLEK, T., BARTELS, S., BOLLER, T., UEDA, T., KUHN, H. & ROBATZEK, S. 2016. Clathrin-dependent endocytosis is required for immunity mediated by pattern recognition receptor kinases. *Proc Natl Acad Sci U S A*.

MCMAHON, H. T. & BOUCROT, E. 2011. Molecular mechanism and physiological functions of clathrin-mediated endocytosis. *Nat Rev Mol Cell Biol*, 12, 517-533.

MCMICHAEL, C. M., REYNOLDS, G. D., KOCH, L. M., WANG, C., JIANG, N., NADEAU, J., SACK, F. D., GELDERMAN, M. B., PAN, J. & BEDNAREK, S. Y. 2013. Mediation of clathrin-dependent trafficking during cytokinesis and cell expansion by *Arabidopsis* stomatal cytokinesis defective proteins. *Plant Cell*, 25, 3910-25.

MELOTTO, M., UNDERWOOD, W., KOCZAN, J., NOMURA, K. & HE, S. Y. 2006. Plant stomata function in innate immunity against bacterial invasion. *Cell*, 126, 969-80.

MEYER, D., PAJONK, S., MICALI, C., O'CONNELL, R. & SCHULZE-LEFERT, P. 2009. Extracellular transport and integration of plant secretory proteins into pathogen-induced cell wall compartments. *Plant J*, 57, 986-99.

MICALI, C. O., NEUMANN, U., GRUNEWALD, D., PANSTRUGA, R. & O'CONNELL, R. 2011. Biogenesis of a specialized plant-fungal interface during host cell internalization of *Golovinomyces orontii* haustoria. *Cell Microbiol*, 13, 210-26.

MIYA, A., ALBERT, P., SHINYA, T., DESAKI, Y., ICHIMURA, K., SHIRASU, K., NARUSAKA, Y., KAWAKAMI, N., KAKU, H. & SHIBUYA, N. 2007. CERK1, a LysM receptor kinase, is essential for chitin elicitor signaling in *Arabidopsis*. *Proc Natl Acad Sci U S A*, 104, 19613-8.

MONAGHAN, J., MATSCHI, S., SHORINOLA, O., ROVENICH, H., MATEI, A., SEGONZAC, C., MALINOVSKY, F. G., RATHJEN, J. P., MACLEAN, D., ROMEIS, T. & ZIPFEL, C. 2014. The calcium-dependent protein kinase CPK28 buffers plant immunity and regulates BIK1 turnover. *Cell Host Microbe*, 16, 605-15.

MOSESSON, Y., SHTIEGMAN, K. & KATZ, M. 2003. Endocytosis of receptor tyrosine kinases is driven by monoubiquitylation, not polyubiquitylation. *J Biol Chem*, 278, 21323-21326.

MUKHTAR, M. S., CARVUNIS, A. R., DREZE, M., EPPEL, P., STEINBRENNER, J., MOORE, J., TASAN, M., GALLI, M., HAO, T., NISHIMURA, M. T., PEVZNER, S. J., DONOVAN, S. E., GHAMSARI, L., SANTHANAM, B., ROMERO, V., POULIN, M. M., GEBREAB, F., GUTIERREZ, B. J., TAM, S., MONACHELLO, D., BOXEM, M., HARBORT, C. J., MCDONALD, N., GAI, L., CHEN, H., HE, Y., EUROPEAN UNION EFFECTOROMICS, C., VANDENHAUTE, J., ROTH, F. P., HILL, D. E., ECKER, J. R., VIDAL, M., BEYNON, J., BRAUN, P. & DANGL, J. L. 2011. Independently evolved virulence effectors converge onto hubs in a plant immune system network. *Science*, 333, 596-601.

NEKRASOV, V., LI, J., BATOUX, M., ROUX, M., CHU, Z. H., LACOMBE, S., ROUGON, A., BITTEL, P., KISS-PAPP, M., CHINCHILLA, D., VAN ESSE, H. P., JORDA, L., SCHWESSINGER, B., NICASE, V., THOMMA, B. P., MOLINA, A., JONES, J. D. & ZIPFEL, C. 2009. Control of the pattern-recognition receptor EFR by an ER protein complex in plant immunity. *EMBO J*, 28, 3428-38.

NIELSEN, M. E., FEECHAN, A., BOHLENIUS, H., UEDA, T. & THORDAL-CHRISTENSEN, H. 2012. *Arabidopsis* ARF-GTP exchange factor, GNOM, mediates transport required for innate immunity and focal accumulation of syntaxin PEN1. *Proc Natl Acad Sci U S A*, 109, 11443-8.

NOMURA, K., DEBROY, S., LEE, Y. H., PUMPLIN, N., JONES, J. & HE, S. Y. 2006. A bacterial virulence protein suppresses host innate immunity to cause plant disease. *Science*, 313, 220-3.

NOMURA, K., MECEY, C., LEE, Y. N., IMBODEN, L. A., CHANG, J. H. & HE, S. Y. 2011. Effector-triggered immunity blocks pathogen degradation of an immunity-associated vesicle traffic regulator in *Arabidopsis*. *Proc Natl Acad Sci U S A*, 108, 10774-9.

NTOUKAKIS, V., MUCYN, T. S., GIMENEZ-IBANEZ, S., CHAPMAN, H. C., GUTIERREZ, J. R., BALMUTH, A. L., JONES, A. M. & RATHJEN, J. P. 2009. Host inhibition of a bacterial virulence effector triggers immunity to infection. *Science*, 324, 784-7.

NTOUKAKIS, V., SCHWESSINGER, B., SEGONZAC, C. & ZIPFEL, C. 2011. Cautionary notes on the use of C-terminal BAK1 fusion proteins for functional studies. *Plant Cell*, 23, 3871-8.

O'CONNELL, R. J. & PANSTRUGA, R. 2006. Tete a tete inside a plant cell: establishing compatibility between plants and biotrophic fungi and oomycetes. *New Phytol*, 171, 699-718.

OHNO, H., FOURNIER, M. C., POY, G. & BONIFACINO, J. S. 1996. Structural determinants of interaction of tyrosine-based sorting signals with the adaptor medium chains. *J Biol Chem*, 271, 29009-15.

PANDEY, K. N. 2009. Functional roles of short sequence motifs in the endocytosis of membrane receptors. *Front Biosci (Landmark Ed)*, 14, 5339-60.

PECK, S. C. 2006. Analysis of protein phosphorylation: methods and strategies for studying kinases and substrates. *Plant J*, 45, 512-22.

PEER, W. A., HOSEIN, F. N., BANDYOPADHYAY, A., MAKAM, S. N., OTEGUI, M. S., LEE, G. J., BLAKESLEE, J. J., CHENG, Y., TITAPIWATANAKUN, B., YAKUBOV, B., BANGARI, B. & MURPHY, A. S. 2009. Mutation of the membrane-associated M1 protease APM1 results in distinct embryonic and seedling developmental defects in *Arabidopsis*. *Plant Cell*, 21, 1693-721.

PEL, M. J. & PIETERSE, C. M. 2013. Microbial recognition and evasion of host immunity. *J Exp Bot*, 64, 1237-48.

POSTMA, J., LIEBRAND, T. W., BI, G., EVRARD, A., BYE, R. R., MBENGUE, M., KUHN, H., JOOSTEN, M. H. & ROBATZEK, S. 2016. Avr4 promotes Cf-4 receptor-like protein association with the BAK1/SERK3 receptor-like kinase to initiate receptor endocytosis and plant immunity. *New Phytol*, 210, 627-42.

PRUITT, R. N., SCHWESSINGER, B., JOE, A., THOMAS, N., LIU, F., ALBERT, M., ROBINSON, M. R., CHAN, L. J. G., DEE, L. D., CHEN, H., BAHAR, O., DAUDI, A., DE VLEESSCHAUWER, D., CADDELL, D., ZHANG, W., ZHAO, X., LI, X., HEAZLEWOOD, J. L., RUAN, D., MAJUMDER, D., CHERN, M., KALBACHER, H., MIDHA, S., PATIL, P. B., SONTI, R. V., PETZOLD, C. J., LIU, C., BRODBELT, J. S., FELIX, G. & RONALD, P. C. 2015. The rice immune receptor XA21 recognizes a tyrosine-sulfated protein from a Gram-negative bacterium. *Science Advances*, 1, 6 e1500245.

RAIBORG, C. & STENMARK, H. 2009. The ESCRT machinery in endosomal sorting of ubiquitylated membrane proteins. *Nature*, 458, 445-52.

RAIBORG, C., WENZEL, E. M., PEDERSEN, N. M., OLSVIK, H., SCHINK, K. O., SCHULTZ, S. W., VIETRI, M., NISI, V., BUCCI, C., BRECH, A., JOHANSEN, T. & STENMARK, H. 2015. Repeated ER-endosome contacts promote endosome translocation and neurite outgrowth. *Nature*, 520, 234-8.

RANF, S., GISCH, N., SCHAFFER, M., ILLIG, T., WESTPHAL, L., KNIREL, Y. A., SANCHEZ-CARBALLO, P. M., ZAHRINGER, U., HUCKELHOVEN, R., LEE, J. & SCHEEL, D. 2015. A lectin S-domain receptor kinase mediates lipopolysaccharide sensing in *Arabidopsis thaliana*. *Nat Immunol*, 16, 426-33.

RAPOSO, G. & STOORVOGEL, W. 2013. Extracellular vesicles: Exosomes, microvesicles, and friends. *JCB*, 200, 373-383.

REYES, F., BUONO, R. & OTEGUI, M. 2011. Plant endosomal trafficking pathways. *Current Opinion in Plant Biology*, 14, 666-673.

RICHARDSON, L. G., HOWARD, A. S., KHUU, N., GIDDA, S. K., MCCARTNEY, A., MORPHY, B. J. & MULLEN, R. T. 2011. Protein-protein interaction network and subcellular localization of the *Arabidopsis thaliana* ESCRT machinery. *Front Plant Sci*, 2, 20.

RICHARDSON, L. G. & MULLEN, R. T. 2011. Meta-analysis of the expression profiles of the *Arabidopsis* ESCRT machinery. *Plant Signal Behav*, 6, 1897-903.

RICHTER, S., KIENTZ, M., BRUMM, S., NIELSEN, M. E., PARK, M., GAVIDIA, R., KRAUSE, C., VOSS, U., BECKMANN, H., MAYER, U., STIERHOF, Y. D. & JURGENS, G. 2014. Delivery of endocytosed proteins to the cell-division plane requires change of pathway from recycling to secretion. *Elife*, 3, e02131.

ROBATZEK, S., CHINCHILLA, D. & BOLLER, T. 2006. Ligand-induced endocytosis of the pattern recognition receptor FLS2 in *Arabidopsis*. *Genes and Development*, 20, 537-542.

ROBINSON, D. G. & PIMPL, P. 2014. Clathrin and post-Golgi trafficking: a very complicated issue. *Trends in Plant Science*, 19, 134-139.

ROCHA, N., KUIJL, C., VAN DER KANT, R., JANSSEN, L., Houben, D., JANSSEN, H., ZWART, W. & NEEFJES, J. 2009. Cholesterol sensor ORP1L contacts the ER protein VAP to control Rab7-RILP-p150 Glued and late endosome positioning. *J Cell Biol*, 185, 1209-25.

ROMEIS, T., LUDWIG, A., MARTIN, R. & JONES, J. 2001. Calcium-dependent protein kinases play an essential role in a plant defence response. *The Embo Journal*, 20, 5556-5567.

RON, M. & AVNI, A. 2004. The receptor for the fungal elicitor ethylene-inducing xylanase is a member of a resistance-like gene family in tomato. *Plant Cell*, 16, 1604-15.

ROSEBROCK, T. R., ZENG, L., BRADY, J. J., ABRAMOVITCH, R. B., XIAO, F. & MARTIN, G. B. 2007. A bacterial E3 ubiquitin ligase targets a host protein kinase to disrupt plant immunity. *Nature*, 448, 370-4.

ROUX, M., SCHWESSINGER, B., ALBRECHT, C., CHINCHILLA, D., JONES, A., HOLTON, N., MALINOVSKY, F. G., TOR, M., DE VRIES, S. & ZIPFEL, C. 2011. The *Arabidopsis* leucine-rich repeat receptor-like kinases BAK1/SERK3 and BKK1/SERK4 are required for innate immunity to hemibiotrophic and biotrophic pathogens. *Plant Cell*, 23, 2440-55.

ROWLAND, A. A., CHITWOOD, P. J., PHILLIPS, M. J. & VOELTZ, G. K. 2014. ER contact sites define the position and timing of endosome fission. *Cell*, 159, 1027-41.

RUSSINOVA, E., BORST, J. W., KWAAITAAL, M., CANO-DELGADO, A., YIN, Y., CHORY, J. & DE VRIES, S. C. 2004. Heterodimerization and endocytosis of *Arabidopsis* brassinosteroid receptors BRI1 and AtSERK3 (BAK1). *Plant Cell*, 16, 3216-29.

SCHEURING, D. & ROBINSON, D. G. 2007. Trans Golgi Network: Meeting Place of Trafficking Pathways.

SCHEURING, D., VIOTTI, C., KRUGER, F., KUNZL, F., STURM, S., BUBECK, J., HILLMER, S., FRIGERIO, L., ROBINSON, D. G., PIMPL, P. & SCHUMACHER, K. 2011. Multivesicular bodies mature from the trans-Golgi network/early endosome in *Arabidopsis*. *Plant Cell*, 23, 3463-3481.

SCHMIDT, S. M., KUHN, H., MICALI, C., LILLER, C., KWAAITAAL, M. & PANSTRUGA, R. 2014. Interaction of a *Blumeria graminis* f. sp. *hordei* effector candidate with a barley ARF-GAP suggests that host vesicle trafficking is a fungal pathogenicity target. *Mol Plant Pathol*, 15, 535-49.

SCHULZE, B., MENTZEL, T., JEHLE, A. K., MUELLER, K., BEELER, S., BOLLER, T., FELIX, G. & CHINCHILLA, D. 2010. Rapid heteromerization and phosphorylation of ligand-activated plant transmembrane receptors and their associated kinase BAK1. *J Biol Chem*, 285, 9444-51.

SCHWESSINGER, B., ROUX, M., KADOTA, Y., NTOUKAKIS, V., SKLENAR, J., JONES, A. & ZIPFEL, C. 2011. Phosphorylation-dependent differential regulation of plant growth, cell death, and innate immunity by the regulatory receptor-like kinase BAK1. *PLoS Genet*, 7, e1002046.

SEDGWICK, S. G. & SMERDON, S. J. 1999. The ankyrin repeat: a diversity of interactions on a common structural framework. *Trends Biochem Sci*, 24, 311-6.

SEGONZAC, C., FEIKE, D., GIMENEZ-IBANEZ, S., HANN, D. R., ZIPFEL, C. & RATHJEN, J. P. 2011. Hierarchy and roles of pathogen-associated molecular pattern-induced responses in *Nicotiana benthamiana*. *Plant Physiol*, 156, 687-99.

SERRANO, M., ROBATZEK, S., TORRES, M., KOMBRINK, E., SOMSSICH, I. E., ROBINSON, M. & SCHULZE-LEFERT, P. 2007. Chemical interference of pathogen-associated molecular

pattern-triggered immune responses in *Arabidopsis* reveals a potential role for fatty-acid synthase type II complex-derived lipid signals. *J Biol Chem*, 282, 6803-11.

SHAHRIARI, M., RICHTER, K., KESHAVAIAH, C., SABOVLJEVIC, A., HUELSKAMP, M. & SCHELLMANN, S. 2011. The *Arabidopsis* ESCRT protein-protein interaction network. *Plant Mol Biol*, 76, 85-96.

SHAN, L., HE, P., LI, J., HEESE, A., PECK, S., NURNBERGER, T., MARTIN, G. & SHEEN, J. 2008. Bacterial effectors target the common signaling partner BAK1 to disrupt multiple MAMP receptor-signaling complexes and impede plant immunity. *Cell Host Microbe* 4, 17-27.

SHARFMAN, M., BAR, M., EHRLICH, M., SCHUSTER, S., MELECH-BONFIL, S., EZER, R., SESSA, G. & AVNI, A. 2011. Endosomal signaling of the tomato leucine-rich repeat receptor-like protein LeEix2. *Plant J*, 68, 413-23.

SHARFMAN, M., BAR, M., SCHUSTER, S., LEIBMAN, M. & AVNI, A. 2014. Sterol-dependent induction of plant defense responses by a microbe-associated molecular pattern from *Trichoderma viride*. *Plant Physiol*, 164, 819-27.

SHIMIZU, T., NAKANO, T., TAKAMIZAWA, D., DESAKI, Y., ISHII-MINAMI, N., NISHIZAWA, Y., MINAMI, E., OKADA, K., YAMANE, H., KAKU, H. & SHIBUYA, N. 2010. Two LysM receptor molecules, CEBiP and OsCERK1, cooperatively regulate chitin elicitor signaling in rice. *Plant J*, 64, 204-14.

SMITH, J. M., LESLIE, M. E., ROBINSON, S. J., KORASICK, D. A., ZHANG, T., BACKUES, S. K., CORNISH, P. V., KOO, A. J., BEDNAREK, S. Y. & HEESE, A. 2014. Loss of *Arabidopsis thaliana* dynamin-related protein 2B reveals separation of innate immune signaling pathways. *PLoS Pathog*, 10, e1004578.

SMITH, K., ANDERSEN-NISSEN, E., HAYASHI, F., STROBE, K., BERGMAN, M., BARRETT, S., COOKSON, B. & ADEREM, A. 2003. Toll-like receptor 5 recognizes a conserved site on flagellin required for protofilament formation and bacterial motility. *Nature Immunology*, 4, 1247-1253.

SONG, W. Y., WANG, G. L., CHEN, L. L., KIM, H. S., PI, L. Y., HOLSTEN, T., GARDNER, J., WANG, B., ZHAI, W. X., ZHU, L. H., FAUQUET, C. & RONALD, P. 1995. A receptor kinase-like protein encoded by the rice disease resistance gene, *Xa21*. *Science*, 270, 1804-6.

SORKIN, A. & VON ZASTROW, M. 2009. Endocytosis and signalling: intertwining molecular networks. *Nat Rev Mol Cell Biol*, 10, 609-22.

SPALLEK, T., BECK, M., BEN KHALED, S., SALOMON, S., BOURDAIS, G., SCHELLMANN, S. & ROBATZEK, S. 2013. ESCRT-I mediates FLS2 endosomal sorting and plant immunity. *PLoS Genet*, 9, e1004035.

SPALLEK, T., ROBATZEK, S. & GOHRE, V. 2009. How microbes utilize host ubiquitination. *Cell Microbiol*, 11, 1425-34.

SPARKES, I., TOLLEY, N., ALLER, I., SVOZIL, J., OSTERRIEDER, A., BOTCHWAY, S., MUELLER, C., FRIGERIO, L. & HAWES, C. 2010. Five *Arabidopsis* reticulon isoforms share endoplasmic reticulum location, topology, and membrane-shaping properties. *Plant Cell*, 22, 1333-43.

SPARKS, J. A., KWON, T., RENNA, L., LIAO, F., BRANDIZZI, F. & BLANCAFLOR, E. B. 2016. HLB1 is a tetratricopeptide repeat domain-containing protein that operates at the intersection of the exocytic and endocytic pathways at the TGN/EE in *Arabidopsis*. *Plant Cell*, 28, 746-69.

SPETH, E. B., IMBODEN, L., HAUCK, P. & HE, S. Y. 2009. Subcellular localization and functional analysis of the *Arabidopsis* GTPase RabE. *Plant Physiol*, 149, 1824-37.

SPITZER, C., REYES, F. C., BUONO, R., SLIWINSKI, M. K., HAAS, T. J. & OTEGUI, M. S. 2009. The ESCRT-related CHMP1A and B proteins mediate multivesicular body sorting of auxin carriers in *Arabidopsis* and are required for plant development. *Plant Cell*, 21, 749-66.

STEGMANN, M., ANDERSON, R. G., ICHIMURA, K., PECENKOVA, T., REUTER, P., ZARSKY, V., MCDOWELL, J. M., SHIRASU, K. & TRUJILLO, M. 2012. The ubiquitin ligase PUB22 targets a subunit of the exocyst complex required for PAMP-triggered responses in *Arabidopsis*. *Plant Cell*, 24, 4703-16.

STONE, S. L., WILLIAMS, L. A., FARMER, L. M., VIERSTRA, R. D. & CALLIS, J. 2006. KEEP ON GOING, a RING E3 ligase essential for *Arabidopsis* growth and development, is involved in abscisic acid signaling. *Plant Cell*, 18, 3415-28.

SU, J. F., WEI, J., LI, P. S., MIAO, H. H., MA, Y. C., QU, Y. X., XU, J., QIN, J., LI, B. L., SONG, B. L., XU, Z. P. & LUO, J. 2016. Numb directs the subcellular localization of excitatory amino acid transporter type 3 through binding the YXNXXF motif. *J Cell Sci*.

SUN, T., ZHANG, Q., GAO, M. & ZHANG, Y. 2014. Regulation of SOBIR1 accumulation and activation of defense responses in *bir1-1* by specific components of ER quality control. *Plant J*, 77, 748-56.

SUN, Y., LI, L., MACHO, A. P., HAN, Z., HU, Z., ZIPFEL, C., ZHOU, J. M. & CHAI, J. 2013. Structural basis for flg22-induced activation of the *Arabidopsis* FLS2-BAK1 immune complex. *Science*, 342, 624-8.

TANAKA, H., KITAKURA, S., DE RYCKE, R., DE GROODT, R. & FRIML, J. 2009. Fluorescence imaging-based screen identifies ARF GEF component of early endosomal trafficking. *Curr Biol*, 19, 391-7.

TATEDA, C., ZHANG, Z., SHRESTHA, J., JELENSKA, J., CHINCHILLA, D. & GREENBERG, J. T. 2014. Salicylic Acid regulates *Arabidopsis* microbial pattern receptor kinase levels and signaling. *Plant Cell*, 26, 4171-87.

THOMAS, C. M., JONES, D. A., PARNISKE, M., HARRISON, K., BALINT-KURTI, P. J., HATZIXANTHIS, K. & JONES, J. D. 1997. Characterization of the tomato Cf4 gene for resistance to *Cladosporium fulvum* identifies sequences that determine recognitional specificity in Cf4 and Cf9. *Plant Cell*, 9, 2209-24.

TILSNER, J., AMARI, K. & TORRANCE, L. 2011. Plasmodesmata viewed as specialised membrane adhesion sites. *Protoplasma*, 248, 39-60.

TOTH, R., GERDING-REIMERS, C., DEEKS, M. J., MENNINGER, S., GALLEGOS, R. M., TONACO, I. A., HUBEL, K., HUSSEY, P. J., WALDMANN, H. & COUPLAND, G. 2012. Prieurianin/endosidin 1 is an actin-stabilizing small molecule identified from a chemical genetic screen for circadian clock effectors in *Arabidopsis thaliana*. *Plant J*, 71, 338-52.

TRUJILLO, M., ICHIMURA, K., CASAIS, C. & SHIRASU, K. 2008. Negative regulation of PAMP-triggered immunity by an E3 ubiquitin ligase triplet in *Arabidopsis*. *Curr Biol*, 18, 1396-401.

UNDERWOOD, W. & SOMERVILLE, S. C. 2008. Focal accumulation of defences at sites of fungal pathogen attack. *Journal of Experimental Botany*, 59, 3501-3508.

UNDERWOOD, W. & SOMERVILLE, S. C. 2013. Perception of conserved pathogen elicitors at the plasma membrane leads to relocalization of the *Arabidopsis* PEN3 transporter. *Proc Natl Acad Sci U S A*, 110, 12492-7.

VAN DER KANT, R., FISH, A., JANSSEN, L., JANSSEN, H., KROM, S., HO, N., BRUMMELKAMP, T., CARETTE, J., ROCHA, N. & NEEFJES, J. 2013. Late endosomal transport and tethering are coupled processes controlled by RILP and the cholesterol sensor ORP1L. *J Cell Sci*, 126, 3462-74.

WAN, J., TANAKA, K., ZHANG, X. C., SON, G. H., BRECHENMACHER, L., NGUYEN, T. H. & STACEY, G. 2012. LYK4, a lysin motif receptor-like kinase, is important for chitin signaling and plant innate immunity in *Arabidopsis*. *Plant Physiol*, 160, 396-406.

WANG, D., WEAVER, N. D., KESARWANI, M. & DONG, X. 2005. Induction of protein secretory pathway is required for systemic acquired resistance. *Science*, 308, 1036-40.

WANG, H., SHI, Y., SONG, J., QI, J., LU, G., YAN, J. & GAO, G. F. 2016. Ebola Viral Glycoprotein Bound to Its Endosomal Receptor Niemann-Pick C1. *Cell*, 164, 258-68.

WANG, J., CAI, Y., MIAO, Y., LAM, S. K. & JIANG, L. 2009. Wortmannin induces homotypic fusion of plant prevacuolar compartments. *J Exp Bot*, 60, 3075-83.

WANG, Y. S., PI, L. Y., CHEN, X., CHAKRABARTY, P. K., JIANG, J., DE LEON, A. L., LIU, G. Z., LI, L., BENNY, U., OARD, J., RONALD, P. C. & SONG, W. Y. 2006. Rice XA21 binding protein 3 is a ubiquitin ligase required for full Xa21-mediated disease resistance. *Plant Cell*, 18, 3635-46.

WATERMAN, H. & YARDEN, Y. 2001. Molecular mechanisms underlying endocytosis and sorting of ErbB receptor tyrosine kinases. *FEBS Lett*, 490, 142-52.

WEISSMAN, A. M. 2001. Themes and variations on ubiquitylation. *Nat Rev Mol Cell Biol*, 2, 169-78.

WESSLING, R., EPPEL, P., ALTMANN, S., HE, Y., YANG, L., HENZ, S. R., MCDONALD, N., WILEY, K., BADER, K. C., GLASSER, C., MUKHTAR, M. S., HAIGIS, S., GHAMSARI, L., STEPHENS, A. E., ECKER, J. R., VIDAL, M., JONES, J. D., MAYER, K. F., VER LOREN VAN THEMAAT, E., WEIGEL, D., SCHULZE-LEFERT, P., DANGL, J. L., PANSTRUGA, R. & BRAUN, P. 2014. Convergent targeting of a common host protein-network by pathogen effectors from three kingdoms of life. *Cell Host Microbe*, 16, 364-75.

WILKINSON, K. A., KONOPACKI, F. & HENLEY, J. M. 2012. Modification and movement Phosphorylation and SUMOylation regulate endocytosis of GluK2-containing kainate receptors. *Communicative & Integrative Biology* 2, 223-226.

WILLMANN, R., LAJUNEN, H. M., ERBS, G., NEWMAN, M. A., KOLB, D., TSUDA, K., KATAGIRI, F., FLIEGMANN, J., BONO, J. J., CULLIMORE, J. V., JEHLE, A. K., GOTZ, F., KULIK, A., MOLINARO, A., LIPKA, V., GUST, A. A. & NURNBERGER, T. 2011. Arabidopsis lysin-motif proteins LYM1 LYM3 CERK1 mediate bacterial peptidoglycan sensing and immunity to bacterial infection. *Proc Natl Acad Sci U S A*, 108, 19824-9.

WINTER, V. & HAUSER, M. T. 2006. Exploring the ESCRTing machinery in eukaryotes. *Trends Plant Sci*, 11, 115-23.

XIN, X. F., NOMURA, K., UNDERWOOD, W. & HE, S. Y. 2013. Induction and suppression of PEN3 focal accumulation during *Pseudomonas syringae* pv. tomato DC3000 infection of Arabidopsis. *Mol Plant Microbe Interact*, 26, 861-7.

YAMAGUCHI, Y., PEARCE, G. & RYAN, C. 2006. The cell surface leucine-rich repeat receptor for AtPep1, an endogenous peptide elicitor in Arabidopsis, is functional in transgenic tobacco cells. *Proc Natl Acad Sci U S A*, 103, 10104-10109.

YUAN, T., LIU, L., ZHANG, Y., WEI, L., ZHAO, S., ZHENG, X., HUANG, X., BOULANGER, J., GUEUDRY, C., LU, J., XIE, L., DU, W., ZONG, W., YANG, L., SALAMERO, J., LIU, Y. & CHEN, L. 2015. Diacylglycerol guides the hopping of clathrin-coated pits along microtubules for exo-endocytosis coupling. *Dev Cell*, 35, 120-30.

ZENG, W. & HE, S. Y. 2010. A prominent role of the flagellin receptor FLAGELLIN-SENSING2 in mediating stomatal response to *lo* pv tomato DC3000 in Arabidopsis. *Plant Physiol*, 153, 1188-98.

ZHANG, J., NODZYŃSKI, T., PĚNČÍK, A., ROLČÍK, J. & FRIML, J. 2010. PIN phosphorylation is sufficient to mediate PIN polarity and direct auxin transport. *PNAS*, 107, 918-922.

ZHANG, Z., SHRESTHA, J., TATEDA, C. & GREENBERG, J. T. 2014. Salicylic acid signaling controls the maturation and localization of the arabidopsis defense protein ACCELERATED CELL DEATH6. *Mol Plant*, 7, 1365-83.

ZHOU, J., LU, D., XU, G., FINLAYSON, S. A., HE, P. & SHAN, L. 2015. The dominant negative ARM domain uncovers multiple functions of PUB13 in Arabidopsis immunity, flowering, and senescence. *J Exp Bot*, 66, 3353-66.

ZIPFEL, C., KUNZE, G., CHINCHILLA, D., CANIARD, A., JONES, J. D., BOLLER, T. & FELIX, G. 2006. Perception of the bacterial PAMP EF-Tu by the receptor EFR restricts Agrobacterium-mediated transformation. *Cell*, 125, 749-60.

ZIPFEL, C., ROBATZEK, S., NAVARRO, L., OAKELEY, E., JONES, J., FELIX, G. & BOLLER, T. 2004. Bacterial disease resistance in Arabidopsis through flagellin perception. *Nature*, 428, 764-767.